Charles University in Prague

Faculty of Pharmacy in Hradec Králové

Department of Biochemical Sciences

Investigation of proteolytic enzymes expression in different tissues at the transgenic animal model of Huntington´s disease by means of biochemical and immunohistochemical methods

Vyšetření exprese proteolytických enzymů v různých tkáních na transgenním zvířecím modelu Huntingtonovy nemoci pomocí biochemických a imunohistochemických metod

Diploma thesis

Supervisors:

Prof. MUDr. Jaroslav Dršata, CSc.

Department of Biochemical Sciences

Faculty of Pharmacy, Charles University in Prague

MUDr. Taras Ardan, Ph.D.

Institute of Animal Physiology and Genetics AS CR, v.v.i.

Laboratory of Cell Regeneration and Plasticity

Hradec Králové 2015

Bc. Gabriela Kocurová

„I declare that this diploma thesis is my original work and I have not received any unauthorized assistance in its completion. All sources are named in references and cited properly.”

„Prohlašuji, že tato práce je mým původním autorským dílem. Veškerá literatura a další zdroje, z nichž jsem při zpracování čerpala, jsou uvedeny v seznamu použité literatury a v práci řádně citovány. Práce nebyla využita k získání jiného nebo stejného titulu.”

.....

Gabriela Kocurová

I would like to express my gratitude to:

My supervisor MUDr. Taras Ardan, Ph.D. for his tremendous patience, advice and guidance throughout the project

Ing. Zdenka Ellederová, Ph.D. for passing me over all pitfalls of biochemical laboratory

Mgr. Jiří Klíma, CSc. for a precise demonstration of working with cells

Prof. MVDr. Jan Motlík, DrSc. for the opportunity to participate in this project

All Ph.D. students who were still next to me at the doubtful times, especially Mgr. Petra Vochozková for her help and motivation

Other members of the Laboratory of Cell Regeneration and Plasticity

Prof. MUDr. Jaroslav Dršata, CSc. for kindly accepting me under his wings

My family

ABSTRACT

Charles University in Prague

Faculty of Pharmacy in Hradec Králové

Department of Biochemical Sciences

Candidate: Bc. Gabriela Kocurová

Supervisor: Prof. MUDr. Jaroslav Dršata, CSc.

Title of diploma thesis: Investigation of proteolytic enzymes expression in different tissues at the transgenic animal model of Huntington´s disease by means of biochemical and immunohistochemical methods

Background: Huntington's disease (HD) is a neurodegenerative disorder that is caused by an expansion of a polyglutamine (polyQ) domain in the huntingtin (Htt) protein. Because it is known that mutant Htt and especially its small proteolytic fragments are toxic to neurons (particularly those in the striatum and cortex), it has been suggested that proteolysis of mutant huntingtin (mHtt) might play an important role in HD pathogenesis. Therefore, the aim of the present study was to examine the expression of endogenous and mtHtt and possible participation of the proteolytic enzymes from the group of caspases, matrix metalloproteinases (MMPs), kallikreins (KLKs) and calpains in HD pathology of brain tissue.

Methods: In this study we used WT and TgHD minipigs for N-terminal part of the human mtHtt (548aaHTT-145Q, both F2 generation, age 36 months; F3 generation, age 48 months in additional experiment), R6/2 mice were used as positive controls. Htt and proteases were examined immunohistochemically (IHC) and by immunofluorescence (IF) on cryostat sections, or biochemically by Western blotting (WB) using the following primary antibodies: anti-BML-PW0595, anti-EPR5526, anti-MAB2166, anti-1C2, anti-3B5H10, anti-MW8, anti-caspase-3, anti-caspase-8, anti-MMP-9, anti-MMP-10, anti-KLK-10, anti-calpain-5.

Results: Endogenous and transgenic Htt was detected in the brain sections of TgHD minipig (F2 generation, 36m), as well as the presence of small proteolytic fragments was confirmed. IHC revealed formation of aggregates of mtHtt. Biochemical detection of proteases in the TgHD minipig brain showed higher levels of caspase-3, MMP-9 and its multiple proteolytic cleavage products (generated from mHtt). Using IHC and WB, we demonstrated significantly increased expression of caspase-3 in nucleus caudatus and cortex area of TgHD minipigs in comparison to WT animals. Immunohistochemically detected MMP-10 level was very weak in all animals studied (TgHD and WT) with small differences between them. Increased levels of MMP-9 were observed by IF in retinal pigment epithelial cells (RPE) of TgHD minipig (48m). In contrary to that the most proteolytic enzymes revealed the same or increased expressions in TgHD brains, the decreased expression of kallikrein-10 was detected in these brains in comparison to WT brains.

Conclusion: Due to different expression of proteolytic enzymes in TgHD brains further studies are necessary to clarify the exact role of these enzymes in etiology of HD.

Key words: proteolytic enzymes, transgenic animal model, Huntington's disease, biochemistry, immunohistochemistry

ABSTRAKT

Univerzita Karlova v Praze

Farmaceutická fakulta v Hradci Králové

Katedra biochemických věd

Kandidát: Gabriela Kocurová

Školitel: Prof. MUDr. Jaroslav Dršata, CSc.

Název diplomové práce: Vyšetření exprese proteolytických enzymů v různých tkáních na transgenním zvířecím modelu Huntingtonovy nemoci pomocí biochemických a imunohistochemických metod

Úvod: Huntingtonova nemoc (HN) je neurodegenerativní onemocnění způsobené expanzí polyglutaminu (polyQ) v proteinu huntingtin (Htt). Protože je známo, že mutantní Htt a zvláště jeho malé proteolytické fragmenty jsou toxické pro neurony (hlavně ty ve striatu a mozkové kůře), proteolýza mutantního Htt (mtHtt) hraje zřejmě důležitou roli v patogenezi HN. Cílem této studie je proto vyšetření endogenního i mtHtt a možné zapojení proteolytických enzymů z rodiny kaspáz, matrix metaloproteináz (MMP), kalikreinů (KLK) a kalpainů v patogenezi HN.

Metody: V této studii jsme použili WT a TgHD miniprasata pro N-koncovou část lidského mtHtt (548aaHTT-145Q, generace F2, věk 36 měsíců; generace F3, věk 48 měsíců pro neplánovaný experiment), R6/2 myši byly použity jako pozitivní kontroly. Htt a proteázy byly zkoumány imunohistochemicky (IHC) a pomocí imunofluorescence (IF) na kryostatových řezech, nebo biochemicky Western blottingem (WB) za použití následujících primárních protilátek: anti-BML-PW0595, anti-EPR5526, anti-MAB2166, anti-1C2, anti-3B5H10, anti-MW8, anti-kaspáza-3, anti-MMP-9, MMP-anti-10, anti-KLK-10, anti-kalpain-5.

Výsledky: Endogenní a transgenní Htt byl detekován v mozkových řezech TgHD miniprasete (F2 generace, 36m), stejně jako byla potvrzena přítomnost malých proteolytických fragmentů. IHC odhalila tvorbu agregátů mtHtt. Biochemická detekce proteáz v TgHD miniprasat mozku prokázala vyšší hladiny kaspázy-3, MMP-9 a jejich mnohých produktů proteolytického štěpení (vzniklých z mHtt). Použitím IHC a WB jsme prokázali významně zvýšenou expresi kaspázy-3 v nucleus caudatus a kortikální oblasti TgHD miniprasat ve srovnání s WT zvířaty. Imunohistochemicky stanovená hladina MMP-10 byla velmi nízká u všech studovaných zvířat (TgHD a WT) s malými rozdíly mezi nimi. Zvýšené hladiny MMP-9 byly pozorovány pomocí IF v retinálních pigmentových buňkách (RPE) TgHD miniprasete (48m). Na rozdíl od ostatních proteolytických enzymů, u kterých byly potvrzeny stejné, nebo zvýšené koncentrace, exprese KLK-10 v mozcích TgHD prasat byly snížené oproti mozkům WT jedinců.

Závěr: Vzhledem k rozdílné expresi proteolytických enzymů v TgHD mozcích, další studie budou zapotřebí pro objasnění přesné role těchto enzymů v etiologii HN.

Klíčová slova: proteolytické enzymy, transgenní zvířecí model, Huntingtonova nemoc, biochemie, imunohistochemie

TABLE OF CONTENTS

1 INTRODUCTION

Huntington's disease (HD) is a hereditary progressive neurodegenerative disease with an autosomal dominant pattern of inheritance and the onset of clinical symptoms about 30 to 50 years.

The earliest symptoms are changes in mood, with the development of the disease appears cognitive impairment, depression, disturbances of motor function with characteristic choreatic movements and in subsequent stages there is an overall personality disintegration (Munoz-Sanjuan *et al.* 2011).

Prevalence is reported to be between 3 to 10/100,000 inhabitants and is characterized by geographical differences, the higher is recorded in Europe and in countries populated by Europeans (Canada, America, Australia). Nevertheless, in Japan and other Far Eastern countries, as well as in Africa, HD cases are also recorded. Due to problems with diagnosis of the disease, it may be difficult to get clear and exact statistical data. According to a study released by Evans *et al.* in 2013, more than a double increase of the prevalence of HD patients has appeared between 1990 and 2010 in the UK, from 5.4 to 12.3 patients (calculated per 100,000 population), while the most significant increase was observed in the age group of 51-60 years. More accurate diagnosis, better treatment and associated prolonged life expectancy might be the factors behind the increasing prevalence of HD in the population. Also, a greater willingness to record HD ongoing electronic health cards plays a role in this increase. Exact number of patients is not known in the Czech Republic, but it is assumed that there are about 1000 (Harper *et al.* 2002).

1.1 Pathological features

HD is characterized by damage of striatal projection neurons. Firstly, GABAergic neurons producing enkephalins, which are stored on D2 dopamine receptors. Subsequently appears the degeneration of neurons with dopamine D1 receptor, producing besides GABA also substance P. Interneurons are not damaged so much. The cell loss is manifested as atrophy of the striatum, which is observable by imaging methods such as CT or MR. Besides striatum, demage of other structures of the brain (e.g. cerebral cortex) occurs in the later stages of the disease. These lesions are often associated with an

increased proliferation of glial cells, indicating the onset of certain reparative processes. The final stage is an overall brain atrophy (Aylward *et al.* 2000).

Genetic basis of the disease is a mutation of the short arm of chromosome 4, namely the region of the first exon of N-terminal Htt protein gene (4p16.3), which leads to a multiplication of CAG repeats. Subsequently, polyglutamine chain is synhesized and we talk about polyQ sequence.

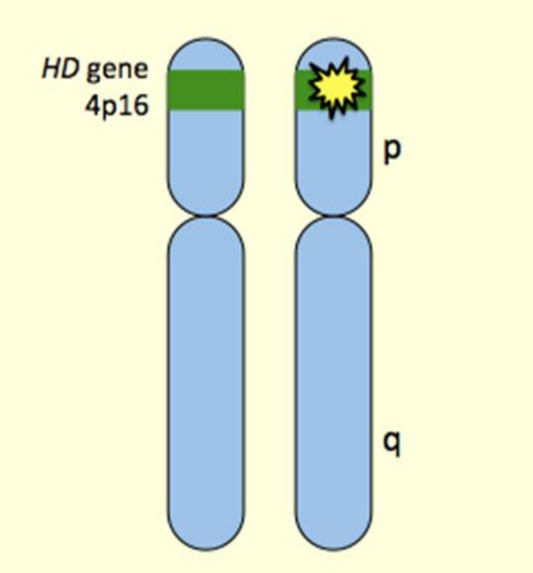

Figure 1. HTT gene located on chromosome 4p16. (Huntington's Disease 2013)

Physiologically, there are in average from 16 to 20 repetitions in the polyQ section. The unstable form of the gene for huntingtin (HTT) is in the case, when the number of repetitions ranges between 27 and 35 and this occurs with up to 10% risk of intergenerational elongation. When the number of repetitions is 36-39, the prognosis is poor, clinical features do not occur, but if so, the average life expectancy is higher than within those with number of triplets higher than 40, where an onset of clinical manifestations of HD is guaranteed (Kremer B *et al.* 1994). In addition, apart from the extension of the section there are documented cases characterized by contraction of the number of triplets (Kovtun *et al.* 2004). The relationship between the number of repetitions and the onset of clinical manifestations of the disease has been described several times so far, but only for people with a very high number of triplets (over 60) and those with a marginal number of triplets (36-39) (Andrew *et al.* 1993). An increased number of triplets is observed rather in persons with paternal transmission because of easy expansion of triplets during spermatogenesis (Wexler *et al.* 2004).

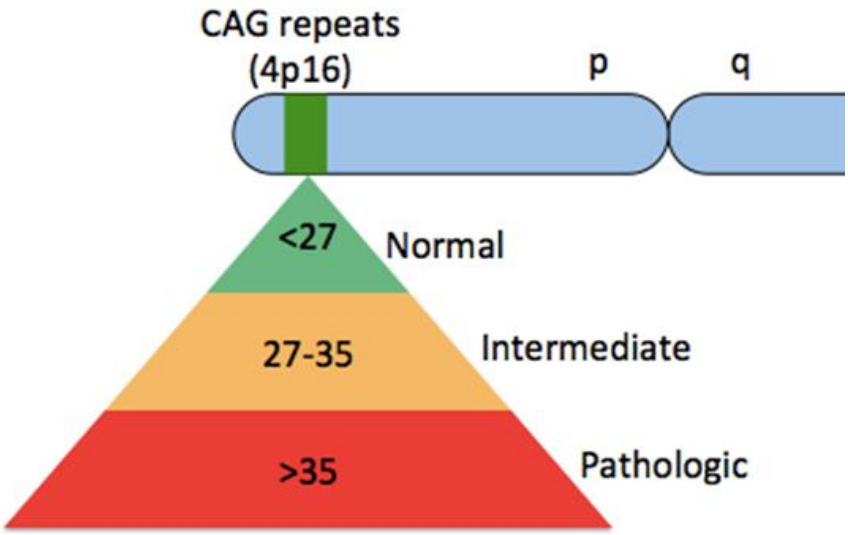

Figure 2. Expansion of a CAG-trinucleotide-repeat sequence in the HTT **gene. (Huntington's Disease 2013)**

The number of triplets is not the only determining factor of the onset of symptoms, but interacting genes polymorphism associated with Htt is also the subject of discussion as a potential factor influencing the age of onset of the disease (Leeflang *et al.* 1995). Several studies have shown the effect of TAA repeats in the 3 'untranslated region of the glutamate receptor gene GRIK2 (GluR6 gene). Other studies suggest S18Y polymorphism in gene for ubiquitin-carboxy-terminal hydrolase L1 (UCHLI) genotype ε2ε3 with apoliproprotein E, polymorphic (Gln-Ala) 38 repeat in the gene for the CA150 transcriptional coactivator and genetic variation in the subunits of NMDA receptors.

1.2 Huntingtin protein

Huntingtin (Htt) is a protein found physiologically throughout the body and its function is unknown. It belongs to ubikvitinuous proteins and is expressed in all cells of the body, mostly in a brain and testis (DiFiglia *et al.* 1995). It is found in the cytoplasm in neuronal cells. Htt participates in transcription processes of axonal transport and is involved in many interactions with other proteins (Borrell-Pagès *et al.* 2006). There is a relationship between Htt and BDNF (brain derived neurotrophic factor), which is the supporting factor in the development of cells within ontogenesis (Zuccato *et al.* 2009). Htt is probably also involved in apoptotic processes. It is a protein, which is completely indispensable for the body. Total loss of the Htt gene (called knock-out) in animal mod-

els has led to a significant failure of neurogenesis incompatible with survival (Zeitlin *et al.* 1995).

As mentioned above, section of CAG repeats are multiplicated, subsequent protein synthesis of long polyglutamine sextion called polyQ chain occurs and we talk about mutated form of Htt (mtHtt). This increase in CAG repetitions is responsible for the pathological protein conformation forming beta-sheet, which does not occur physiologically. Due to a mutation of the protein, its function is changed, which conveys toxic consequences. The pathogenesis associated with mtHtt is still under investigation, but excitotoxicity, oxidative stress, apoptotic processes, activation of microglia, mitochondrial dysfunction, defect in neurogenesis (Roth *et al.* 2009), as well as disorders of axonal vesicular transport, disturbances in postsynaptic signaling and transcription disorders (Gil *et al.* 2008) are considered as the main that contribute to this process. It is also expected, that pathological Htt has a negative effect on ubiquitin-proteasome system (Petrucelli *et al.* 2004) and lysosomal system (Ravikumar *et al.* 2002). The mutant Htt tend to aggregate due to its conformation and defects in proteolytic systems and Htt inclusions are found in the later stages of the disease in the nuclei of neurons, while Htt aggregates are found in the cytoplasm of cells. Function of aggregates still has not been fully understood. Despite initially presumed toxic function, the hypothesis about gain of function, when toxic aggregates are supposed to be created as protective elements against the harmful effects of free and intermediary forms of Htt, has appeared in more recent studies. According to some studies, neurons without inclusions and aggregates die faster than neurons with these formations (Saudou *et al.* 1998).

1.3 HD animal models

When a mutation causing development of HD is inserted to the genome of various organisms, then they can share some pathophysiological mechanisms and cellular processes with humans.

Scientific research possibilities rely on the availability of suitable animal models that provide insight into genetics and the pathophysiology of the disease. From identification of the gene responsible for HD, several animal models of this disease have been developed. Large animal models, such as domestic livestock, offer some significant advantages compared with rodents including bigger brain that is accessible for viewing and intracebral therapy, longer life, or similar morphology and organ function. But the most common question is, which of these models recapitulates the human disease the best way.

The most frequently studied animal models are rodents, but there are also used non-mammalian models of HD such as Caenorhabditis elegans, Drosophila melanogaster and zebrafish Danio rerio, which belong to intervertebrates and allow s rapid testing of specific hypotheses and new therapeutic strategies (Brignull *et al.* 2006). These animals recapitulate human disease in many ways and their undoubtable advantage is the prize and ease of their breeding, as their lifespan is quite short and allows have a large number of animals. However, a further evaluation of processes causing HD are essential for a development of new therapeutic approaches and this finally leads to a creation of more complex models of the disease (Ramaswamy *et al.* 2007).

1.3.1 Mouse models

The dominant character of gene mutations in HD allowed to easily create genetic models in several species carrying the mutation, which cause abnormal neurological phenotype in all animals expressing the mutation. Knock-in mouse and rat models were created by inserting either abbreviated or full-length forms of the mutated gene for Htt specifically into the gene locus for Htt, or these forms of the mtHtt were inserted randomly (transgenic models).

Transgenic models

R6/1 and R6/2 transgenic mice models were firstly characterized by Bates (Carter *et al.* 1999) and they still have been the most widely used transgenic mice models (Mangiarini *et al.* 1996). Well described and the most often used model is the R6/2 mice model bearing 144Q. This model is characterized by progressive physical deficits, rapid weight loss and learning and memory disorders (Ramaswamy *et al.* 2007). The large number of repetitions in the model R6/2 corresponds to the juvenile type of HD symptoms in humans. For some R6/2 mice it is known that the symptoms occur by 4 weeks, even though the average time of onset of symptoms is from 9 to 11 weeks. The average lifespan of animals is about 10-13 weeks, rarely they can survive more than 14 weeks. Mice R6/1 carry less CAG repeats than mice R6/2, and therefore we observe milder symptoms, later onset of the disease (about 13 to 20 weeks) and a longer survival time, usually more than year. This transgenic model is not used as frequently as a model R6/2 and that is why has not been so well described. Borchelt *et al.* (1999) created N171-82Q transgenic mice model expressing the 171 N-terminal amino acid of the human Htt under control of the mouse promoter whose fragment contained 82 CAG repeats. Therefore, the lower number of repeats, the later onset of symptoms occur (in months) and the individuals die around 5th month of life (Schilling *et al.* 1999). The lateness of the symptom onset and the striatal degeneration is the main advantage making this model attractive for studies of presymptomatic therapy.

Knock-in models

Creating knock-in mice involves replacing a part of the mouse gene for the Htt by human mHtt copy containing an expanded part of CAG repeats. These mouse models face later onset of behavioral and neuroanatomical changes. However, they do not have their behavioral problems so distinctive as transgenic models do (Ramaswamy *et al.* 2007).

Conditional models

The group of Yamamoto *et al.* (2000) created a conditional mouse model of HD, where it is possible to inactivate the mutated gene by tetracycline lodged in the diet. Surprisingly, the decline in Htt aggregates and the amelioration of clinical symptoms were observed on animals after inactivation (Yamamoto *et al.* 2000). The availability of

numbers of different mouse models of HD provides powerful tool for preclinical testing of therapeutical strategies as mice share the similar genetic background and the lenght of CAG repetitions with humans. Additionally, therapeutics could be tested on animal models before the onset of clinical symptoms and the data could be gained relatively quickly due to the short life span of mouse animal models (Rubinsztein *et al.* 2002). However, the small size of their brain and the difference in its architecture in comparison with humans are the reasons that do not allow use these models for detailed neuroanatomical characterization associated with HD (Zuccato *et al.* 2010).

1.3.2 Large animal models of HD

Huntington's disease is a late-onset disease. The short duration of life of rodents has resulted in very early signs and symptoms of the disease and a long-term research is not possible. Therefore, mammals are suitable for this particular research. With their long life they are great representatives for long-term monitoring of behavioral and motor changes, neuroanatomical characterization and testing of presymptomatic therapy (Jacobsen *et al.* 2010). Another advantage of the large animal models is the possibility of using non-invasive in vivo imaging techniques such as PET (Positron Emission Tomography) and MRI (Magnetic Resonance Imaging) to detect anatomical changes (Jacobsen *et al.* 2010). Currently, domestic sheep (Ovis aries L.), miniature pig (Sus scrofa domesticus), and primates (genus Macaca) lie under the main investigation. Phylogenetically, primates are the closest relatives of humans, they have similar genomes and structure of the brain as humans have and therefore represent a unique animal model for the study of pathogenesis and progression of disease. There are only few groups handling with primates as models of HD, among them Chan *et. al.* (unpublished) with a group of HD and control individuals of Macaque rhesus (Macaca mulata). They have a long time study of cognitive and behavioral deficits using MRI (Chan *et al.* unpublished). Another group around J. McBride works with Macaque rhesus model holding one goal, searching markers and symptoms of the disease (McBride *et al.* unpublished). However, work with primates renders certain difficulties. Animals have motoric, but also cognitive and psychical symptoms, which could be a real ethical problem. Also, breeding of primates is supposed to be in a monkey colony, and this is not possible in a case of HD, when the disease inquire an isolation of HD individual and this altogether can lead to a deprivation of primates.

Domestic sheep is a suitable model for pharmacological testing associated with surgery and transplants because sheep brain is similar to human forebrain (Jacobsen *et al.* 2010). Also, sheeps share a similar body weight and body systems. It makes them a good model for studying of reproducion, respiratory and cardiovascular physiology, etc. Furthermore, sheeps have a good memory and the ability to learn and also the gene for Htt coincides with sheep one in 88% of nucleotides of the Htt (Jacobsen *et al.* 2010). Therefore, J. Morton and her team provided several cognitive tests, which were very similar to tests on humans (Morton *et al.* 2013).

Great potential for the study of human disease has minipig model with short generation interval and larger number of offspring. Thanks to a long period of life and relatively undemanding breeding, this model allows study of preclinical (asymptomatic) stage of the disease and testing of new drugs. A brain of minipig is in its size, complexity and cognitive circuits similar to human one. Recent progress has been documented in defining the porcine genome (Archibald *et al.* 2010), porcine single nucleotide polymorphisms (Ramos *et al.* 2009), microRNAome (Kim *et al.* 2008) and improved techniques for genetic modification of pigs (Hofmann *et al.* 2003). The porcine homologue of the HTT gene has a large ORF of 9417 nucleotides encoding 3139 amino acids with a predicted size of 345 kDa (GenBank, Accession No. AB016793). There is a 96% similarity between the porcine and human HTT genes (GenBank, Accession No. AB016794). CAG repeats have polymorphic signs in porcine HTT gene and vary from 8 to 14 units. As well as in humans, porcine HTT consists of two trancripts of approximately 11 and 13 kb (Matsuyama *et al.* 2000). The close similarity between porcine and human HTT genes and proteins is another reason for using the minipig model. Altogether, it makes minipigs an ideal model for HD research (Swindle *et al.* 2012). Recently, team around Yang *et al.* (2010) published work about generating transgenic HD pigs that express N-terminal (208 amino acids) of mHtt with an expanded polyQ tract (105Q). Primary porcine fetal fibroblast cells expressing N-terminal mutant Htt fragments were used for the nuclear transfer, and pig eggs containing these nuclei were developed to early embryos that were then transferred to surrogate pigs to produce newborn pigs.

Although all five newborn trasgenic pigs appeared normal at birth, three of them were unable to gain weight and died several hours after birth. Another trangenic pig

lived for 25 days and then died prematurely. Only one piglet was still alive (4 moth old at that time, no more recent data). Interestingly, expression of mutant Htt resulted in more neurons with activated caspase-3 in transgenic pig brains than in transgenic mouse brains (Yang *et al.* 2010).

Another team working with this animal model is a group around Jan Motlik at the IAPG of AS CR (Institute of Animal Physiology and Genetics, Academy of Sciences, Czech Republic) in Liběchov.

Liběchov minipigs from IAPG

The IAPG in Liběchov imported the first miniature pigs in 1967 from the Hormel Institute at the University of Minnesota (two boars and three sows) and from the Institute for Animal Breeding and Genetics from the University of Göttingen (two boars and four sows). Subsequently, breeding, animal health and their body shape have been thoroughly controlled and oubreeding conditions maintained by import of several additional boars from Göttingen (Vodicka *et al.* 2005). The animals were bred at about 5 months of age when they reached sexual maturity. At this stage they weigh about 12-15 kg. In our minipig colony the life expectancy is unknown, because of maximum 8-year housing of animals. However, the survival of parental minipig breeds (Hormel and Göttingen) has been reported to be from 12 to 20 years. Animals in Liběchov breeding are mainly white and adults weight about 60-75 kg.

In 2009, the IAPG of AS CR Liběchov made the first attempt to create a transgenic minipig as a model of HD.

N-terminal fragment of human Htt was prepared from a plasmid comprising cDNA pFLmixQ145 145 CAG/CAA repetitions. The nucleotide sequence for the first 548 amino acids including the 145 glutamines has been associated with HD promoter and introduced into a plasmid carrying CPPT pHIV7 (central polypurine tract) and WPRE (Woodchuck hepatitis post-transcriptional regulatory element) of cis-enhancing element. Co-transfecting HEK293T cells with this plasmid were obtained from lentiviral vector carrying the designation pHIV1-HD-548aaHTT-145Q. This vector was injected by microinjection into single-celled embryos perivitelline space. The embryos were cultured in vitro to the blastocyst stage and then transferred into the oviduct of

sows laparoscopically. It has been shown that lentiviral construct does not affect the survival and development of minipigs.

The presence of the transgene was verified by PCR (Polymerase Chain Reaction) in skin cells of born piglets. Sequence-coding human HTT and WPRE area were amplified. Localization of incorporated transgene into the q arm of chromosome 1 was determined by FISH analysis (Fluorescent in Situ Hybridization) and the number of copies of the transgene integrated into the genome was determined by relative comparison between the pig's endogenous and the transgenic human Htt by quantitative PCR. PCR with primers flanking the CAG/CAA repetitions also determined the number of glutamines in transgenic Htt. It results in pigs carrying one copy of the 548 amino acids long N-terminal part of the human mutated Htt HTT1-548 (124Q), which is under the control of the human htt promoter on the long arm of the first chromosome.

This animal model of minipigs is able to naturally reproduce and transmit the introduced gene to progeny. The first transgenic minipig was gilt Adéla (Figure 3), who became the founder of transgenic minipig lines with inserted HD gene (HD-transgenic TgHD) and nontransgenic WT (wild type). The proportion of transgenic individual litters is approximately 40%. By crossing TgHD and WT minipigs, 4 filial generations (F1, F2, F3, F4) arose gradually. Boars from the F1 generation were over the first year of life andrologically examinated, then were taken into a reproductional process and stay behind the formation of the second generatin F2. Currently, we have approximately 208 minipigs, including TgHD and WT (Baxa *et al.* 2013).

Figure 3. The first transgenic minipig Adéla (TgHD) with her littermate Adam (WT). (Archiv of the IAPG CAS CR, Liběchov)

The presence of the mtHtt was demonstrated in almost all tissues of transgenic animals with preserved number of glutamines. Expression of the mtHtt is comparable to the wild-type form. The rate of transmission to subsequent generations corresponds to the laws of Mendelian inheritance. So far, all born transgenic pigs are heterozygous for the mtHtt.

Based on analyzes AGERA (Agarose Gel Electrophoresis for Resolving Aggregates) and filter retardation, the formation of aggregates of mtHtt in the brain of transgenic minipigs was demonstrated, and in nuclei of neurons were visible inclusions as one of the main symptoms of the HD manifestation. Using immunohistochemistry, it was shown that Htt is more expressed in a gray matter than in a white one. In boars, formation and quality of sperm was monitored with foundings, that the transgenic pigs at 13 months of age have a decrease in amount of sperm and also their ability to penetrate into the oocyte through zone pellucida is reduced (Baxa *et al.* 2013).

1.4 Proteolysis

One of the key mechanisms in the pathogenesis of Huntington's disease (HD) is a proteolysis of mtHtt. Some of the first studies revealed that small proteolytic fragments have particular cytotoxic characteristics. Proteolytic cleavage as a source of these breakdown products was considered as an early or initial step in HD pathogenesis (Ikeda *et al.* 1996; Mangiarini *et al.* 1996). This theory is commonly known as a toxic fragment hypothesis (Goldberg 1996; Wellington and Hayden 1997). Recent studies indicate that a mutated form of Htt and especially its small proteolytic fragments are highly toxic to neurons, which are located in the striatum and cortex, and inhibition of proteolysis of mutant Htt significantly reduces neurotoxicity. Although the mechanism of activation of proteases in HD is still under investigation, it is believed that in the early stages of the disease mutant form Htt sensitizes N-methyl-D-aspartate receptors (NMDARs) and there is an influx of Ca^{2+} ions into the intracellular space. As a result of the influx of calcium ions are activated Ca^{2+}-dependent enzymes and talk about excitotoxic action of mtHtt. In dysregulation of Ca^{2+} homeostasis in HD play a role not only ionotropic NMDARs, but metabotropic glutamate receptors (mGluRs), which are numerous in the striatal cells (Fan and Raymond 2007).

On cleavage of mtHtt involve different groups of proteolytic enzymes. HD was the first polyQ disease where the discovery of the caspase-mediated cleavage was made (Goldberg *et al.*1996).

Apart from caspases, Htt is cleaved by other proteases including aspartyl proteases, calpains, γ-secretase, lysosomal proteases, matrix metalloproteinases (MMPs) (Goldberg *et al.* 1996; Wellington *et al.* 1998; Gafni and Ellerby 2002; Lunkes *et al.* 2002; Gafni *et al.* 2004; Kegel *et al.* 2010). Caspases, calpains and MMPs belong to the most explored ones (Goldberg *et al.* 1996).

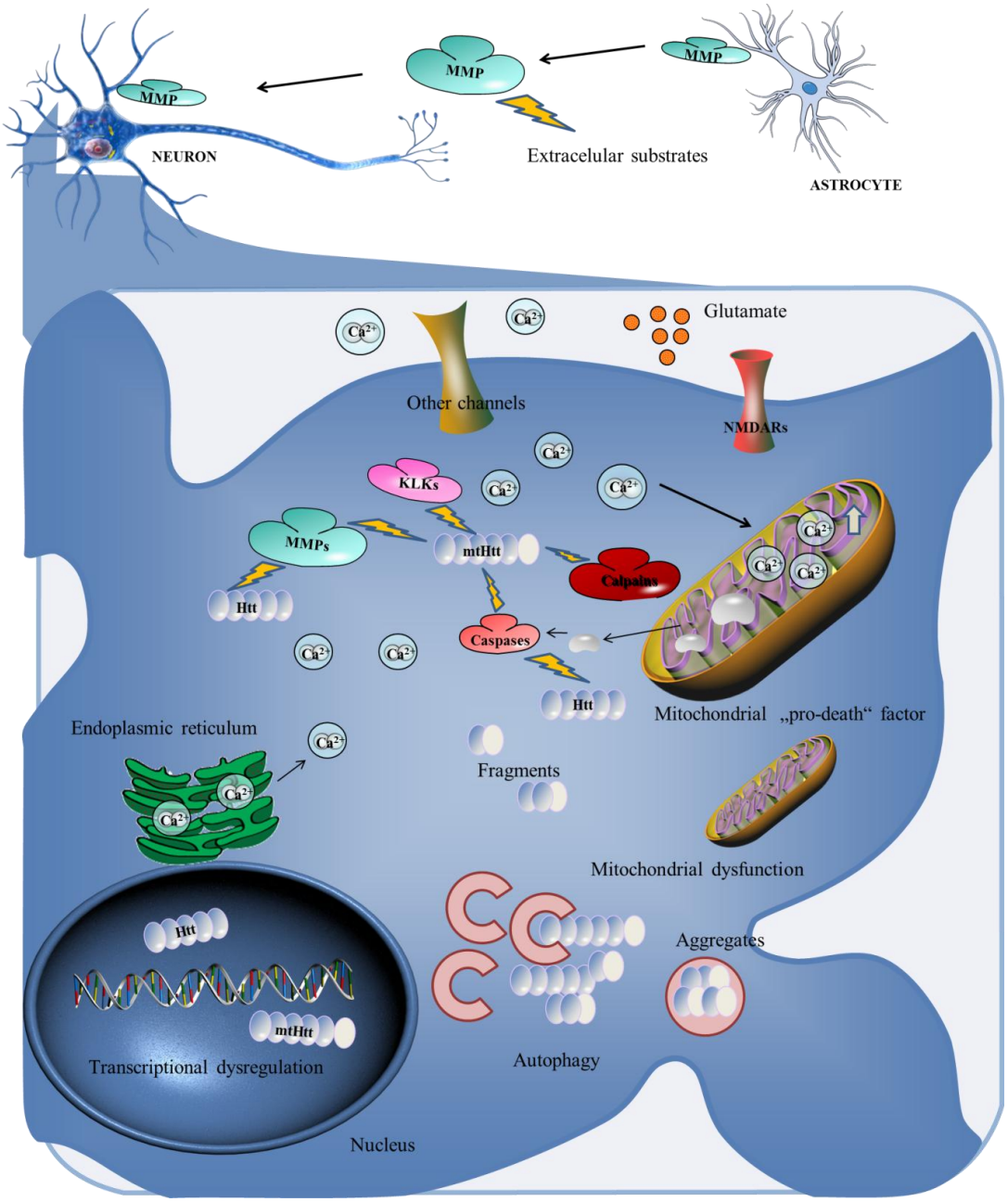

Fig. 4: Cleavage of mtHtt by various proteolytic enzymes with production of toxic fragments of mtHtt.
High concentrations of mtHtt in cell cause formation of aggregates, which undergo autophagy. Accumulation of small mtHtt fragments lead to a transcriptional dysregulation and many organelle dysfunctions. In the extracellular space, the activation of membrane-bound or secretory MMPs results in a cleavage of substrates involved in inflammation, which may also enhance the neurotoxic effect of these enzymes. (Kocurova and Ardan 2015)

1.5 Proteases

A protease means, according to a basic definition, an enzyme that hydrolyzes peptide bonds in proteins. It is considered to be roughly 2% of the human genome or about 700 individual structures with proved or putative proteolytic activity (Goldberg *et al.* 1996). Proteases share some signs as an ability to catabolize proteins, but they also have many other attributes, which distinguished them from one another. They may differ in their size, localization, quaternary structure, and are sorted into families for simplification. In human bodies, there are five groups of proteases including aspartyl, cysteine, metallo, serine, and threonine proteases, and enzymes are divided into them on the basis of catalytic activity. Cysteine, serine, and threonine proteases use nucleophilic active-site residues to hydrolyze peptide bonds, aspartyl and metalloproteases to activate water molecules using active-site residues and promote nucleophilic attack (Graham *et al.* 2006). Some biological processes require proteolytic activity such as development, differentiation, or the immune response (Baumgartner *et al.* 2009). What is very important in proteolysis is high regulation as it is an irreversible process. That is the reason why proteases are translated as inactive zymogens containing inhibitory prodomains. Once the protease is approved to be active, the prodomain must be removed. There are some proteases, which do not operate with inhibitory prodomains, and need another type of regulatory unit, e.g. cofactor binding or posttranslational modification. When the enzyme is activated, endogenous protein inhibitors change their subcellular localization and therefore the protease activity can be limited (Figure 5). Due to numerous posttranslational modifications not only conventional proteomic and transcriptomic methods are used in examination of these proteins, but also their protease activity is measured for better understanding of their biological functions (Chen *et al.* 2000).

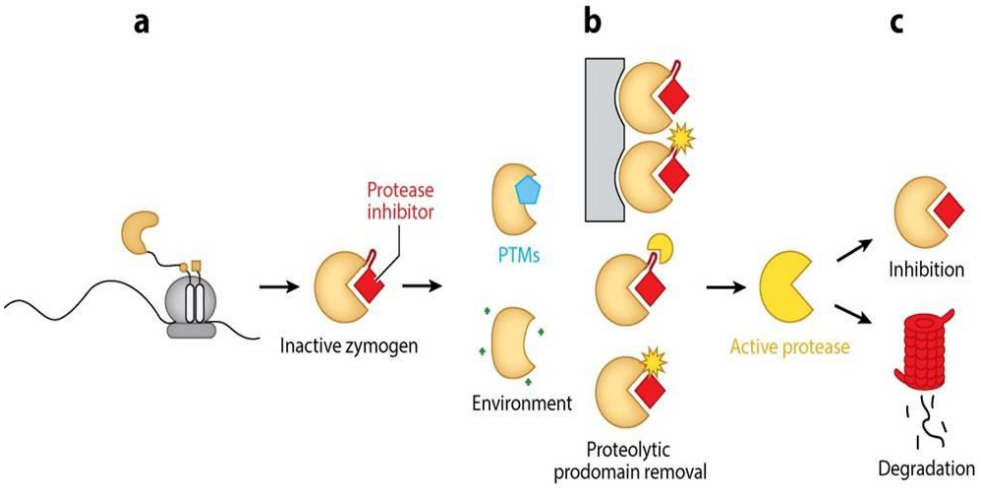

Figure 5. Activity-based profiling of proteases
Proteases are often synthesized as inactive zymogens (left) that are activated by several mechanisms including posttranslational modifications (PTMs), cofactor binding, pH change, and proteolytic prodomain removal (center). Prodomain hydrolysis (yellow stars) can occur at a macromolecular signaling complex (top), by the action of another individual protease (middle), or by autocatalysis (bottom). After activation, protease activity can be limited by endogenous inhibitors or by degradation by the proteasome (right). (Sanman and Bogyo 2014)

1.5.1 Caspases

Caspases are cysteine-aspartate proteases that are involved in processes associated with apoptosis, cell proliferation, diferentiation and migration, or inflammatory reactions. Caspases are involved in cell death mechanisms and the presence of cell death and caspase activation was observed in human HD brain as well as in mouse and cell models of HD (Chen *et al.* 2000; Hermel *et al.* 2004; Kim *et al.* 1999; Portera-Cailliau *et al.* 1995; Lunkes *et al.* 1998; Ona *et al.* 1999; Li *et al.* 2000; Zhang *et al.* 2003).

11 genes were already found to encode 11 human caspases in the human genom. Caspase 1 up to caspase 10, and caspase 14. They dispose a couple of features distinguishable from other proteases. Caspases are synthesised as inactive proenzymes consisting of a prodomain, a large (p20) and a small (p10) subunit.

The classification is based either on their mayor function–differentianted into pro-apoptotic caspases subfamily and pro-inflammation subfamily, or on the length of their prodomains– divided into groups of initiator and exucution caspases, which correspond to their positions in their apoptotic signaling cascade. Initiator caspases activated within the programmed cell death are dependent on stress and cell type and organize a highly efficient proteolytic cascade leading to the activation of caspases and sub-

sequent execution of cell death. Initiator caspases involved in the apoptotic cascade, mainly in mediating cell death signaling transduction, possess long prodomains that contain one of the two characteristic protein-protein interaction motifs: the death effector domain (DED) or the caspase recruitment domain (CARD) and interact with the upstream adapter molecules. The group of initiator caspases include caspase-2, -8, -9, -10, and to form the active dimer the activation is required. Among execution include caspase-3, -6, -7, and shaping the active heterodimer requires proteolytic cleavage, which is typically secured by upstream proteases. They perform downstream execution steps of apoptosis by cleaving many cellular substrates. This upstream and downstream relationship is not permanent and absolute and may only exist transiently in very early phases of apoptosis.

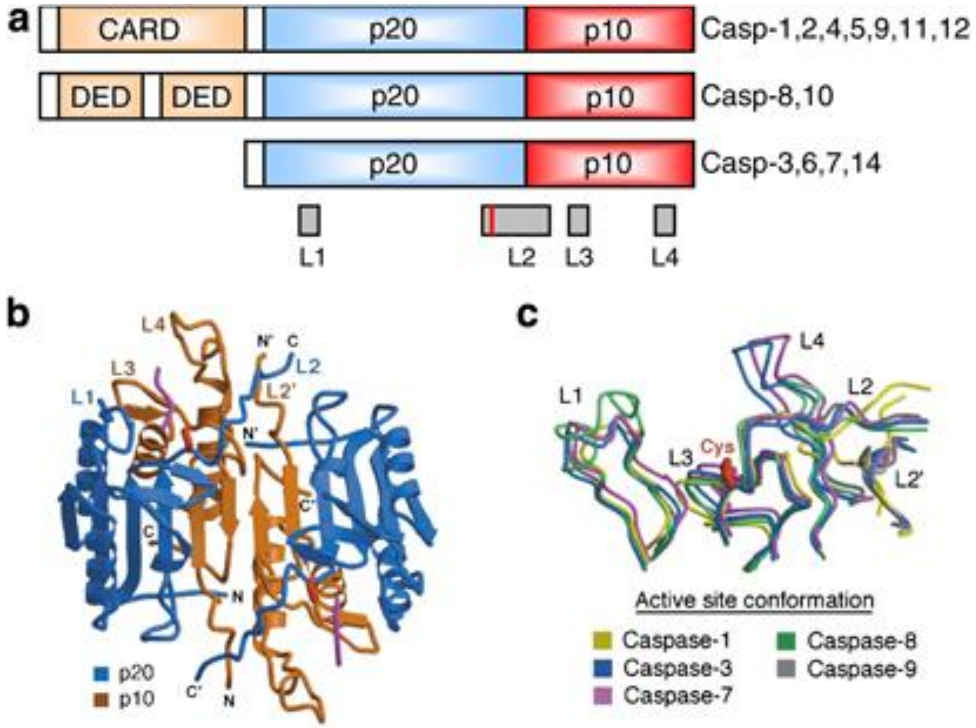

Figure 6. Structure and domain organization of mammalian caspases.
(a) Domain organization of caspases and the location of catalytic center loops (L1-L4). Initiator caspases have long prodomains, CARD or DED, whereas executioner caspases have short prodomains. Loops are shown in gray. The active site Cys is shown by a red line. Processing that separates p20 and p10 subunits occurs in L2. The resulting large subunit potion of the L2 loop of one monomer and small subunit portion of the L2 loop of the neighboring monomer (L2´) are involved in loop bundle formation (band c). (b) Ribbon representation of the active caspase-3 structure showing the positions of the active center loops (L1-L4, L2´) based on the crystal structure of the complex of caspase-3 with peptide inhibitor (in pink). (c) The active site conformations of the caspases with known structures. Loops L1 and L3 are highly conserved, whereas L2 and L4 are responsible for the differences in substrate binding specificity. (Li and Yuan 2008)

Because of these distinct roles, also the activation mechanisms are different. The upstream caspases require proximity-based dimerization for activation and the cleavage of their intradomain linkers to get the stabilization of the molecule. There are various types of apical caspases activation and they differ depending on the pathway in which a particular caspase operates. For instance, caspase 2 is activated by cytotoxic stress at the PIDDosome, extrinsically triggered apoptosis activates caspase 8 at the death-inducing signaling complex (DISC), whether caspase 9 is activate during intrinsically triggered apoptosis at the apoptosome. Caspase 1 is activated by self-association as part of the "inflammasome", which forms in response to inflammatory stimuli. In such a manner, many apoptotic stimuli can converge upon effector caspases to elevate proteolytic signaling and apoptosis. Upstream caspases need both cleavage and dimerization for proper signaling, which is one of the safety requirement how cells defend against spurious activation of death signaling. Among crucial regulators the apoptotic caspase pathway belongs X-linked inhibitor of apoptosis (XIAP), which directly binds and inhibits the initiator caspases 3, 7 and the executive caspase 10 activity. This way XIAP can counteract an apoptotic signal by blocking both of these caspase ways of effect. On the other hand, the regulator protein SMAC (second mitochondrial derived activator of caspases) can counteract this blockade restoring the activity (Mace *et al.* 2014).

Pro-inflammatory caspases (caspase-1, 4, 5) regulate cytokine maturation in inflammation (Li and Yuan 2008).

It has been reported in literature that almost 400 substrates are cleaved by caspases up to now. As mentioned above, one of the substrates of caspases is Htt protein (Lüthi and Martin 2007). It was the first neuronal protein identified as a substrate for caspases mediating cleavage (Goldberg *et al.* 1996). Cleavage of mHtt produce toxic polyQ fragments-containing sequence and its accumulation can lead to activation of other caspases and subsequent cell damage. Cleavage site is located in the N-terminal region between amino acids aa460 and aa600.

Some studies have defined the Htt cleavage sites for caspase-3 at amino acids (aa) Asp-513 and Asp-552, for caspase-2 at aaAsp-552, and for caspase-6 at the IVLD aa Asp-586 site (Wellington *et al.*1998, 2000; Hermel *et al.* 2004). Caspase-6 binds to Htt and dominant-negative caspase-6 blocks HD striatal neuronal degeneration (Hermel

et al. 2004). Further, the processed form of caspase-6 can be found activated in mouse and human HD striatum (Hermel *et al.* 2004; Graham et al 2010).

The resulting fragments are different in length and distribution in the cell. The fragments resulting from cleavage by caspase-2 and -3 of 75 kDa and 70 kDa are localized perinuclear, whereas highly toxic fragments formed by cleavage of a caspase-6 are accumulated in the nucleus. Also, TgHD murine models have shown toxicity other fragments: exon 1 Htt fragment (R6/2 mice) and aa171 Htt N-terminal fragment (N171-82Q mice) (Huttenlocher *et al.* 1997).

Although cleavage mtHtt probably plays an important role in the pathogenesis of HD, it is possible that not all fragments are toxic.

Recent studies suggest that the cleavage of caspase-6 in the position Asp586 is considered especially important for the pathogenesis of HD. It was proved in a YAC128 mouse model genetically modified to express caspase-6-resistant (C6R) whole form of human mHtt. Mice expressing C6R mHtt did not develop striatal neurodegenerative symptoms and were protected from motor deficits and the depressive phenotype observed in HD mouse models. Moreover, neurotoxicity caused by multiple stressors such as NMDA, quinolinic acid and staurosporine was not presented (Graham *et al.* 2010).

Improvement in HD mice phenotype has been found when caspase 6 is blocked, as well as in the case of using pharmaceuticals blocking activity of caspases. The most recent investigation described ED11, a novel peptide inhibitor based on the Htt caspase-6 cleavage site (aa550-560). ED11 compete with Htt for the caspase-6 active site and thus reduce Htt cleavage. In experiment of Aharony *et al.* (2015), striatal extracts from BACHD mice were incubated with caspase-6 in the presence of ED11.

Interestingly, the presence of Htt fragments is consistent with cleavage at amino acid Asp-586 of Htt in the BACHD Casp6−/− mouse was showed in a study by Gafni *et al.* (2012), indicating that caspase-6 activity cannot fully account for the generation of the Htt586 fragment in vivo.

1.5.2 Calpains

Calpains are a family of Ca^{2+} -dependent intracellular cysteine proteases including μ- and m-calpains. Both types are heterodimers consisting of a larger 80 kDa catalytic and a smaller 28 kDa regulatory subunit. The large subunit differs between members of a protein family and is active even without the small subunit. The transition to the active state μ-calpains sufficient levels of calcium ions in the order of micromolar, while the m-calpains require Ca^{2+} values in the order of millimoles. Binding of Ca^{2+} ions leads to autolytic process and the catalytic subunit in the case of μ-calpain cleaved from originally 80 kD protein to a large protein of size 76 kDa, in the case of m-calpain subunit is cleaved to 20 kDa regions. Regulatory subunit, which is common to both forms of calpain, is from the original 28 kDa truncated to 21 kDa. Activation of calpain is mediated by many apoptotic and necrotic stimuli. Physiological function and possible differences between the two μ- and m-calpains are yet unclear. It is assumed their participation in both the division and migration of cells (Kulkarni *et al.* 1999), and integrin-mediated signal transduction and apoptosis (Wellington *et al.* 2000). While Htt is cleaved by caspases into fragments of molecular weight 70, 75 and 80 kDa (Graham *et al.* 2011) calpains produced smaller fragments (62, 67, 72 kDa). Extent of the cleavage Htt is in direct proportion to the length of polyQ chain. Calpain activation was confirmed in human tissues HD patients. The total amount of activated and non-activated calpain is increased in HD patients compared with controls (Gafni *et al.* 2004). Lower concentrations of calpain produced fragments with molecular weights 67 kDa and 62 kDa, and in higher concentrations appear cleavage products with a length of 47 kDa. As mentioned above, the μ-calpains and m-calpains cleave Htt in the same places, but at different intracellular Ca^{2+} concentration: μ -calpain cleaves Htt in the presence of calcium ions at low concentrations (3 mM) and m-calpains only at high concentrations (10 mM). Also self-activation of calpain is influenced by Ca^{2+} homeostasis. Preincubation with calpain inhibitor 1 leads to complete blockage of Htt cleavage of both types of calpain. By using an inhibitor of Ca^{2+}/Mg^{2+}-ATPase of the endoplasmic reticulum, the Ca^{2+} ion levels increase inside the cell and there is a higher level of 28-kDa calpain regulatory subunit.

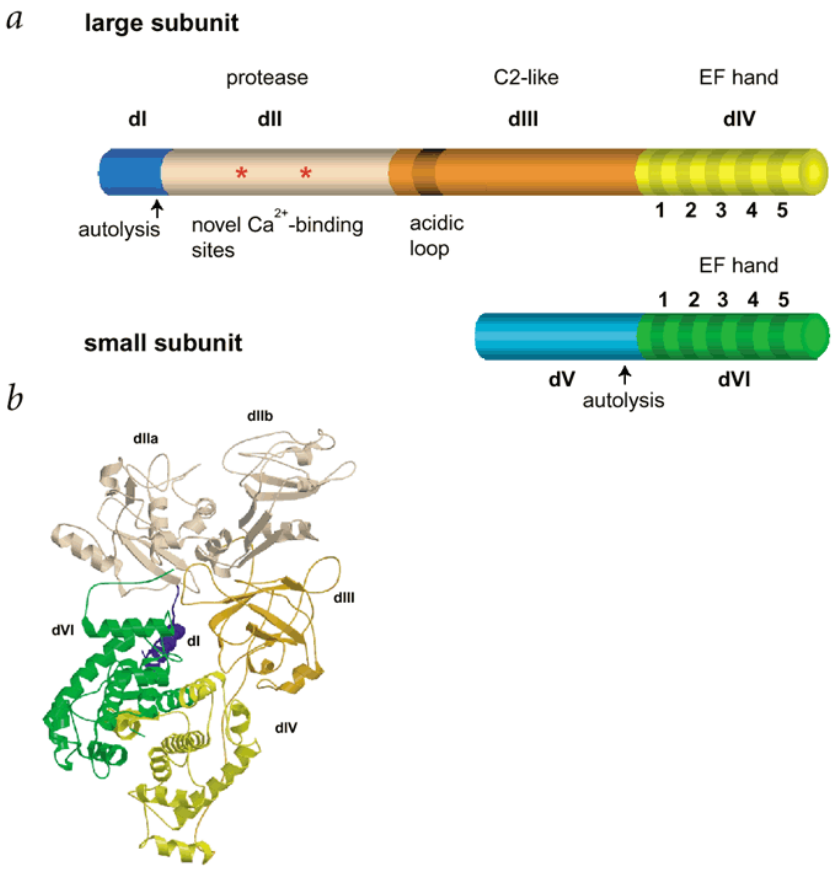

Figure 7. Schematic diagram of human m-calpain.
a, Schematic representation of the domain structure of the large and small subunits of m-calpain. Novel Ca^{2+}-binding sites in their structure of a mini-calpain, are depicted by asterisks and sites of autolysis by arrows. *b*, Ribbon drawing of m-calpain in the absence of calcium[6] (Knorchid and Ikura 2002)

Levels of Htt fragments increase after cleavage by caspase-2 and -3, representing about 5 % of the total number of fragments. The residue is cleaved by calpain and other proteases. Gafni *et al.* (2002) confirmed that most of the fragments of a size of 72 kDa, in the case of mutant Htt length 15Q, or 82 kDa in mutant Htt with 135Q. The cleavage site of calpain was determined by using deletion analysis at position aa535-537 (serine-serine-serine). Once the position was deleted, there was a reduction of 72 kDa grafts. Amount of 67 kDa fragments was reduced by deletion at aa468-470 (leucine-threonine-alanine). Although the cleavage site of Htt characteristic for the formation of 62 kDa fragment was not specified, it is not so significant deficiency, because such large fragments represent a minority of the total number of fragments. Fragments of Htt 138Q-(1-1212) were reduced compared to Htt fragments 15Q-(1-1212) thanks to the accumulation of polyQ Htt in stacking gel. Elimination of production of specific grafts has led to further reduction in Htt proteolysis, when the amount of

both low molecular weight fragments (probably arised in aspartic protease cleavage) and Htt aggregates was diminished (3.7× less).

The presence of the Htt fragments in the cell nucleus correlates with the cytotoxicity, which may be increased by activation of the cellular localization signals and decreased by activation of cellular export signals. The whole form of Htt contains naturally occurring export signals which enable it to pass from the nucleus to the cytoplasm, and vice versa. Most Htt is in the cytosol (> 95%). It is noted in many studies, that the requirement for entry into the nucleus is fragment size lower than 50 kDa. These conclusions are based mainly on immunofluorescence analysis of Htt aggregates, but not for subcellular fractionation. It is necessary to clarify, whether the fragments can be transported from the cytoplasm to the nucleus, and vice versa, and whether a small percentage of Htt normally occurring in the nucleus also undergoes cleavage. Calpain- and caspase-cleaved Htt fragments accumulates in the cytoplasm and nucleus at the size of 72/82 kDa and especially in the nucleus at 67/77 kDa.

Characterization of calpain is not as advanced as for caspases. Three out of fifteen enzymes calpain family, calpain-1, calpain-2, and calpain-4, were already largely studied, the other three - calpain-5, 7-calpain and calpain-10 are known for their high expression in brain tissue, thus their role in the Ca^{2+}-mediated pathogenesis is presumed, which is also confirmed by the increased level of mRNA in the R6/2 mouse model of HD. Both active and inactive form of calpain-2 were found primarily in the cytoplasmic fraction, calpain-7 and calpain-10 had its inactive form localized both in the nucleus and in the cytoplasm, while the active form only in the nucleus, and both forms of calpain-5 were present in the cytoplasm and the cell nucleus. Thapsigargin is a drug selectively inhibiting sarco-endoplasmic Ca^{2+}-ATPase, resulting in a large increase in intracellular Ca^{2+}. After application of thapsigargin, the regulation of calpain-activation was confirmed. Semi-quantitative PCR revealed an increased amount of transcripts calpain-5, -7 and -10. The higher levels of proteins and their active forms were also observed (Gafni *et al.* 2002).

1.5.3 MMPs

Matrix metalloproteinases (MMPs) are zinc-dependent proteolytic enzymes that are involved in many physiological and pathological processes. Above all, they are known for their involvement in the degradation of extracellular proteins, but their importance is much greater because the substrates find chemokines, cell receptors, cytokines and growth faktors (Miller *et al.* 2010). Along with adamalysin, serralysins, fragilysins and astacins belongs to the large family of Zn-dependent metalloproteinases called metzincins. Most MMPs contain a characteristic sequence HEXXH, which interacts with zinc (López-Pelegrín *et al.* 2015). There are more than twenty MMPs, which occur in humans.

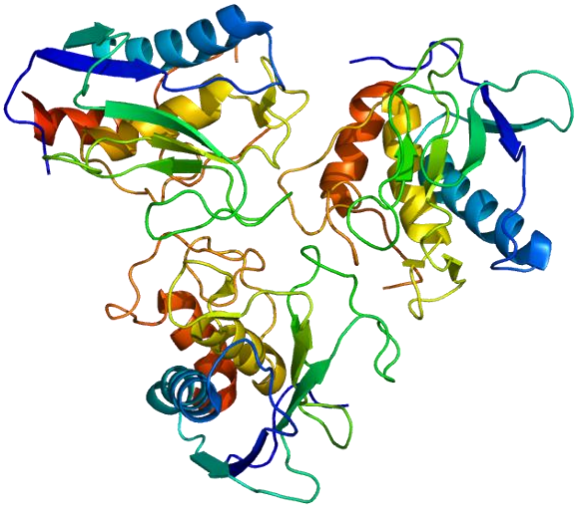

Figure 8. Structure of the MMP-10 protein. (Emw 2009)

An extensive study mapping the proteolytic enzymes responsible for elevated levels of a small 48 kDa N-terminal fragment of mtHtt was published by a group of Miller *et al.* (2010). In a screening of 514 siRNA all known human proteases, 41 proteases were identified affecting accumulation of Htt fragments, while 11 of them were confirmed by retesting. Among the proteases were three MMPs (MMP-10, MMP-14, MMP-23B) (Krawitz *et al.* 2005). This study demonstrates an increased activity of these enzymes both in cell cultures and animal models of HD. MMP-10 was shown to be involved in the direct cleavage of Htt, while MMP-14 and MMP-2 were not. In a subsequent study, the effects of MMPs on cell toxicity confirmed, that the knock-down (inhi-

bition of gene expression) significantly reduces neuronal death in striatum. Using NNGH (N-isobutyl-N- (4-methoxyphenylsulfonyl) glycyl hydroxamic acid), a pharmacological inhibitor of MMPs, as well as endogenous inhibitors TIMP1, TIMP2, TIMP3, led to a blocking of Htt-mediated toxicity in Hdh111Q/111Q cells. We also recorded in those cells 5.7× higher incidence of cleaved forms of MMP-10 compared to Hdh7Q/7Q cells. Nevertheless, this did not mean that also levels of activated MMP-10 are increased in cells with mtHtt, analysis using the enzyme with fluorogenic substrate was performed. Results of the analysis confirmed a significant increase in the activation of MMPs in Hdh(111Q/111Q) cells. Subsequently, YAC128 mice models of HD (full-length of mtHtt) and R6/2 (fragment of mtHtt) were used. The results obtained in these mouse models confirm the 1.6 to 1.8-fold increase of MMP activity in the striatum of YAC128 (age 16 months), and R6/2 (age 10 weeks) compared to healthy controls. After precipitation and subsequent zymography increased levels of activated MMPs were found in cortical and striatal lysates of R6/2 mice (in a range from 50 kDa to 90 kDa). The 50 kDa-graft corresponds to active form of MMP-10. The graft of a size of 90 kDa represents MMP-9 (92 kDa), which undergoes an activation by MMP-10 (Miller *et al.* 2010).

Although MMPs can be produced in neurons and glial cells, their co-localization with glial (GFAP) and neuronal (NeuN) markers showed, that the most of active MMPs are present in neurons. To determine whether Htt is a direct substrate of MMP-10 and MMP-14, the cell lysate expressing mtHtt was incubated with recombinant MMPs. MMP-2, which has not previously been confirmed as one of the proteases inducing proteolysis and cell toxicity, was used in this study as a control. Htt was determined as a substrate for MMP-10, but not for MMP-14 and MMP-2, in connection with finding the 48 kDa fragment in normal Htt and 70 kDa fragment in mtHtt148Q. In vitro translation of Htt15Q also confirmed this fact. All these three MMPs were equally active after adding the fluorescent substrate. Unlike a MMP-14 knock-down, a knock-down of MMP-10 directly inhibited mtHtt toxicity. Compared to the caspases and calpains, MMP-10 cleaves Htt near its N-terminus. To determine the exact cleavage site of MMP-10, Htt15Q(1-469) and Htt138Q(1-469) were incubated with MMP-10 in vitro. Molecular weight analysis of Htt15Q cleavage products specified the cleavage site at position aa414. Investigation of the amino acid sequence in the region and comparison with the known substrates of Htt showed a possible cleavage site at position aa402. The cleavage

site is within the sequence S/T XXGG I/L, which is conserved in multiple species (Barret *et al.* 2012, p775). Deletion analysis at region aa402-403 of Htt was performed to test this hypothesis, and resulted in reduction of proteolysis mediated by MMP-10. Likewise, the application of MMP-10 in the post-mortem cell lysate caused an increased level of 50 kDa cleavage product.

Although most MMP is expressed as proenzymes and their cleavage to the active form takes place outside the cell, MMP-10 cleaves Htt intracellularly. Examination of colocalization of endogenous Htt and MMP-10 showed, that these two proteins together highly colocalize, moreover in the cells undergoing cell death there is a significantly higher degree of colocalization. Colocalization is not found due to the direct protein interaction as the coimmunoprecipitation of MMP-10 and Htt was negative.

Previously known information indicates that selective inhibition of MMPs might potentially be an effective tool in the treatment of HD. For instance, knock-out mice for MMP-9 were less sensitive to cerebral ischemia, which could be directly associated with post-mortem analysis of brains of HD patients, where an increased concentration of MMP-9 was found, while in the brain of healthy people it was not (Silvestroni *et al.* 2009).

1.5.4 KLKs

Kallikreins, or kallikrein related peptidases (KLKs) forms S1 family of 15 (chymo) trypsin-like serine proteases (KLK1-15), which belongs to clan SA (Brix *et al.* 2005) and have pleiotropic physiological roles and also participate in disease states. These enzymes are encoded by 15 structurally similar, steroid hormone-regulated genes (KLK) co-localizing to chromosome 19q13.4. This part of the genome represents the largest cluster of contiguous protease genes, which is not interrupted by any non-KLK genes. The length of a single-chain of preproenzyme encoded by each KLK gene varies between 244 and 293 amino acid residues and among them there is approximately 40% protein identity (Turk *et al.*2012). The nuclear signaling regulates the expression of most KLK genes, while the activation of zymogens is under the control of multiple proteolytic cascades leading to sequential activation of multiple KLK enzymes.

Tissue KLKs are usually divided into two groups, classical and non-classical. The „classical“ KLKs group includes the first identified members (KLK1, KLK2, KLK3/PSA), whereas the rest of KLKs belong to the“non-classical“ group.

Inactive preproforms (containing a signal peptide of signal 16-30 amino acid residues) are proteolytically processed and forms inactive proforms (proKLK/zymogens). This process is accompanied by the removal of an N-terminal propeptide of 4-9 amino acids, except the KLK5, where a 37-amino acid long activation peptide is reported. Activation of proforms is executed by specific proteolytic removal of their N-terminal part through their own autocatalytic activity, or by another KLK zymogen, or other proteases, which overall leads to a sequential activation of multiple KLK enzymes. „KLK activome” term was used to signalize participation of many KLK zymogens in an activation process. It has been proposed, that more than 99 proKLK/KLK pairs might constitute the activome due to 225 possible combinations (Yoon *et al.*2007, 2009).

Invariant residues of the active-site catalytic triad (His57, Asp102 and Ser195), as well as a conserved Gly193 (human chymotrypsin numbering system) are characteristic features of KLKs. The last mentioned Gly193 plays a role in stabilizing the oxyanion intermediate of the internal peptide bond during hydrolysis (Schwabish *et al.* 2006).To their common features belong exon/intron organization, exon lengths and conserved intronic intervals.

Protein folding is enabled by five or six disulfide bonds. Two interacting β-barrels and α-helices bridged by the active site belonging to common structural features. Only KLK1, KLK2 and KLK3/PSA contain characteristic loop of 9-11 amino acid residues located ahead of the active site Asp, which convey specificity for kininogenase activity, particularly ability to release kinin from kininogen.

It was showed that KLK1-/- mice had an impaired renal Ca^{2+} reabsorption soliciting hypothesis that KLK1 could be involved in regulation of Ca^{2+} homeostasis (Duncan *et al.* 2008). Recently, KLK6 was considered to be important in pathogenesis of the central nervous system inflammation and multiple sclerosis. Also, KLK6 is profusely expressed in the EAE mouse model of multiple sclerosis, at the sites of demyelinization, and also in the lesions of patient brains (Turk *et al.*2009). Proteolysis of myelin in vitro supports a potential role of KLK6 in demyelination and/or remyelination (Asagiri *et al.*2007). Parkinson’s disease and other synucleinopathies seem to be also the diseases,

where KLK6 play a role. In a study based on foundings with cultured cells was showed, that KLK6 degrades α-synuclein and co-localizes with pathological inclusions such as Lewy bodies and glial cytoplasmic inclusions (Ceru *et al.* 2010). KLK6 upon cellular stress is released into the cytoplasm from mitochondria, where is normally stored. The released enzymes commence limited proteolysis of α-synuclein, which leads to inhibition of polymerization by reducing the amount of monomer. That all cause a prevention of the formation of aggregates, a hallmark of these pathologies (Ceru *et al.* 2010). KLK5, 7 and 14 are involved in skin diseases, especially skin desquamation and KLK2, KLK3, KLK5 take a part in seminal plasma liquefaction (Santos-Rosa *et al.* 2008). KLK3/PSA has been established as a mayor representant and the mostly used biomarker of prostate cancer for almost three decades. PSA from the beginning of the usage in 1986 as a reccurance prediction tool remains the gold standard in defining biochemical relapse. The wide application of PSA screening in asymptomatic men (approved by FDA in 1994) led to a great decrease of the diagnosed patients with advanced disease (Lee *et al.*1990; Sol-Church *et al.* 2000). Although most of the studies of KLKs as biomarkers of the disease concern human malignities, an increasing number of studies handling with KLKs and their participation in non-malignant diseases, mainly in the diseases of the CNS (Wiley *et al.* 1985; Brguljan *et al.* 2003). KLKs levels in serum or CSF (cerebrospinal fluid) are assumed to become good biomarkers for mayor CNS diseases.

1.5.5 Cathepsins

Among the approximately 50 characterized lysosomal proteolytic enzymes are particularly important aspartic, serine and cysteine proteases (Brix et al.2005).

Cathepsins are enzymes belonging to a CA clan of cysteine peptidases, more specifically, they are members of a C1 family of papain-like cysteine proteases with unique reactive-site properties and the differing tissue-specific expression pattern (Turk et al. 2012). They were discovered in the first half of the 20th century hand by hand with the discovery of lysosomes. However, not much was known about the physiological or pathological role of these proteases until the 1990s, when more clues of the functions of cysteine proteases was provided as a highlight of the physiological roles of cathepsins, as they were considered for a long time to be mainly mere scavengers (Guha *et al.*2008). Cathepsins are divided into three groups accordingly to their amino acids of their active sites that confer catalytic activity. It has been discovered 11 cathepsins of a

cysteine subfamily (the cathepsins B, C, F, H, K, L, O, S, V, X and W), two aspartyl cathepsins (cathepsins D and E), and serine cathepsins (cathepsins A and G) (Zhang *et al.* 2009). Human cathepsins require a lysosomal slighty acidic and reducing environment for their optimal functions. Therefore, these enzymes were initially considered as lysosomal/endosomal enzymes, which are responsible for the bulk proteolysis of intracelular and extracellular proteins. Recently, other localizations of cathepsins were proved, such as the nucleus, cytoplasm and plasma membrane (Turk *et al.* 2012). It was previously shown that cathepsin L variants are responsible for the proteolytic processing of the N-terminus of the histone H3 tail and also interact with the histones H2A.Z, H2B and H3 (Santos-Rosa *et al.* 2008; Duncan *et al.* 2008; Ceru *et al.* 2010). Also, a significant increase was noted in activity of aminopeptidase II, cathepsin H and cathepsin D in the caudate tissue of HD patients (Mantle *et al.* 1995). Additionally, cathepsins D, B and L affected mHtt processing and the levels of cleavage products (cp) known as A and B (Kim *et al.* 2005). Cp A formed nuclear inclusions and therefore might be involved in generating of nuclear aggregates (Lunkes *et al.* 2002). mHtt in vitro increases autophagy and the levels of lysosomal proteases cathepsin D and cathepsin L (Kegel *et al.* 2000; Qin *et al.* 2003). Proteasome inhibition stimulates macroautophagy in cultured cortical neurons and increased formation of lysosomes containing cathepsin D (Rideout 2004). Hence, this could be a reason of elevated levels of cp A and cp B due to cathepsin D mediated proteolysis of mHtt (Lunkes *et al.* 2002). When inhibiting cathepsin D, B and L in clonal striatal cells, the reduce of mHtt occured, especially mHtt fragment cp A. mHtt was fully degraded in cathepsin-L-treated lysates but formed stable N-mHtt fragment under exposure to cathepsin D. It was suggested by using mutational analysis that cathepsin D and the protease for cp A may cleave Htt in the same region (Kim *et al.* 2005). Intermediate and active forms of cathepsin D migrating at about 46 kDa and 34 kDa both in crude nuclear fractions and supernatants from clonal striatal cells expressing FH400-100Q were detected by WB analysis. One prominent wild-type N-Htt fragment and up to four fragments of mHtt protein were detected in the presence of cathepsin D. Interestingly, an increased concentration of cathepsin D also increased a formation of wild-type N-Htt, but two fragments of mHtt with the strongest signal on WB were stable in a condition of rising concentration of cathepsin D suggesting their resistance to protease degradation. However, when the aspartyl protease inhibitor pepstatin A was added, all of the N-Htt fragments that appeared in the presence of cathepsin D

did not occur (Kim 2005). Also Ratovitski *et al.* (2009) mentioned short N-terminal proteolytic fragments named cp-1 and cp-2. Using HEK293 cells expressing the first 511 residues of Htt were determined the cp-1 and cp-2 cleavage sites. Concerning cp-1, the cleavage of Htt occurred between residues 81 and 129. The finding was based on epitope mapping with Htt-specific antibodies and the further purification of Htt was performed by affinity and size exclusion chromatography. To analyse whether these fragments are corresponding to cp-A and cp-B previously described by Lunkes *et al.* (2002), who mapped the cleavage site of cp-A at the possition 105-114, the deletion of this site failed to prevent the formation of any fragment. This suggests that cp-A is distict from cp-1. Furthermore, the cp-2 fragment generated by cleavage of Htt at position Arg167 was detected using mass spectrometry, which was confirmed by deletion analysis and specific detection with a custom-generated cp-2 site neo-epitope antibody. When altered these cleavage sites from Htt-N511-52Q, it resulted in a lowering of Htt aggregation in neuronal cells.

2 AIMS

The main aims of this study were as follows:

a. Investigate the expression of Htt in WT and TgHD minipigs and compare them
b. Detect by specific antibodies (EPR5526, 1C2) Htt fragments - typical cleavage products of proteases
c. Try to detect aggregates of mutant Htt in a brain of TgHD minipigs as a consequence of proteolytic processes
d. Investigate the expression of caspases, MMPs, KLKs, calpains in a brain of TgHD and WT minipigs using immunohistochemical and biochemical methods

3 MATERIALS AND METHODS

3.1 Experimental animal

The Liběchov minipigs, model of HD carrying two alleles of porcine endogenous Htt along with a single allele of the human mtHtt, were used for our experiments. All experimental procedures were carried out in a strict accordance with Czech legislation and approved by the Animal Ethics Committee in Prague, Czech Republic.

The R6/2 mice were used in some experiments as possitive controls.

3.2 WB analysis

We examined 3 WT (K48, K64, K103) and 3 TgHD (K100, K63, K104) minipigs of F2 generation (36 month old).

3.2.1 Tissue processing

Slaughtered pig was rinsed with ice-cold PBS (phosphate-buffered saline) the brain was removed and dissected into various parts, which were snap frozen in liquid nitrogen and stored at -80 °C for following usage in a Western blotting (WB). We had two options how to subsequently handle with samples.

a. Before use, the tissue was removed from the freezer and kept for approximately one hour at a room temperature for rising the temperature up to -20 °C. Then the samples were prepared by cutting frozen tissue on the Cryo-cut (CM 1950, Leica) at -20° C into 50 slices with a thickness of 10 microns, and they were lysed immediately.

b. A piece of tissue was cut off with a scalpel and crushed in liquid nitrogen (N2). The resulting powder was divided into several Eppendorf tubes, returned to boxes with N2 and then stored until use at -80 °C.

3.2.2 Lysis

The prepared tissue sample was mixed with the range of 50ml (for small pellets) up to 300 ml (cut from large tissue) of RIPA lysis buffer (150 mM NaCl, 5mM EDTA (pH 8), 50mM Tris HCl (pH 7,4), 0,05% NP-40, 1% sodium deoxycholate, 1% Triton X-100, 0,1% SDS, inhibitors of proteases and phosphatases (Calbiotech)). Lysed tissue was vortexed (MACSmixTM Tube Rotator, Miltenyi Biotec) and then sonicated (Bandelin Sonorex Digitec, Fisher Scientific) for 10 minutes. Subsequently, lysates were

centrifuged at 10,000 G for 10 min in 4 °C (Allegra X-22R Centrifuge, Beckman Coulter) to avoid gelification, which may occur without centrifugation.

3.2.3 Protein concentration measurement

After each lysis the protein concentration was measured using BCA Protein Assay Kit 660nm (Pierce). Because RIPA buffer made some problems in measurment, a modified protocol was used, where samples are three times diluted in saline. Measurement is performed in 96-well plates. Firstly, the blank is pipetted (5 ml of saline solution + 1 ml of RIPA buffer), then the reference series of BCA in saline solution (in the kit, 3 ml + 2ml of saline + 1 ml of RIPA buffer) and finally also samples (5ml of saline solution + 1ml of sample). RIPA buffer was pipetted into a blank and a series of reference samples should correspond to the one used in the lysis buffer (the same stock and inhibitors). The samples were always meausured in duplicates and then their average was counted. In cases where samples were too concentrated (over the span of the reference range), they were diluted in RIPA buffer and then the result was recalculated. After pipetting of the samples, 90 ml of agent was added to each well (using a multichannel pipette and the dish with a groove, reverse pipetting avoided bubbles making and was performed quickly in order to preserve the same incubation time for all samples).

Consequently, the samples were incubated for 2 minutes and measured spectrophotometrically (SynergyHT, Biotek) using program Gen5 1.05 with exporting of the acquired data to Excel sheet. In Excel, the reference series values were plotted in a graph and an equation was calculated. Then the concentration of samples was calculated using the equation and the diameter of each sample absorbance value.

3.2.4 Electrophoresis

For SDS-PAGE (Sodium Dodecyl Sulfate Polyacrylamide Gel Electrophoresis) were used NuPage 3-8% Tris-Acetate (4-12% Bis-Tris) gradient gels (Life Technologies) accordingly to the kit instructions. Gels were pulled out from the bag, washed by destilated water and checked for cracks (which may have spoiled the experiment). After tracing the wells, a comb and the white tape from the bottom were pulled out, the wells were rinsed by destilated water and installed in the Novex Mini-Cell tub (Invitrogen). Running buffer was prepared from the 20× concentrated stock of NuPAGE Tris-Acetate (Bis-Tris) running buffer (Life Technologies) and destilated water, which was pre-

cooled down in a refrigerator. For analysis within one tub is needed 800 ml of buffer consisting of 40ml stock and the destilated water replenishing the rest of volume up to 800 ml. Firstly, cathode buffer was poured to the tub and 500 ml of NuPAGE antioxidant (Invitrogen) was added to avoid unwanted reoxidation of protein samples. Then an anode buffer was poured to fill the tub.

Samples were loaded in an amount ranging from 5 to 20 μg of total protein per sample (calculated by measuring concentrations). Based on volume of the less concentrated sample which was needed, the rest of samples were supplemented with a lysis buffer to the certain volume. When analysing calpain-5 expression in tissue, HeLa Whole Cell Lysate was loaded as a positive control. The appropriate amount of 4× concentrated LDL Sample Buffer with 10× concentrated NuPAGE Sample Reducing Agent was added and samples were boiled in Cooling/Heating Thermostat (BioTech) at the temperature of 95 °C for 5 minutes. After cooling, the samples were centrifuged in a tabletop centrifuge (Micro Centrifuge, Roth) and loaded on the gel together with a marker (for 3-8% gels was used HiMark, for 4-12% gels marker Dual, both BioRad). Electrophoresis ran at 150 V for approximately one hour and half.

3.2.5 Western blotting

Before blotting the equipment was cooled down for about 15 minutes (PowerPac 1000, BioRad; Fastblot B34, Biometra) using the cooling water pump (Pharmacia Biotech, AP Czech). The gel was removed from the apparatus and then incubated in a blotting buffer (Towbin 20% for smaller proteins, Towbin 10% for larger proteins) (25 mM Tris-HCl, 125 mM glycin, 0,1% SDS, 20% metanol, pH 8,1–8,4) about 15 minutes. The gel was remeasured and the nitrocellulose membrane 8×7 cm was cut out, described and the bottom left corner was cut off for later good identification. The nitrocelulose membrane (BioRad) was equilibrated along with the gel in Towbin. Then two filter papers of the same size as a membrane were cut off and soaked in Towbin. After equilibration of all components, the blotting sandwich was compiled in the following order – filter paper, membrane (in the right orientation), gel, filter paper. Excessive blotting buffer was removed with gauze, lid was carefully and properly closed with a load of about 1 liter of solution. Blot ran at 275 mA for 45 minutes (which was considered as enough time for blotting our proteins. After 45 minutes, the sandwich was dismantled, the gel and the membrane were further used.

3.2.6 Staining gels by CBBG

The gel was removed from the apparatus and "glasses" were separated using a metal spatula and gel was incubated on a shaker (Laboratory Shaker, 358S, Elpan) in a Coomassie Brilliant Blue (CBBG) G250 solution (400ml methanol, 100ml acetic acid, 1g Coomasie, destilated water) in a glass dish for 20 minutes. This solution simultaneously fixed and stained the gel, which was consequently transferred to a destain solution (800ml methanol , 200ml acetic acid) and bleached about 2 hours with an exchange of solution, or left in the solution overnight in the refrigerator. After sufficient discoloration, the gel was imposed into a plastic foil, sealed with a melter and stored in the fridge.

3.2.7 Immunolabeling

Primary antibody used were:

Rabbit-derived anti-EPR5526 (Abcam, 1:50 000)

Mouse-derived anti-3B5H10 (Sigma-Aldrich, 1:3000)

Mouse-derived anti-1C2 (Millipore, 1:1500)

Rabbit-derived anti-caspase 3 (Acris, 1:200)

Mouse-derived anti-caspase 8 (Millipore, 1:500)

Mouse-derived anti-MMP-9 (Aviva, 1:500)

Rabbit-derived anti-MMP-10 (Aviva, 1:400)

Rabbit-derived anti-calpain 5 (1:200)

Goat-derived anti-KLK10 (Santa-Cruz Biotechnology, 1:200)

Mouse-derived anti-β-tubulin (Sigma-Aldrich, 1:30 000)

Secondary antibody used were:

Donkey-derived anti-rabbit IgG (Jackson Laboratories, 1:10 000)

Donkey-derived anti-mouse IgG (Jackson Laboratories, 1:10 000)

The membrane was blocked in 5% skimmed milk in TTBS (Tris- Tween Buffered Saline) (136mM NaCl, 0,0005% Tween, 2M Tris-HCl, pH 7,6) for 1 hour and placed in Falcon conical centrifuge tube with primary antibody diluted in 5% milk. For

50 ml tubes was used usually 2-5 ml of diluted antibody, however when smaller tubes were used, volume of diluted antibody was even 1 ml. Incubation with primary antibody took place on a roller (SRT1, P-LAB) in the refrigerator overnight (or at least for one hour on the roller at RT). After incubation, membrane was washed 3× for 10 minutes in approximately 15 ml of TTBS and sodium azide was added to the Falcon with the used antibody, which preserved it and therefore it could be used for other experiments.

Then the membrane was incubated in secondary antibody (10 ml of the diluted antibody in 5% milk) at rocking platforms (the dilution ratio was 1:10,000) and washed 3× in TTBS, 10 minutes each.

3.2.8 Film development

Solutions in the darkroom (developing solution, developer and fixer) have been pulled out of the fridge about an hour before use, to get the room temperature. Solutions were prepared in appropriate containers, boxes of film were placed on the table and the red lamp was turned on. The membrane was arranged on a glass plate and doused by queuing solution Amersham ECL about 1.5 ml / membrane (mixing the equal volumes of the two solutions, mixed by pipette and spotted on the membrane), then incubated for 5 min and gently dried, followed by to plastic foil in the developer cartridge, position of foil was fixed with a scotch tape. Lower left corner of the membrane (cut off) was located in the higher left corner of the cassette, the white light was switched off and the film was cut in a size covering all membrane with cutting off the lower left corner for good orientation recognition and localization of membrane. After that the film had been attached onto the same posisiton as the membrane was and the film was developed. After removing and incubating for 1 minute in the developer (FOMA LP-T Developer concentrate for manual processing of X-ray films, Foma Bohemia), rinsing with water and incubating for about 10 seconds in fixative (FOMAFIX Concentrate rapid fixer for manual processing of X-ray films, Foma Bohemia), the lights were lit. According to the results exposure was repeated as necessary (length 1 second to 1 hour, depending on a signal strenght). After completion of exposure, the membrane and markers were traced on the film. The membrane was washed 3× in TTBS for 5 minutes and dried on a filter paper. The dried membranes were stored in envelopes of filter paper in a box in the refrigerator for further use.

3.2.9 Re-labeling with a loading control

β-tubulin antibody was used as a control of loading volume and sample concentration. Membrane was stripped in 30% hydrogen peroxide solution (Sigma-Aldrich), which provides chemical deactivation of peroxidase (Sennepin *et al.* 2009) and does not have such an harmful effect on the superficial protein layer.

After washing from the queuing solution, membrane was incubated in a Falcon tube with 2 ml of 30% H2O2 over 30 minutes at the roller at RT, washed 3× in TTBS for 5 minutes each and blocked in 5% milk for 30 minutes. Then was incubated with anti-β-tubulin antibody and handled as described previously.

3.2.10 Data scanning

Data were scanned (Scanner GS-800, BioRad) after each analysis using the program "Quantity One". The scanned images were saved in an original Quantity One format and were also exported to a .tif file.

3.3 Immunohistochemistry

In this analysis we used 3 WT (K48, K64, K103) and 3 TgHD (K100, K63, K104) minipigs of F2 generation (36 month old). For every tested animal we examined 5 coronal brain sections (40 μm thickness), one coronal section was employed for the negative (shame) control where the primary antibody was omitted.

3.3.1 Tissue processing

Slaughtered pigs were rinsed with ice-cold PBS, the right hemisphere of each perfused brain was immersed in a fixative solution composed of 4% paraformaldehyde (PFA) in phosphate buffer saline (PBS, pH 7.4) for 24h and then placed into 30% sucrose-containing 0.01% sodium azide. 40 um thick coronal brain sections were cut usinga clinical cryostat (Leica Biosystems, CM1950), put in a plastic tray with cryomedium (de olmos solution) (ethylene glycol, VWR; Fluka; sucrose, VWR; PVP, Sigma-Aldrich; Na2HPO4 × 2H2O, VWR; NaH2PO4 × H2O; VWR) and stored at least 12h before staining at -17 °C (up to 3 weeks without loosing enzymatic activity).

3.3.2 Immunolabeling

Primary antibody used were:

Rabbit-derived anti-BML-PW0595 (Enzo Life Sciences, 1:200, 1:500, 1:1000)

Rabbit-derived anti-EPR5526 (Abcam, 1:5000)

Mouse-derived anti-MAB2166 (Millipore, 1:1000)

Mouse-derived anti-1C2 (Millipore, 1:1000)

Mouse-derived anti-3B5H10 (Sigma-Aldrich, 1:1000)

Mouse-derived anti-MW8 (Baria, shipped as a supernatant without dilution needed)

Rabbit-derived anti-caspase 3 (Acris, 1:200)

Mouse-derived anti-caspase 8 (Millipore, 1:500)

Mouse-derived anti-MMP-9 (Aviva, 1:500)

Rabbit-derived anti-MMP-10 (Aviva, 1:400)

Rabbit-derived anti-calpain 5 (1:200)

Goat-derived anti-KLK10 (Santa-Cruz Biotechnology, 1:200)

Secondary antibody used were:

Donkey-derived Amersham anti-rabbit IgG biotinylated secondary antibody (Amersham, 1:400)

Sheep-derived Amersham anti-mouse IgG biotinylated secondary antibody (Amersham, 1:400)

Free-floating sections were washed 3× for 5 minutes each in 1× PBS. Then were pretreated with 90% formic acid for 30 minutes and rinse several times in PBS over 5 minutes, while PBS was added into acid to prevent damaging of the sections, which occurs if slices are firstly pulled out from the acid and subsequently rinsed in PBS.The endogenous peroxidase activity was blocked with a solutin of 0.3% of hydrogen perox-ide (H2O2) in 100% methanol for 20 minutes and rinsed several times in PBS over 5

minutes. The treatment by 0.5% freshly prepared sodium borohydride in PBS followed for 30 minutes with repeated rinsing in PBS over 10 minutes. And the slices were blocked 3× in 0,4% Triton-X-100 in PBS (PBSTx) for 10, 30 and 10 minutes. Incubation of sections in primary antibody lasted for 1-2 days.

After incubation the sections were rinsed 4× for 5 minutes each in PBSTx and incubated for 1 hour in Vector biotinylated secondary antibody diluted in PBSTx. Then rinsing 2× for 10 minutes in PBSTx and incubation for 1 hour in Vector ABC Elite solution (Vector ABC Elite reagent diluted 2 drops reagent A and 2 drops reagent B in 5 ml of PBSTx, mixed immediately and incubated for 30 minutes before use). Subsequent rinsing 3× for 5 minutes each in PBSTx, 2×5 minutes each in 1× Tris-imidazole buffer (TI) (0,5M Tris, 0,5 imidazole), 1× for 5 minutes in 1× substrate buffer (SB) (0,6% nickel sulfate) were followed by incubation for 5 minutes in SB with 0,1% diaminobenzidine (DAB) (Sigma-Aldrich), 1 to 2 U/ml glucose oxidase (Sigma-Aldrich), 0,2% glucose, and 0.004% ammonium chloride. After that, the sections were rinsed with TI buffer and water, finally mounted with DPX Mountant (Sigma-Aldrich) and coverslipped.

The specificity of primary antibodies was verified by WB and/or comparative IHC of mouse WT and TgHD (R6/2, 12 weeks old) brain sections. The specificity of secondary antibodies was confirmed by using negative controls.

3.3.3 Image analysis

The evaluation and quantification of immunoreactivity was performed using a densitometric measurement of staining by image analysis software VS-Desktop (Olympus, Tokyo, Japan) and ImageJ (Rasband, W.S., U. S. National Institutes of Health, Bethesda, Maryland, USA). According to the 3D view model of pig brain (from program 3D Slicer; slicer.org) optical sections were divided into substructures (caudate nucleus, putamen, motor and somatosensory and insular cortex), in which the mean of intensity was measured (Figure 9).

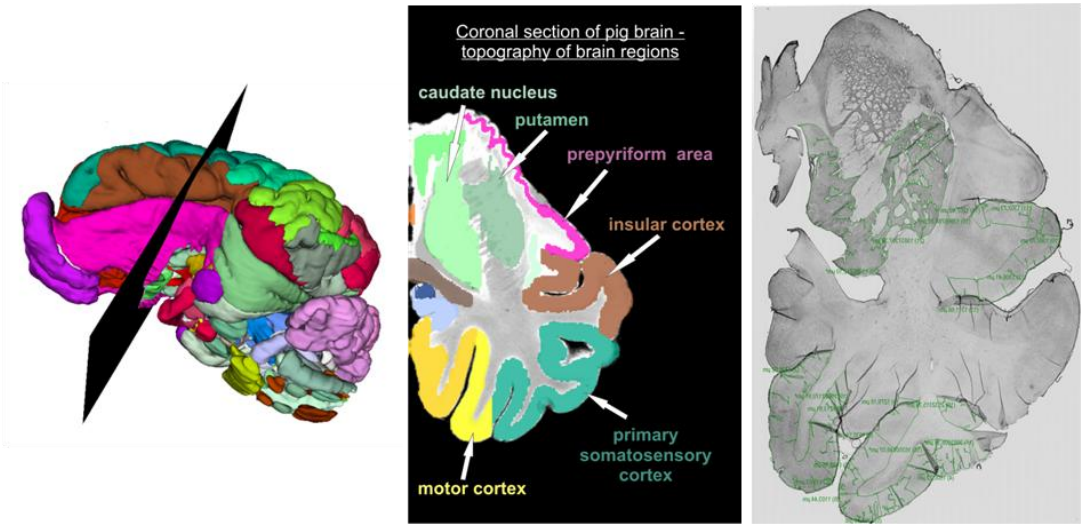

Figure 9. Model of pig brain and picture of brain segmentation into regions for intensity measurement.

3.4 Immunofluorescence

3.4.1 Tissue processing

Immunofluorescence (IF) analysis was performed both on brain tissue and retinal pigment epithelial (RPE) cells.

20 µm thick coronal brain sections (K64 WT and K63 TgHD minipigs, F2 generation, 36m; WT and R6/2 mouse, 12w). Tissue was processed as described above (see the Immunohistochemistry part). Sections were stretched on silanized glass (2% solution of 3-aminopropyl-triethoxy-silane (Sigma-Aldrich) dissolved in acetone).

RPE cells were isolated from the eyes of experimental minipigs (K14 WT and K101 TgHD, F2 generation, 48months). The eyes were gently cut from the eye socket and cleaned from surrounding connective tissue. They were inserted into the Falcon tube with a little amount of PBS and immediately transported to the laboratory where were processed. A small amount of PBS was used just to form a humid chamber as the PBS reduces tonus of the eyes and hence a subsequent handling is more difficult. The eyes were rinsed with 1 ml of ethanol and the remaining tissue was removed. Then the eyes were inserted into a sterilizing solution of 10% betadine (povidonum iodiratum, 100 mg, Egis Pharmaceuticals) in PBS. The amount of solution used was 20 ml for each three eyes. Sterilization took 10 minutes.

3.4.2 Isolation and cultivation of RPE cells

Flow Box (L.12 Jouan) was sterilized by UV radiation for 20 minutes before use. Sterilized eyes were pulled out from Falcon to Petri dishes and rinsed 2× with 1 ml of PBS. Eyball was incised using scalpel few mM below the iris and the anterior eyeball segment was trimmed and the remaining eyeball was tickled on the inner side by blunt scissors edge. This was performed for facilitation of retina detachment when the vitreous floated out and therefore retina is simply attached to the vitreous and subsequently cut off from the optic nerve. If the retina remained inside the eyeball, 1 ml of PBS was pipetted into the eyeball, the retina was relaxed, visualized and then removed with forceps and cut off from the optic nerve. Retinas were frozen at -80 °C for further use in other analysis. Every eye was poured with 1 ml of PBS to prevent drying out of the cells and placed in a 12 well plate. After processing the last of the eye, PBS was taken out, into each eye 1 ml trypsin (Sigma-Aldrich) + EDTA (ethylendiamintetraacetic acid, Sigma-Aldrich)was pipetted and eyes were incubated for 20 minutes in a thermostat at 37 °C and 5% CO2. After removal from the thermostat, trypsin was poured out from the globe and 1 ml of α-MEM (Minimum Essential Medium - Alpha Medium) (Life Technologies) with FBS (Fetal Bovine Serum) (Sigma-Aldrich) and gentamicin (Sigma-Aldrich)were added to each eye, pipetted repeatedly while rinsing the inner surface of the globe and flushing digested RPE cells. The medium was finally released with the cells and transferred to sterile 1.5 ml Eppendorf tube. When the medium was aspiring, it is preferred not to touch the pipette tip near the nerve as it may causecontamination by fibroblasts and other cells. Those cells have a growth advantage compared to RPE cells, therefore it can complicate cultivation.

Thereafter, cells were centrifuged in a tabletop centrifuge (Centrifugy MiniSpin Eppendorf, P-LAB) for 3 minutes at 300g, then the tubes were rotated by 180 °C, and centrifuged again for 3 minutes at 300 g (the centrifuge has a rotor angle). The supernatant was pipetted off and 3 ml of culture medium was added to each well. Some of this volume, from 500 µl to 1 ml, was used for resuspendation of the cells from the centrifugated pellet of cells in an Eppendorf tube. The cells were resuspended by gentle pipetting strokes, all volume was transfered to the remaining medium in the corresponding well of the plate and the medium was again repeteadly pipetted back and forth. When finished all the cells, the plate was capped and mixed by a couple of shaking from the

top to the bottom and from the left to the right, which guarantees, if possible,the best spreading of the cells on the surface of platelets. The plate was allowed to stand for 5 minutes in a flow box, and then was placed in thermostat. The first medium exchange was carried out on the day 2 (day cultivation = day 0) and thereafter every second to third day. The cells were cultured until confluent.

3.4.3 Cell harvesting and cultivation in Lab-Tek Chamber Slide system

Cells were harvested using 0.5% trypsin + EDTA, counted on the VicellXR device (Beckman Coulter) and pipetted into Labtek Chamber slide 8 well (Thermo Fisher Scientific), in an amount of 25,000 cells per well. They were cultured in thermostat while exchanging medium until confluence.

3.4.4 Immunolabeling

Primary antibody used were:

Mouse-derived anti-MMP-9 (Aviva, 1:500)

Secondary antibody used were:

Alexa Fluor® 647 goat anti-mouse (Life Technologies, 1:500)

Material (brain sections/cells) was fixed with 4% PFA for 30 minutes at 4° C, briefly rinsed with distilled water and PBS for 5 minutes. Blocking solution (1% goat serum in 0.4% Triton-X in PBS) was pipetted onto the glass, blocking was carried out for 60 minutes. After removing the blocking solution, the primary antibody was added without rinsing the glass (200µl, antibody diluted in a blocking solution) and incubated for 1.5 hours at RT. After incubation, the glass was rinsed 4× with PBSTw (0.05%) for 5 minutes and incubated with the secondary antibody for 1.5 h at RT and rinsed again 4 times for 5 min with PBSTw and finally with distilled water for reducing the particles of PBSTw (salts would have precipitated and interfere with results). Glasses were dried and mounted in the mounting medium with DAPI covered with the cover glass and kept at 4 ºC. The slides were kept in dark during all the steps.

3.4.5 Fluorescence detection

Immunofluorescence was scanned using the virtual microscopy system VS-120 FL equipped with Olympus VS Desktop software (Olympus, Tokyo, Japan).

4 RESULTS

We investigated expression of Htt as it is a substrate for proteolytic enzymes participating in a cleavage processes, and also tried to detect large Htt forms - inclusions and aggregates. Then we focus on examination of proteolytic enzymes themselves.

4.1 Qualitative and quantitative characterization of huntingtin

Detection and analysis of expression of Htt was performed using antibodies against both N-terminal part of Htt and polyQ stretch of mtHtt protein.

4.1.1 Characterization of huntingtin with antibodies against N-terminus

Detection of Htt was performed using immunohistochemical and biochemical techniques with following primary antibodies: BML-PW0595, EPR5526, MAB2166.

We used 3 WT (K48, K64, K103) and 3 TgHD (K100, K63, K104) minipigs of F2 generation (36 month old). For every tested animal we examined 5 coronal brain sections (40 μm thickness) (Figure 9), one coronal section was employed for the negative (shame) control where the primary antibody was omitted. The specificity of primary antibodies was verified by WB and/or comparative IHC of mouse WT and TgHD (R6/2, 12 weeks old) brain sections. The specificity of secondary antibodies was confirmed by using negative controls. The evaluation and quantification of immunoreactivity was performed using a densitometric measurement of staining by image analysis and statistical analysis was employed by an unpaired t-test or a one-way ANOVA test with a Bonferroni's (Tukey's) post-test multiple comparison.

Immunostaining with rabbit polyclonal BML-PW0595

We detected moderate expression of Htt (endogenous and mutant) by using both anti-huntingtin rabbit polyclonal BML-PW0595 and rabbit polyclonal EPR5526 antibody in brain tissue of all animals (WT and TgHD) with small changes between them. A relatively high expression of Htt was observed in cortical pyramidal neurons in comparison with other cells.

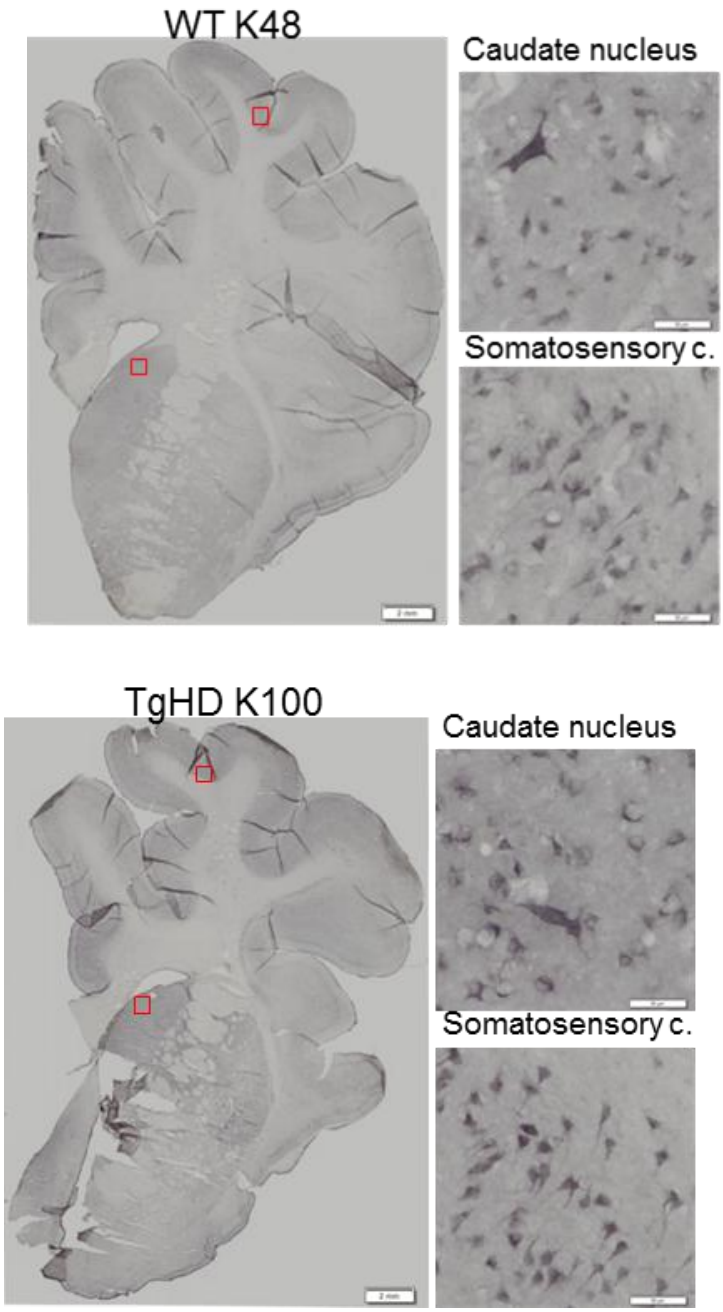

Figure 10. Immunostaining with rabbit polyclonal BML-PW0595 antibody. Immunohistochemical staining in minipig brain coronal sections. Scale bar = 2 mm, scale bar of high-magnification = 50 μm.

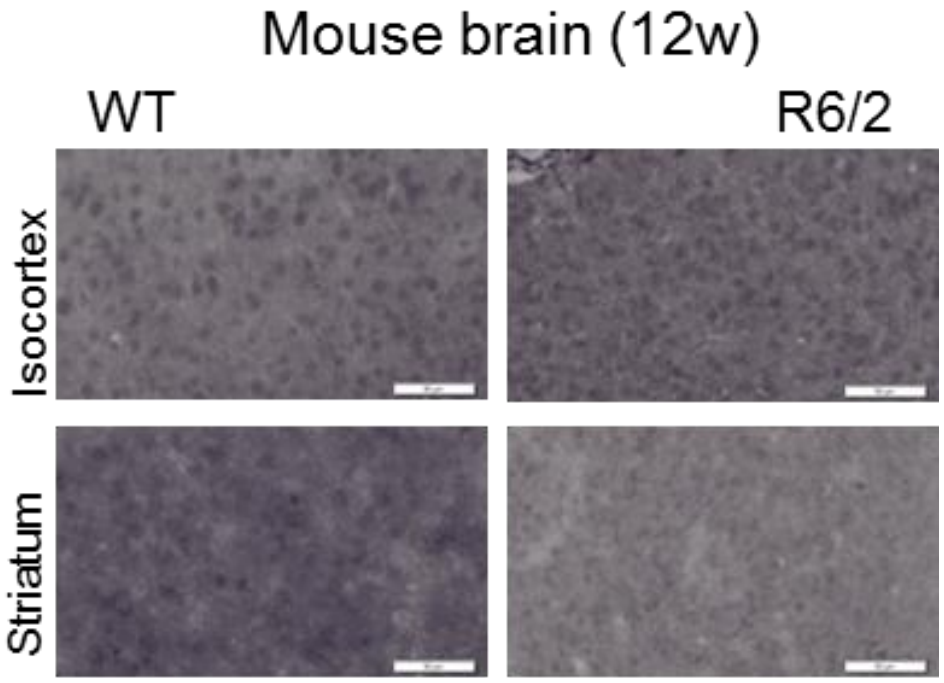

Figure 11. Immunostaining with rabbit polyclonal BML-PW0595 antibody.
Immunohistochemical staining in mouse brain coronal sections. Scale bar = 50 μm. Although we found a slightly increased expression ofHtt in TgHD brain, the quantitative analysis showed a significant increase mainly in somatosensory cortex of TgHD (BML-PW0595, K100, K104) or in some pairs of animals such as K103/K104 (EPR5526, caudate nucleus, motor and somato-sensory cortex).

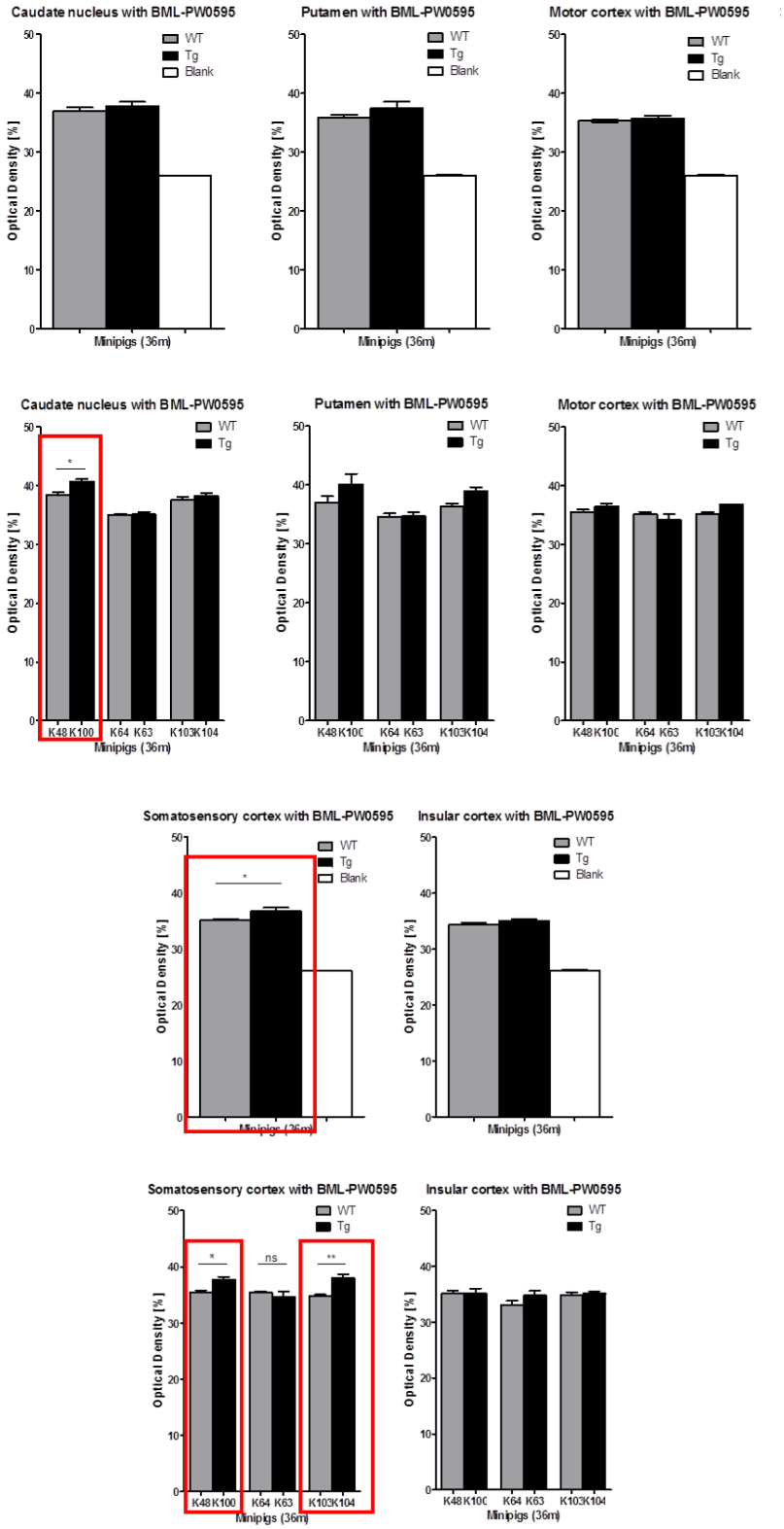

Figure 12. Results of Tukey´s tests. Comparison of the expression of mtHtt/Htt in the brain substructures (caudate nucleus, putamen, motor and somatosensory and insular cortex) between wild type (WT) and transgenic (Tg) minipigs.

Immunostaining with rabbit polyclonal EPR5526 antibody

We detected both forms of Htt by using anti-huntingtin EPR5526 in brain tissue of all animals (WT and TgHD). The expression was relatively mild, accordingly to result observed in the previous analysis with BML-PW0595 antibody.

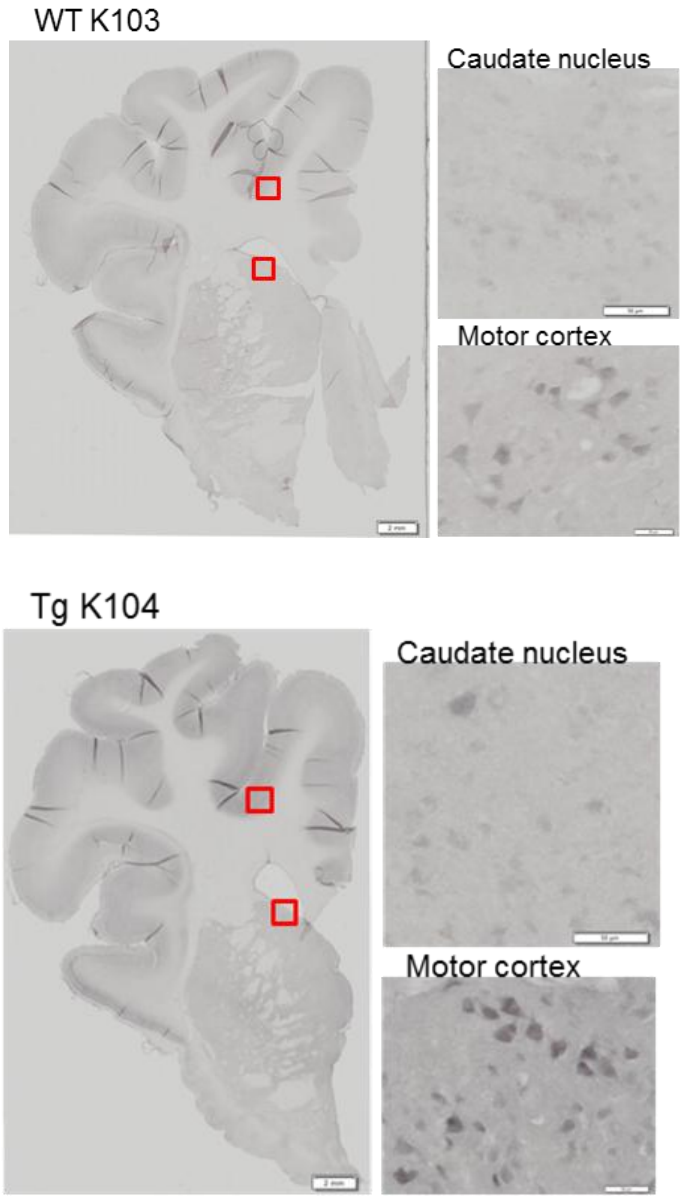

Figure 13. Immunostaining with rabbit polyclonal EPR5526 antibody
Immunohistochemical staining in minipig brain coronal sections. Scale bar = 2 mm, scale bar of high-magnification = 50 µm.

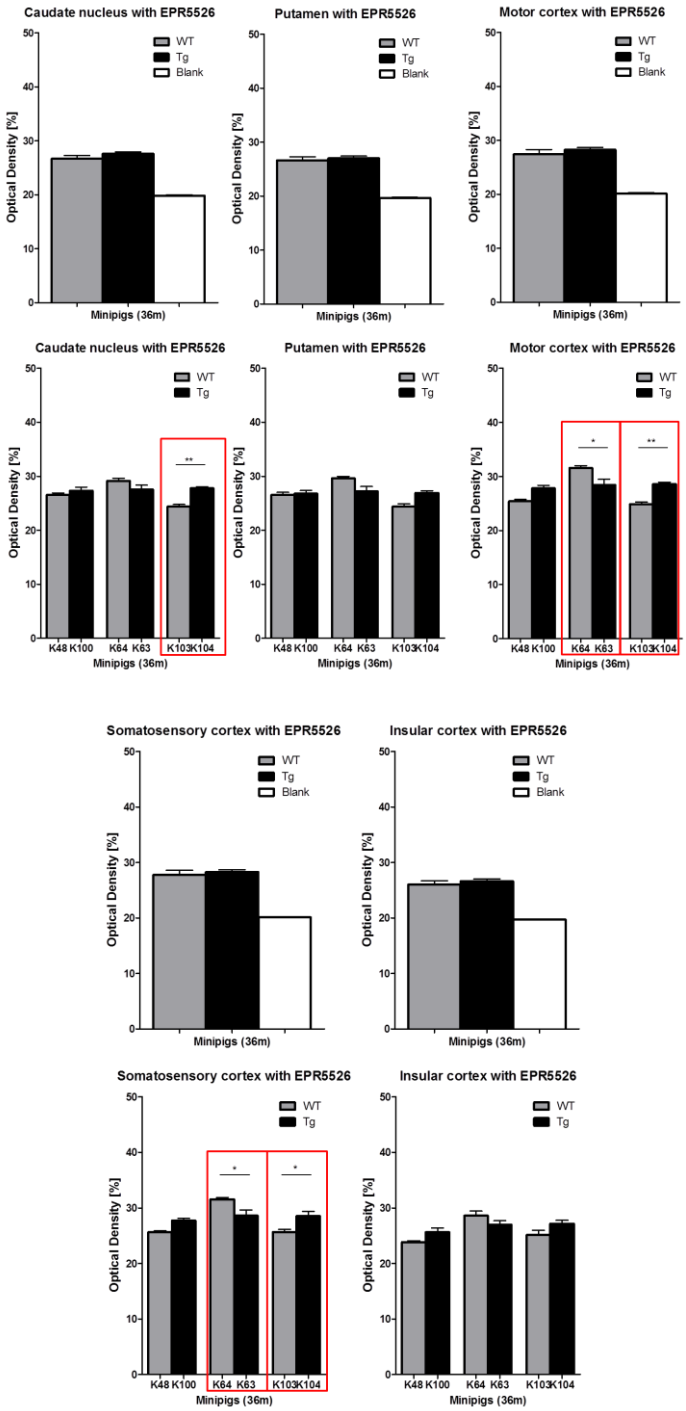

Figure 14. Results of Tukey´s tests. Comparison of the expression of mtHTT/HTT in the brain substructures (caudate nucleus, putamen, motor and somatosensory and insular cortex) between wild type (WT) and transgenic (TgHD) minipigs.

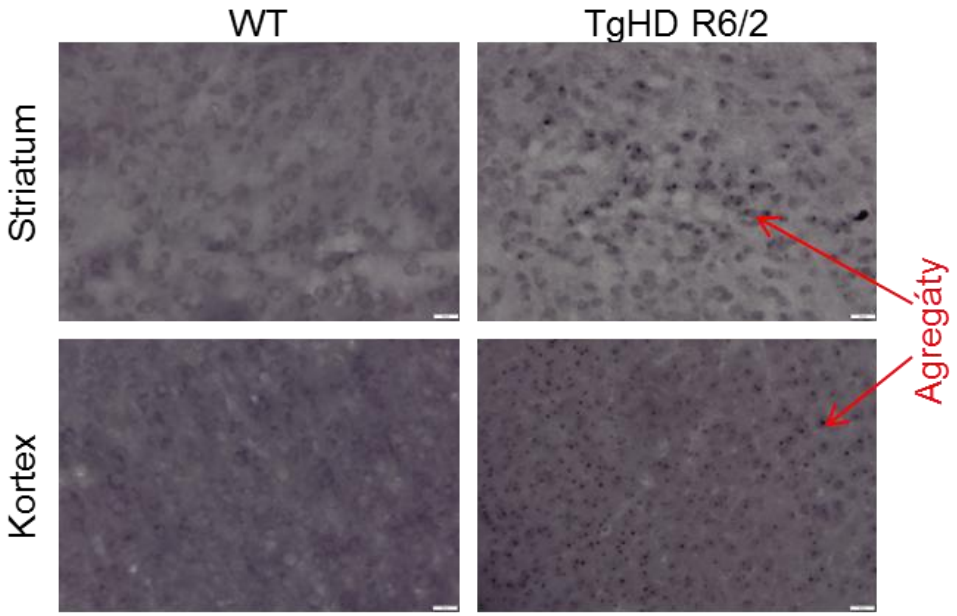

Figure 15. Immunostaining with rabbit polyclonal EPR5526 antibody. Immunohistochemical staining in mouse brain coronal sections. Scale bar = 50 μm.
The fragments of Htt were detected by WB analysis using anti-EPR5526 antibody specific for N-terminal part of both endogenous and mutant Htt. As we can see, Htt undergoes the proteolytic processes and smaller fragments of this protein are present in TgHD and WT animals. The fragment of MW = 125 kDa represents inserted form of human mtHtt in TgHD minipig. Interestingly, we also observed smaller fragments of MW lesser than 50 kDa in TgHD, which are supposed to migrate into the nucleus and therefore act cytotoxically.

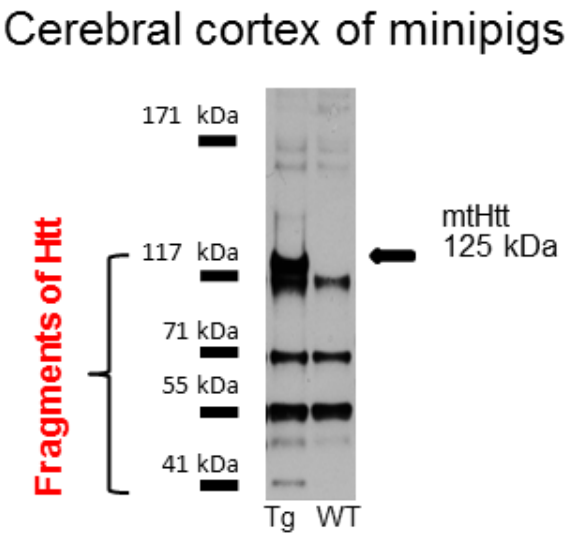

Figure 16. WB of minipig cerebral cortex with rabbit polyclonal EPR5526 antibody. Fragments of mtHtt smaller than 50 kDa detected in TgHD minipig.

Immunostaining with mouse monoclonal MAB2166 antibody

Immunolabeling with anti-MAB2166 antibody indicated very weak staining and was not evaluated by image analysis method.

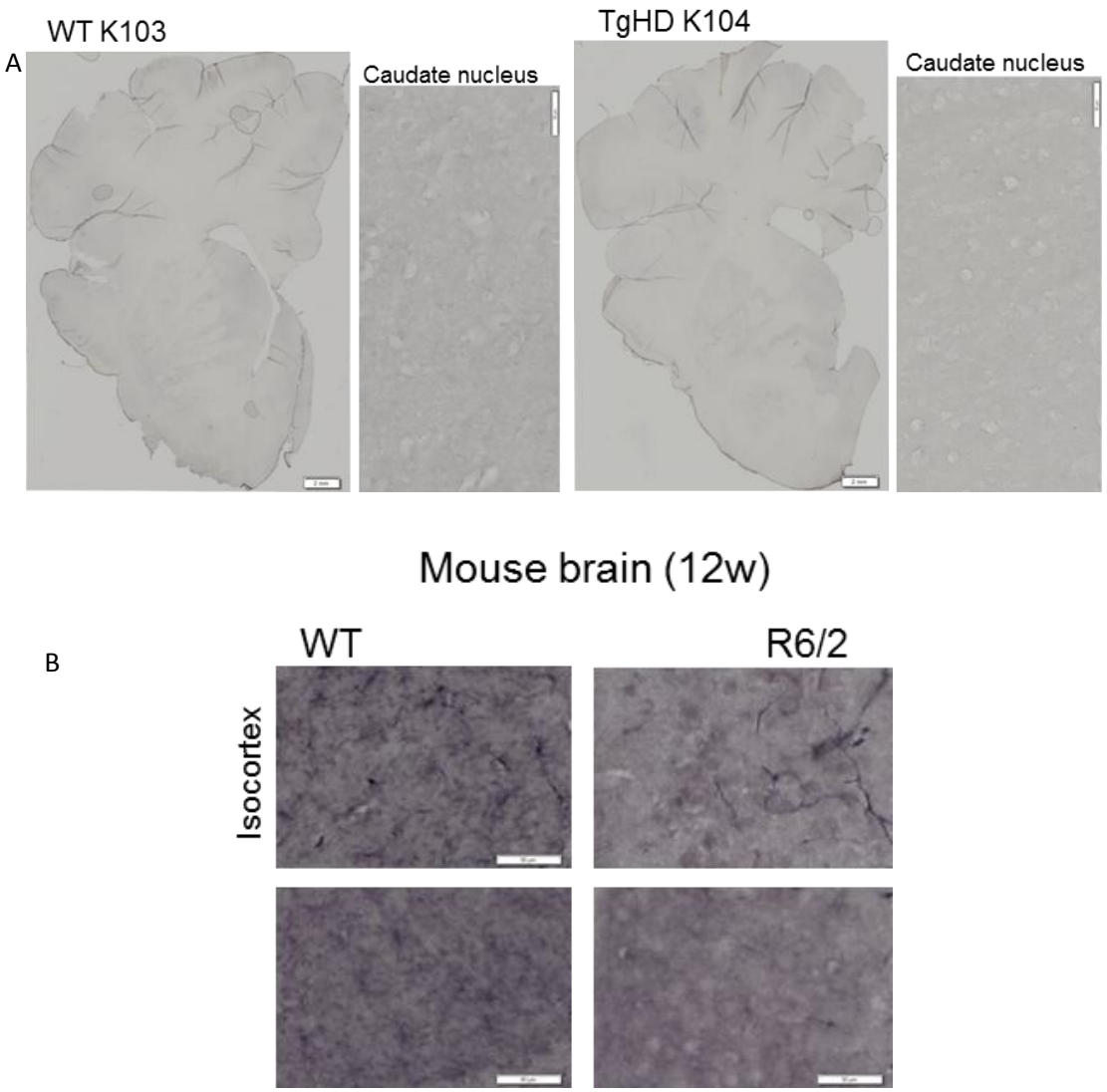

Figure 17. Immunostaining with mouse monoclonal MAB2166 antibody. Immunohistochemical staining of aggregates in minipig brain coronal sections. Scale bar = 2 mm, scale bar of high-magnification = 50 µm (A) and in mouse brain coronal sections. Scale bar = 50 µm (B).

4.1.2 Characterization of huntingtin with antibodies against polyglutamine stretch

We also performed IHC staining with anti-polyQ 1C2 and anti-3B5H10 antibodies that exhibited an increased perinuclear immunoreactivity (localized to Golgi apparatus or endoplasmic reticulum) in striatal and cortical cells of TgHD minipig brain.

In WB analysis using anti-1C2 antibody, the small proteolytic fragments of mtHtt in TgHD minipig were detected, whereas no bands were observed in WT animal.

Immunostaining with rabbit polyclonal 1C2 antibody

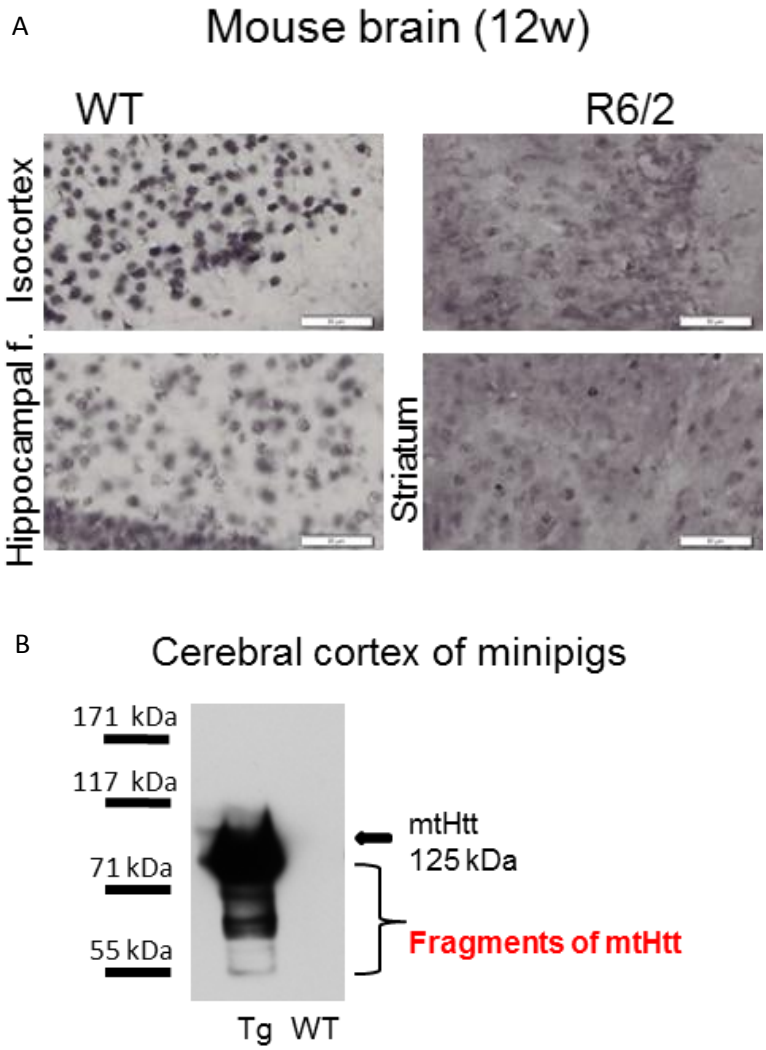

Figure 18. Immunostaining with rabbit polyclonal 1C2 antibody. Immunohistochemical staining in mouse brain coronal sections. Scale bar = 50 µm (A). WB of minipig cerebral cortex. WB shows transgenic inserted form of mtHttandits smaller fragment (B).

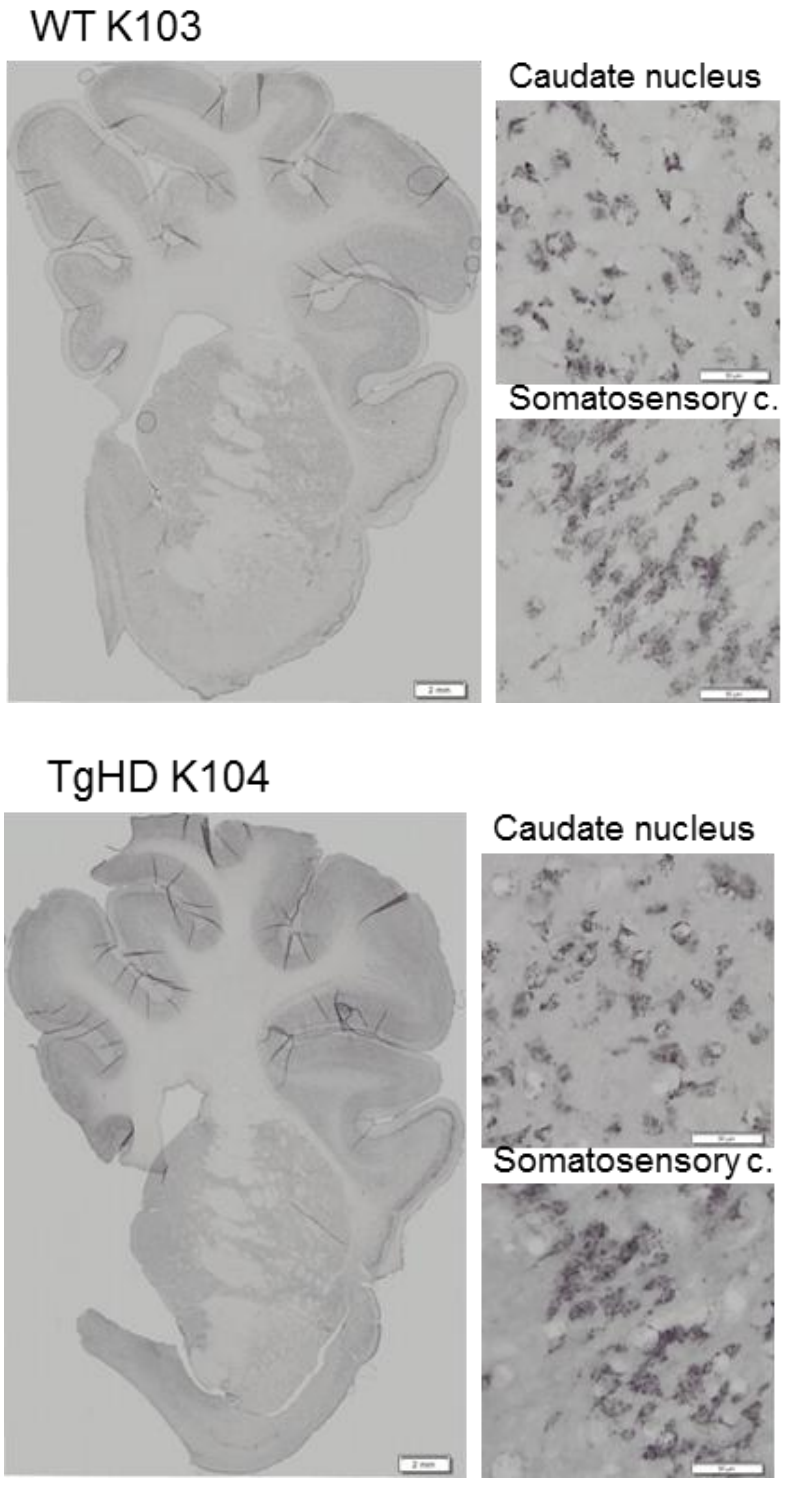

Figure 19. Immunostaining with rabbit polyclonal 1C2 antibody. Immunohistochemical staining in minipig brain coronal sections. Scale bar = 2 mm, scale bar of high-magnification = 50 μm.

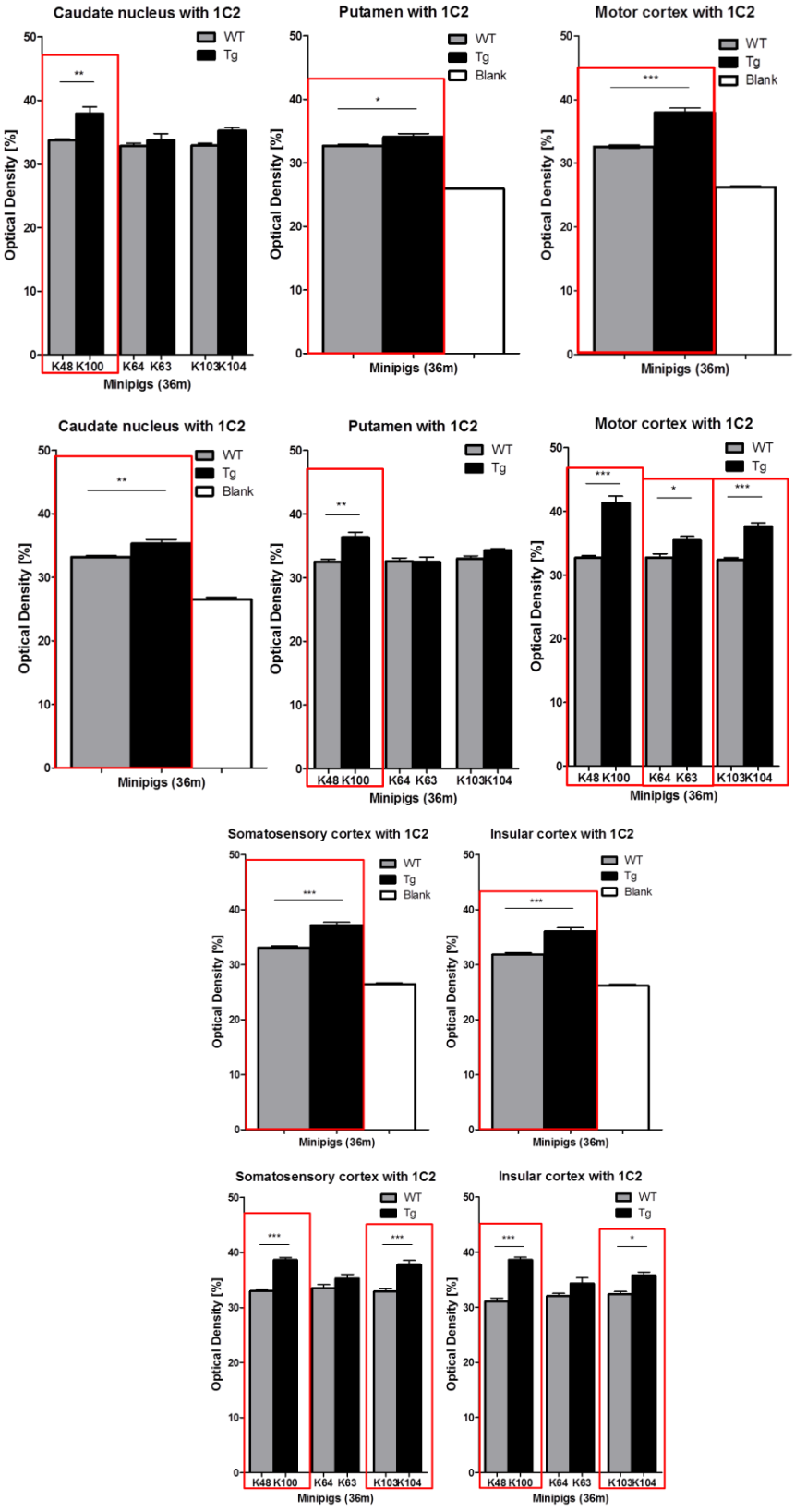

Figure 20. Results of Tukey´s tests. Comparison of the expression of polyQ protein in the brain substructures (caudate nucleus, putamen, motor and somatosensory and insular cortex) between wild type (WT) and transgenic (Tg) minipigs (D).

Immunostaining with mouse monoclonal 3B5H10 antibody

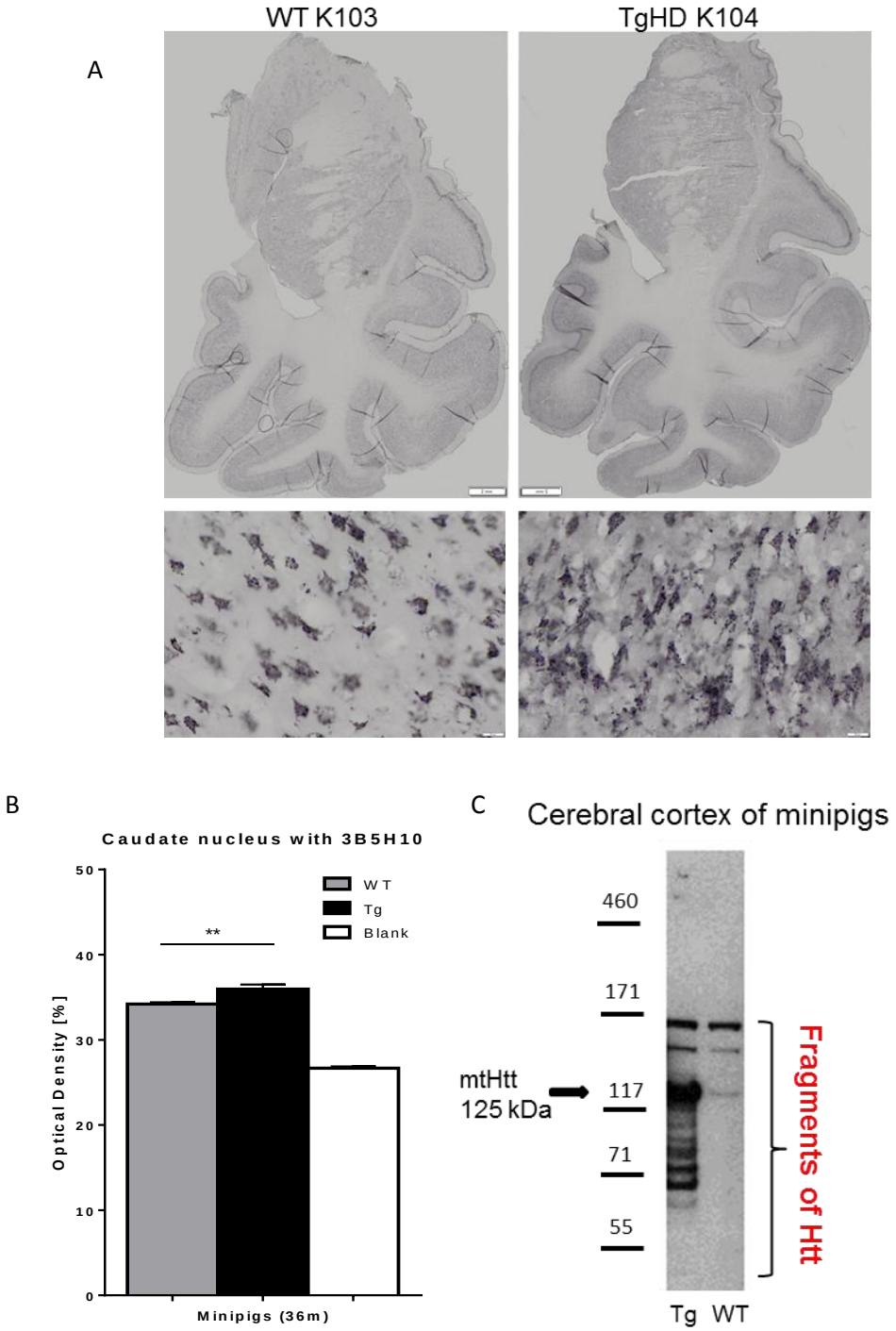

Figure 21. Immunostaining with mouse monoclonal 3B5H10 antibody. Immunohistochemical staining in minipig brain coronal sections. Scale bar = 2 mm, scale bar of high-magnification = 50 µm (A). Results of Tukey´s tests. Comparison of the expression of polyQ protein in the brain substructures (caudate nucleus, putamen, motor and somatosensory and insular cortex) between wild type (WT) and transgenic (Tg) minipigs (B).WB of minipig cerebral cortex. (C).

4.1.3 Detection of huntingtin large aggregated form

We tried to detect Htt large forms with a specific antibody MW8 preferentially binding Htt in tissue sections when Htt is in aggregates rather than when it is in the cytoplasm. We probably detected the first mtHtt aggregates (5-10 µm in diameter) with antibody MW8 in TgHD minipig brain (K104, K63). The shape and density of aggregates was similar to that we observed in TgHD (R6/2) mice (Figure 23). We did not see any aggregates in brain sections of WT animals (minipig and mice).

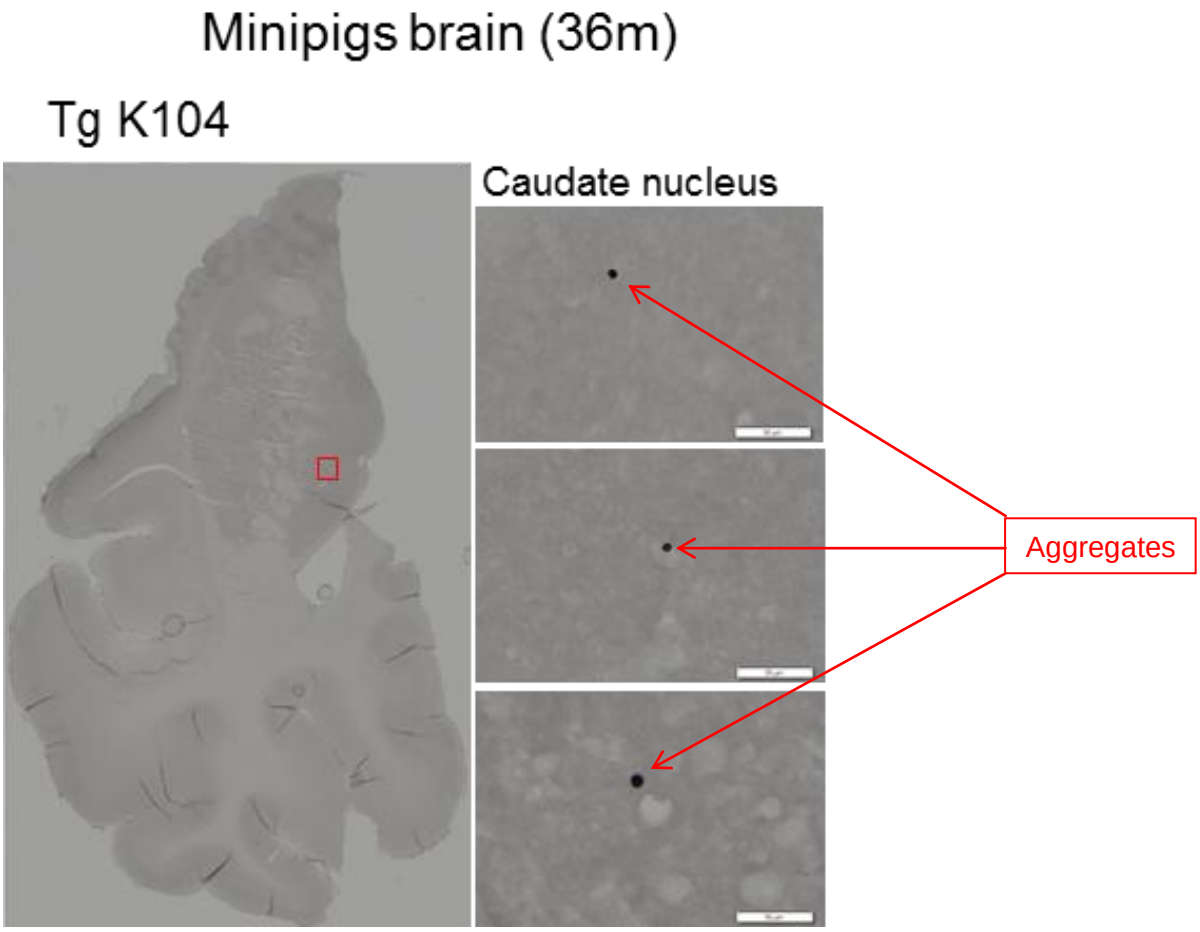

Figure 22. :Immunostaining with mousemonoclonal MW8 antibody.
Immunohistochemical staining of aggregates in minipig brain coronal sections . Scale bar = 2 mm, scale bar of high-magnification = 50 µm and in mouse brain coronal sections (B).

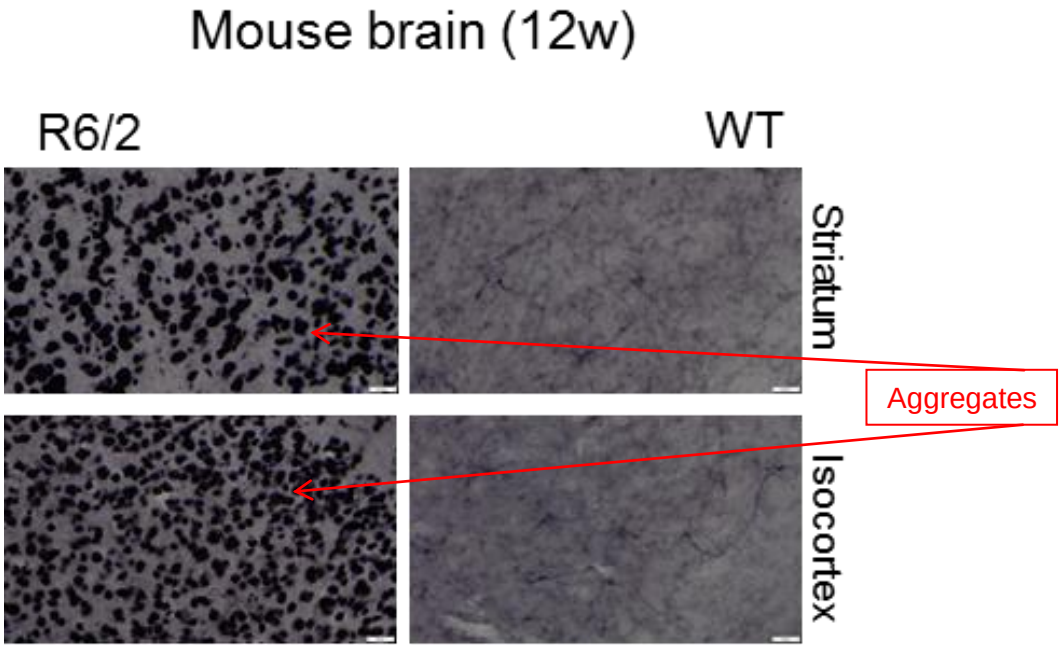

Figure 23. Immunostaining with mousemonoclonal MW8 antibody. Immunohistochemical staining of aggregates in mouse brain coronal sections. Scale bar = 2 mm, scale bar of high-magnification = 50 μm.

4.2 Qualitative and quantitative characterization of proteolytic enzymes

We performed detection and quantification analysis of proteolytic enzymes with folowing primary antibodies: caspase-3, caspase-8, MMP-9, MMP-10, KLK-10, calpain-5.

We used the same range of experimental animals 36 month old for IHC and WB as described previously. In addition, we analyzed an expression of caspase-3 in cortex and putamen of minipig brain sections (K64 WT, K63 TgHD minipigs, 36 month, F2 generation) (20 μm thickness), and mouse cortical WT and transgenic R6/2 part of brain using IF. One pair of 48 month old minipigs (K14 WT and K101 TgHD, F2 generation) was used for detection of MMP-9 in RPE cells isolated from the eyes of sacrificed animals by IF technique.

4.2.1 Caspases

IHC and WB analysis showed increased levels of caspases expression in brain areas of TgHD minipigs. Concerning caspase-3, there were observed increased levels both in the striatum (caudate nucleus, putamen) and cortex of TgHD animal by IHC methods, as well as increased levels of caspase-3 were detected by IF. This result was confirmed also by IHC and IF analysis in the WT and R6/2 mouse cortex. Anti-caspase-3 primary antibody used for WB detected increased levels of caspase-3 proenzyme and its cleaved form in cortex of TgHD animals.

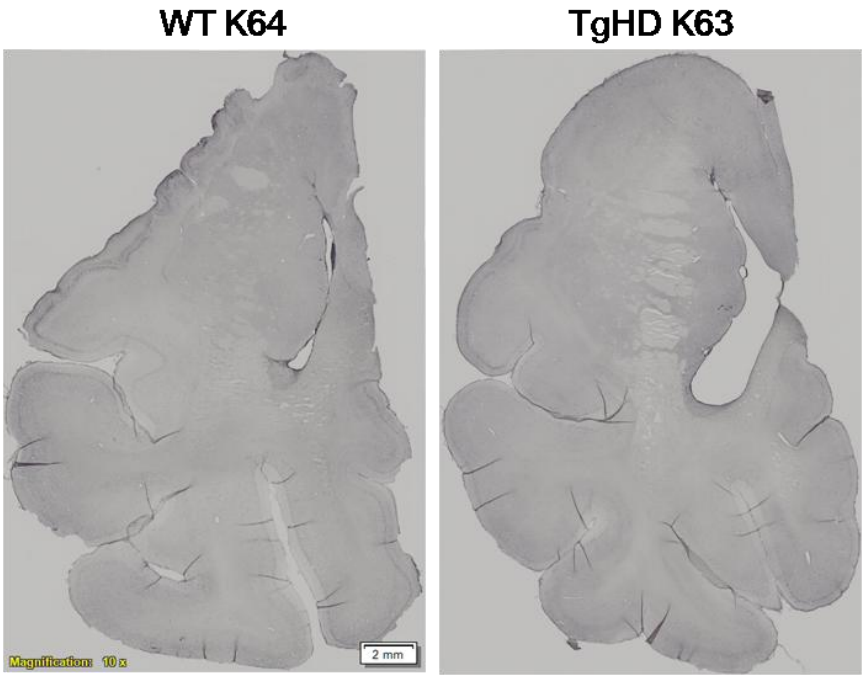

Figure 24. IHC of caspase-3 in the brain of WT and TgHD minipigs (36m)

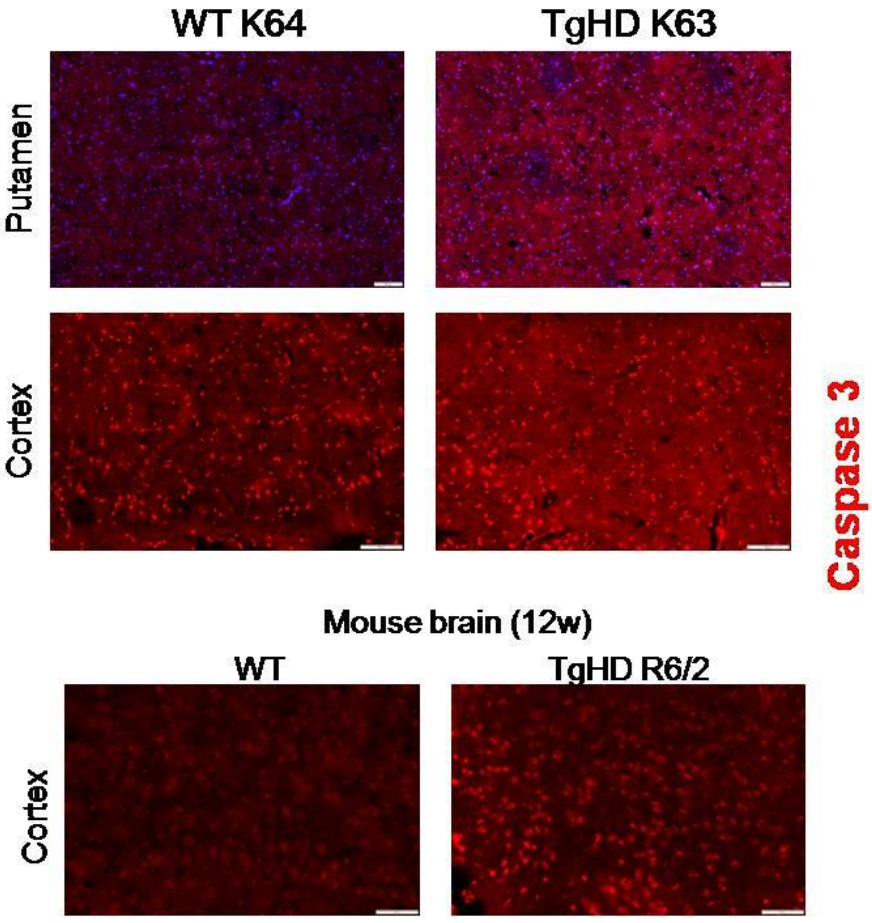

Figure 25. IF of caspase-3 in the brain of WT and TgHD minipigs (36m) and mouse brain (12w)

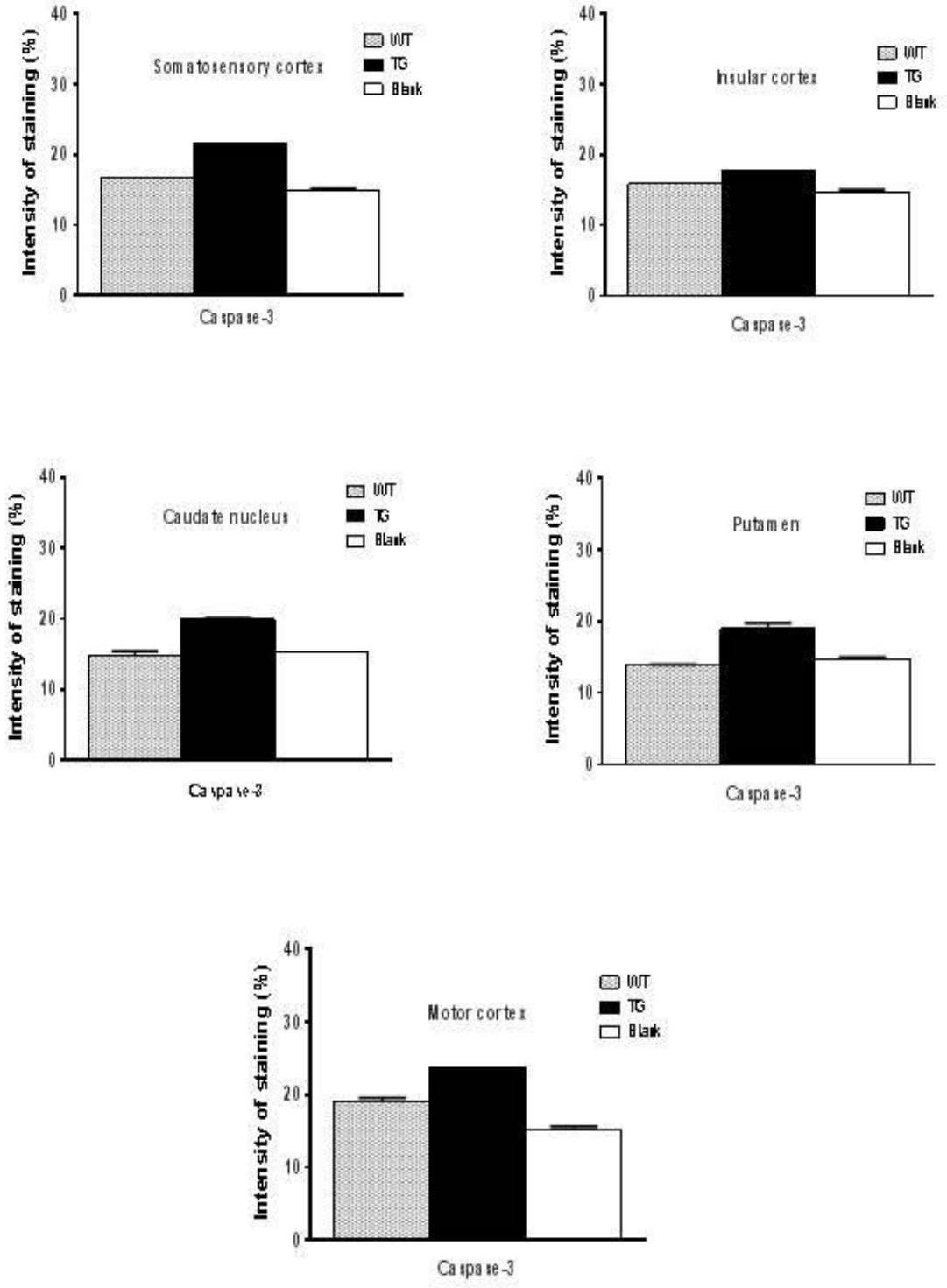

Figure 26. Image analysis of caspase-3 immunohistochemistry in striatum and cortex

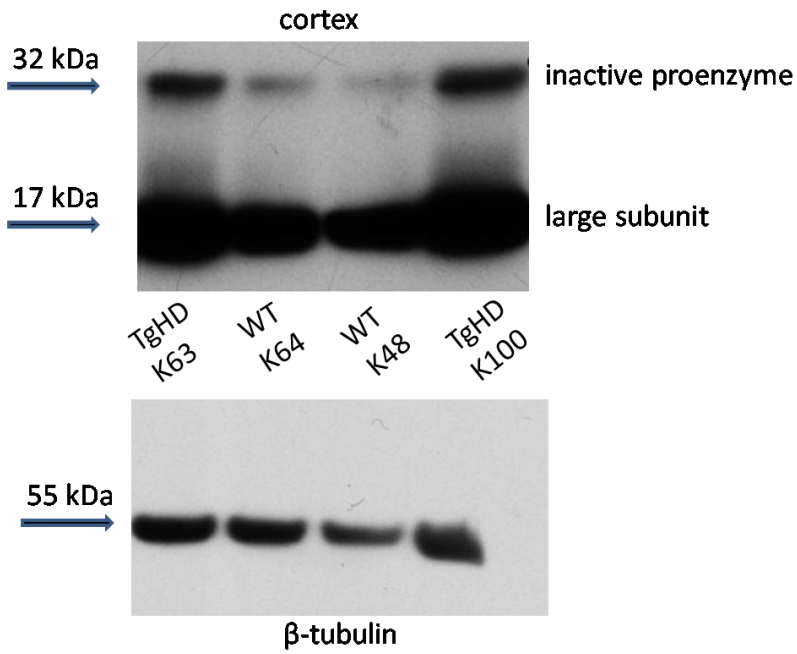

Figure 27. WB of caspase-3 in cortex (36m)
The increased level of proenzyme-8a/8b and the same levels of processed forms p43/41 and p26/24 in TgHD minipig cerebellum were showed by using anti-caspase-8 antibody.

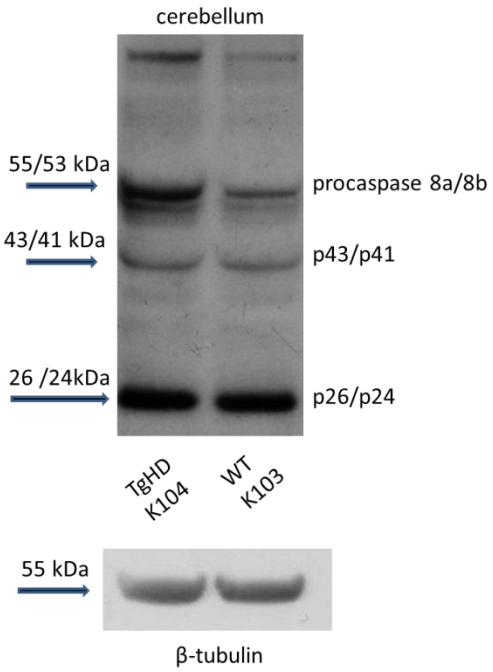

Figure 28. WB of caspase-8 in cerebellum (36m)

4.2.2 MMPs

Among MMPs, there were analyzed MMP-9 and MMP-10. Increased MMP-9 expression was detected immunohistochemicaly in the striatum and cortex of TgHD minipig, and also biochemically were showed increased levels of processed forms of MMP-9 in cortex and cerebellum of TgHD minipig. MMP-10 expression was detected immunohistochemically in both WT and TgHD porcine brains, when the mildly increased expression was seen in the caudate nucleus of TgHD minipig.

We also performed IF of MMP-9 expression in RPE cells of one pair of 48m old minipigs. The increased levels of MMP-9 were observed in these cells in TgHD animal.

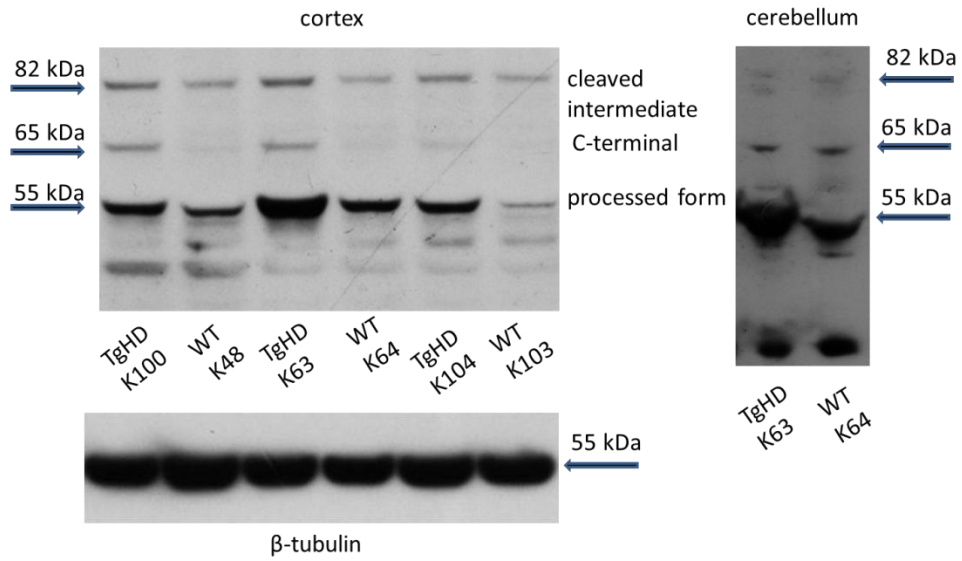

Figure 29. WB of MMP-9 in cortex and cerebellum (36m)

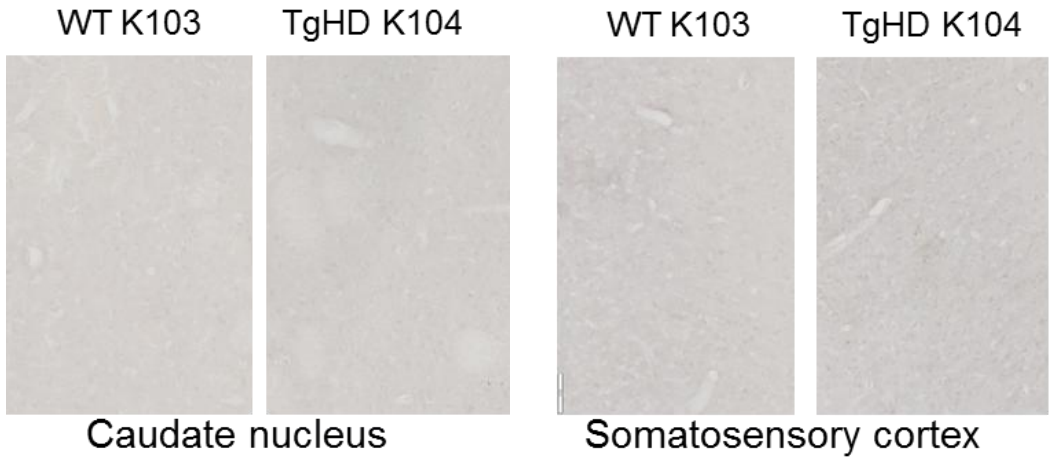

Figure 30. IHC of MMP-9 in the brain of WT and TgHD minipig (36m)

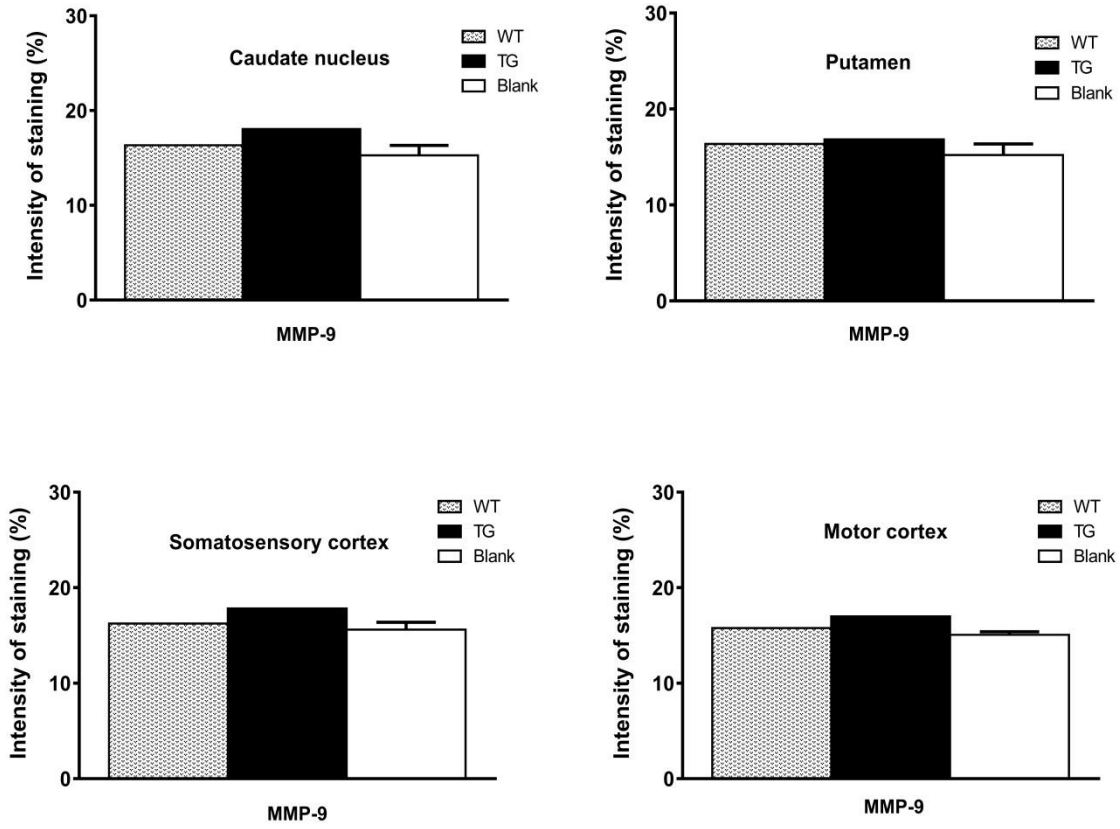

Figure 31. Image analysis of MMP-9 immunohistochemistry in striatum and cortex

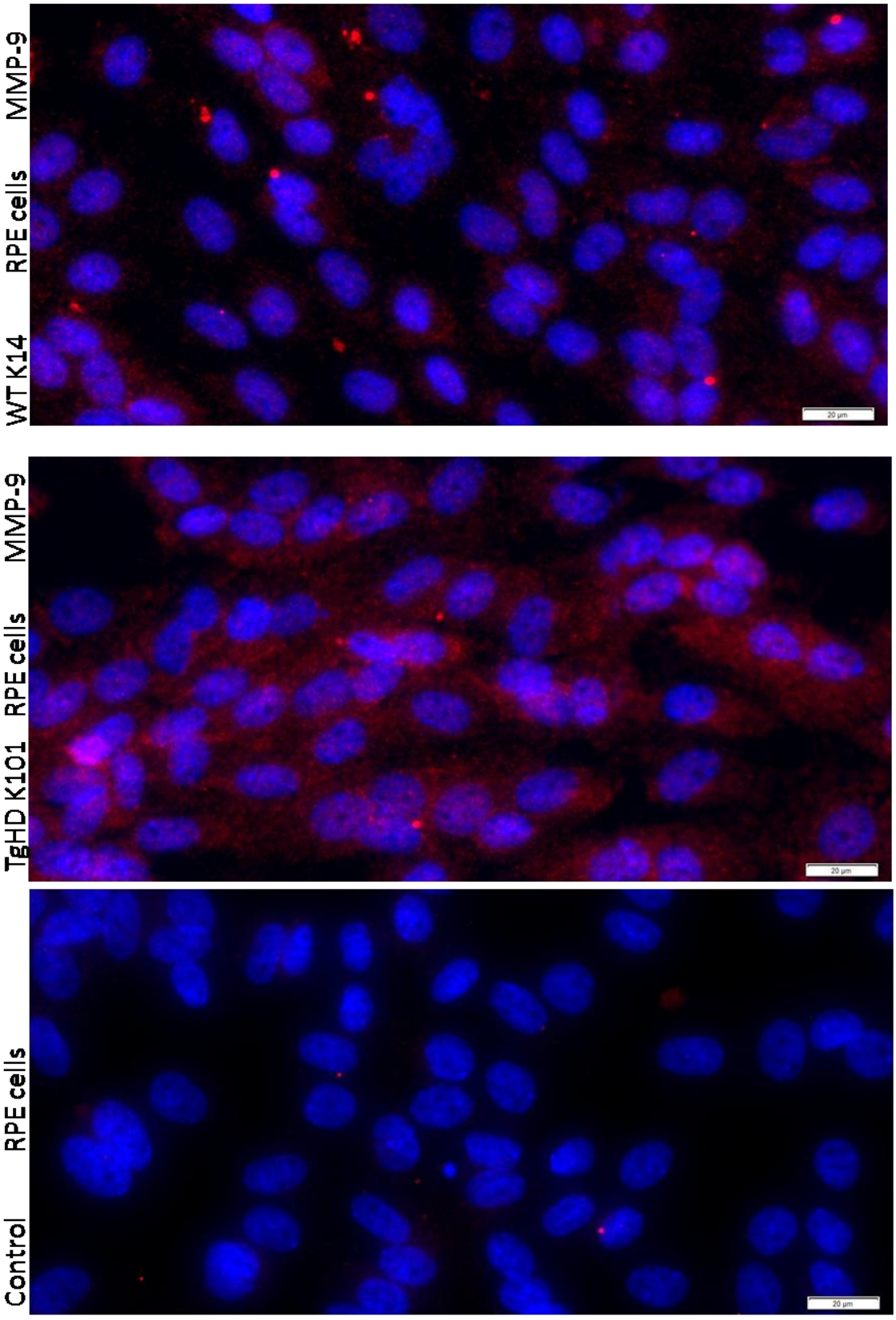

Figure 32. IF of MMP-9 in the RPE cells of WT and TgHD minipigs (48m)

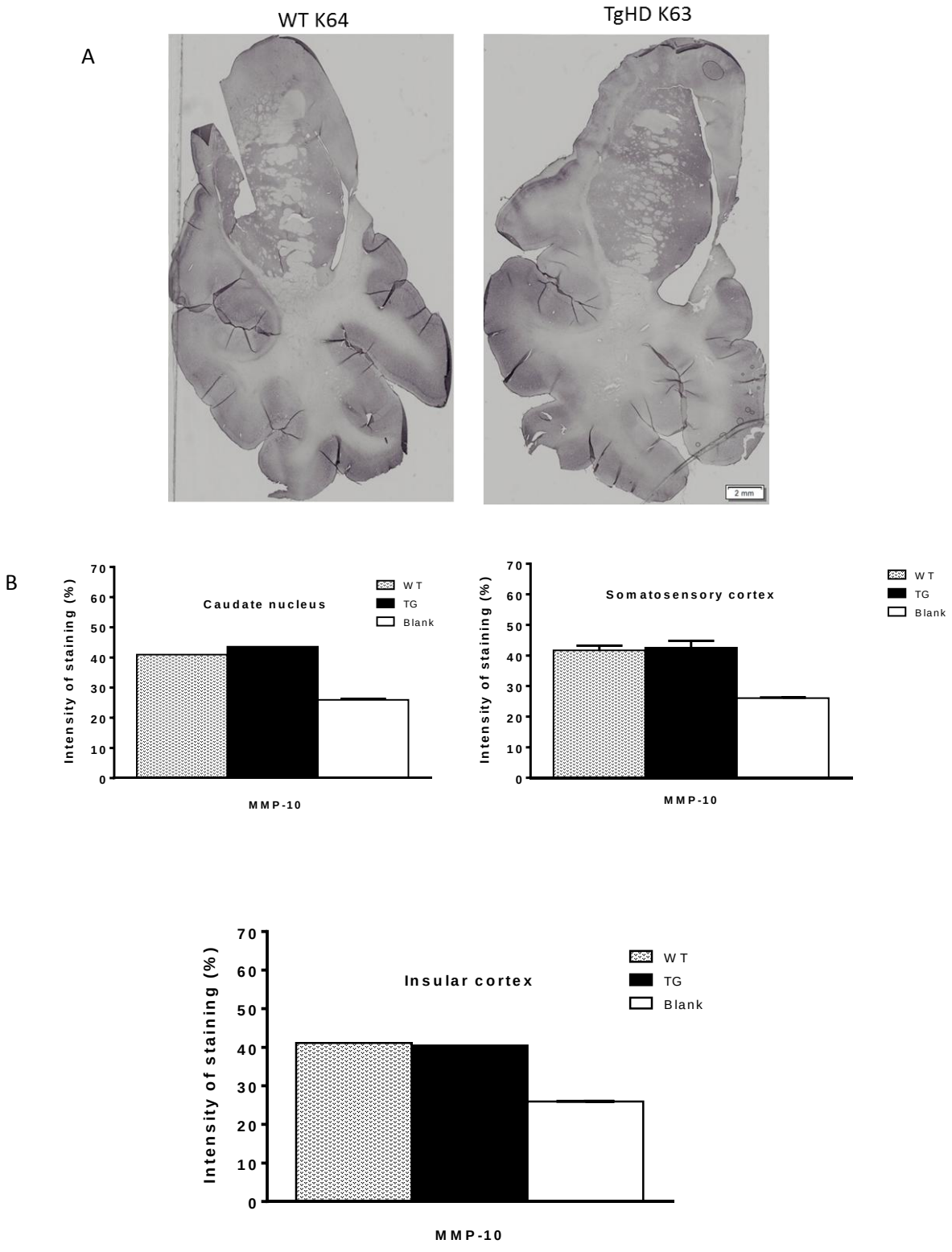

Figure 33. IHC of MMP-10 in the brain of WT and TgHDminipig (36m) (A) Image analysis of MMP-10 immunohistochemistry in striatum and cortex (B)

4.2.3 KLKs

In a family of KLKs, we focused on KLK-10. Using anti-KLK-10 primary antibody in WB analysis were showed slightly increased concentration levels of this enzyme in cerebellum, whereas a slightly decreased level was found in the cortex of 36m TgHD minipig. Immunohistochemically, a decreased expression of KLK-10 was detected in the striatum and cortex of 36m TgHD minipig.

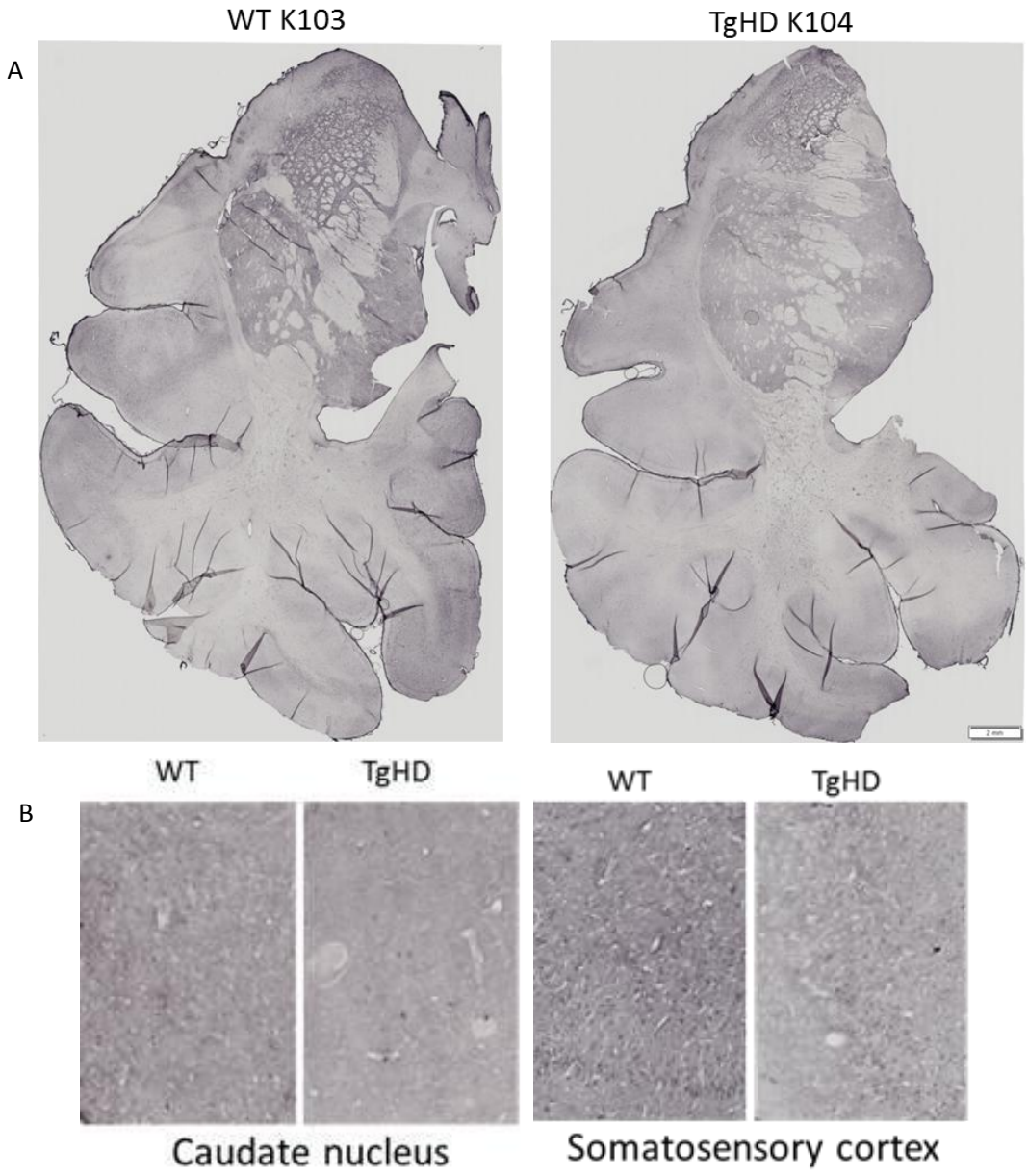

Figure 34. IHC of KLK-10 in the brain of WT and TgHD minipigs (36m).

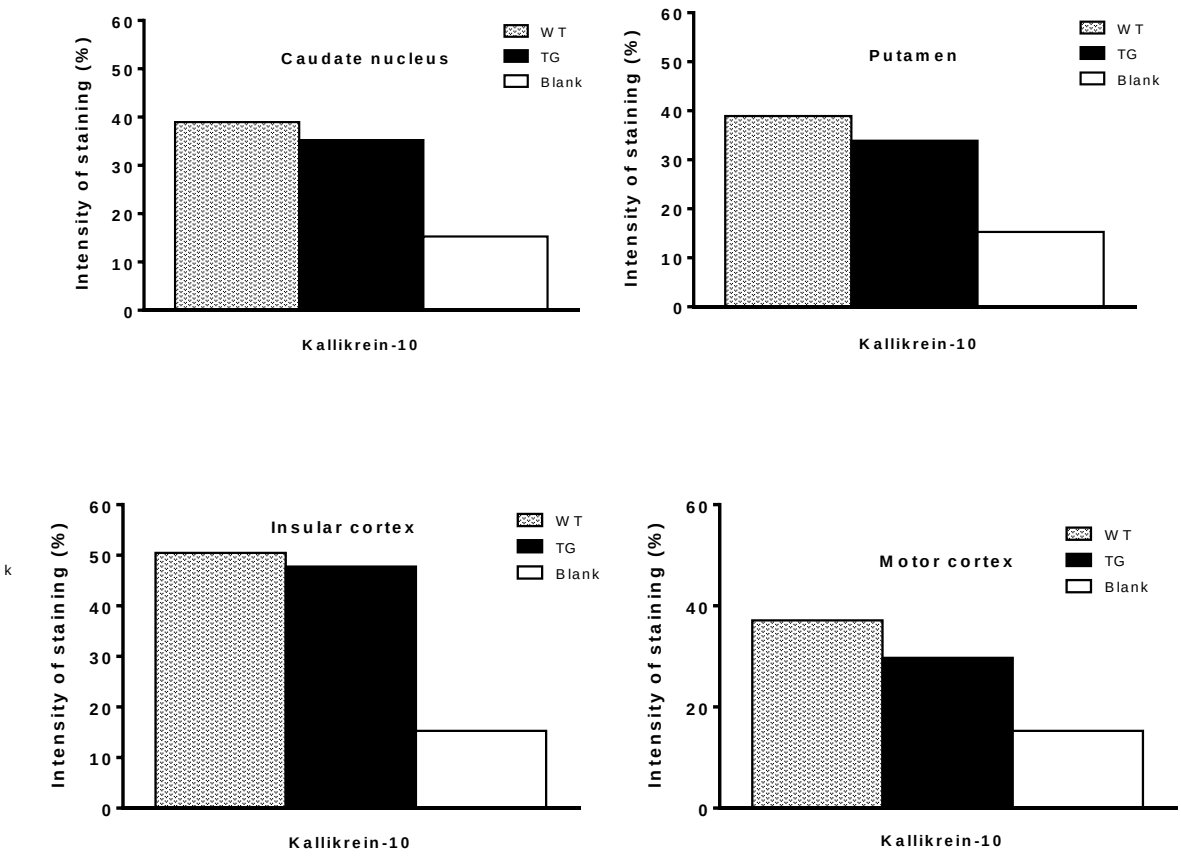

k

Figure 35. Image analysis of KLK-10 immunohistochemistry in striatum and cortex.

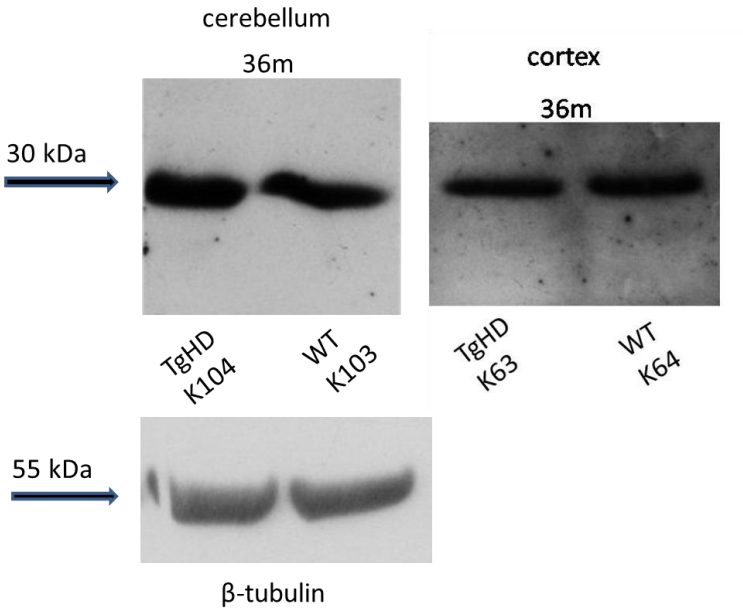

Figure 36. WB of KLK-10 in cortex and cerebellum of WT and TgHD minipigs (36m)

4.2.4 Calpains

The last examined protease was calpain-5, when using IHC we found wide expression of this enzyme both in WT and TgHD animals, however with no difference between them (data not shown). On WB we can also see similar result, calpain-5 was biochemically detected in 36m old minipigs at quite high concentration levels, with no observed differences between WT and TgHD animals.

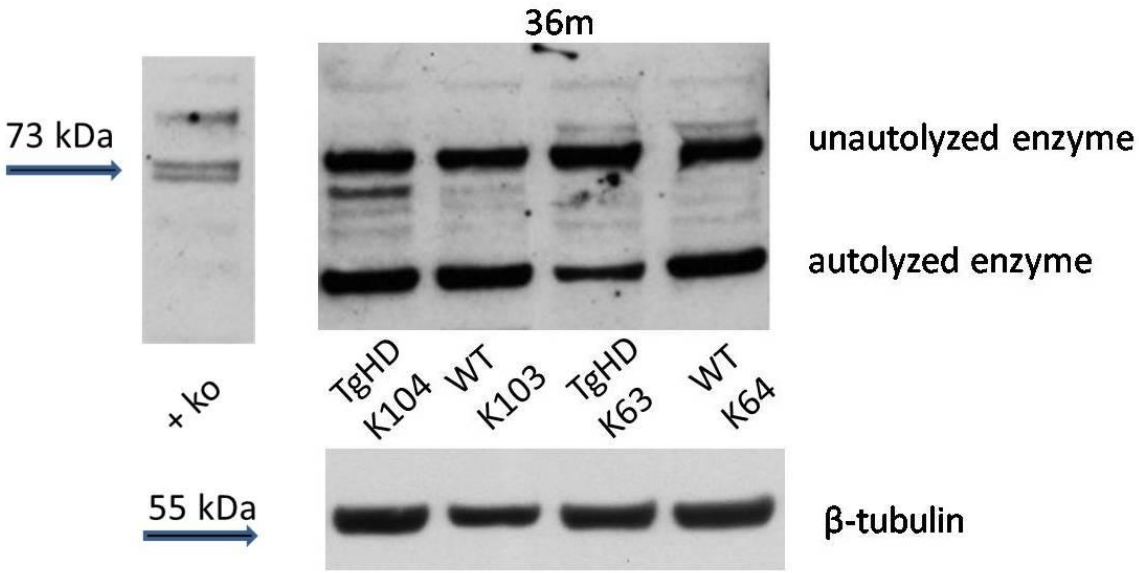

Figure 37. WB of calpain-5 in cortex of WT and TgHD minipigs (36m)

5 DISCUSSION

A crucial step in HD pathogenesis is the cleavage of mtHtt, which is accompanied by releasing smaller N-terminal fragments containing the polyQ stretch and that are toxic to neurons. Such fragments has been demonstrated in many studies in human HD brains and HD mouse models (Kim *et al.* 2001; Mende-Mueller *et al.* 2001; Wellington at al. 2002; Wang *et al.* 2008; Landles *et al.* 2010). Several proteolytic enzymes from families of caspases, MMPs, calpains and cathepsins, have already been reported as actors in these proteolytic processes (Goldberg *et al.* 1996; Kim *et al.* 2001, 2006; Gafni and Ellerby 2002; Lunkes *et al.* 2002; Miller *et al.* 2010; Tebbenkamp *et al.* 2012; Hermel *et al.* 2004; Ratovitski *et al.* 2009).

In this study, we investigated the expression of proteolytic enzymes from the families of caspases, MMPs, KLKs and calpains on the transgenic minipig model of Huntington´s disease at the Institute of Animal Physiology and Genetics, Academy of Sciences in Liběchov, Czech Republic. It is known, that as a consequence of proteolytic processing of mtHtt, short mtHtt fragments occur in affected cells, which finally lead to a formation of aggregates of mtHtt. Hence, we decided to also detect and quantify expression of mtHtt and its cleavage products and evaluate aggregates formation.

Although the studies in rodent models have helped to elucidate important pathways that are detrimental and contribute to the HD pathogenesis, there is a need of use more complex models of the disease, which correspond, or at least closely resemble, the physiology of humans. Pigs, and mainly minipigs, are the suitable candidates. Additionally, pig brain permit detailed identification of brain structures by imaging techniques and the slow disease progression allows longitudinal studies.

The Liběchov minipig was created in 2009 and information coding the sequence of N-terminal part of human mtHtt was transferred to subsequent generations from both female and male sides. The ratio of transgenic (TgHD) and wild-type (WT) newborn piglets was approximately equal in each litter. Up to now, 4 filial generations have arised (F1, F2, F3, F4) and current work of the laboratory is ongoing to characterize the phenotype of transgenic minipigs of F2 generation.

At present, a complex of non-invasive and invasive experimental approaches to WT and TgHD minipigs is used to elucidate pathologic pathways responsible for development of HD symptoms.

The latest experiments focus on behavioral tests over all generations in an attempt to capture the first changes in behavior of HD animals.

Biomarkers are, accordingly to a proper definition, some cellular, biochemical, or molecular characteristics that can be objectively measured and evaluated as indicator of normal biological processes, pathological processes, or pharmacological responses to a therapeutic intervention (Biomarkers Definitions Working Group 2001). The identification of such markers is now the subject of a high interest among the HD research groups.

In our laboratory, the semen, blood and cerebrospinal fluid (CSF) is continuously collected from F3 generation of WT and TgHD individuals and examinated with one goal to find a reproducible, sensitive and specific biomarker with such an outcome measure that can be used to track the disease progression in patients.

Our work contributes to the efforts to better understand the essence of HD and shed a light on a characterization of mtHtt in terms of its presence in minipig brain, differences in expression of mtHtt among striatal and cortical parts within animal, as well as differences in expression levels between WT and TgHD individuals of F2 generation of transgenic minipig model at the age of 36 months.

We used several antibodies raised both against the N-terminal of Htt and polyQ stretch for qualitative and quantitative analysis of mtHtt.

First, we used a series of antibodies directly binding N-terminus of Htt. Immunohistochemically, we detected moderate levels of endogenous and mtHtt in caudate nucleus and somatosensory cortex, without distinctive changes between WT and TgHD animals, with rabbit polyclonal BML-PW0595 antibody against aa2-17 sequence of endogenous and mutant Htt, and also rabbit polyclonal EPR5526 antibody corresponding to aa1-100 part of Htt. Interestingly, a relatively high expression of Htt was observed in cortical pyramidal neurons in comparison with other cells, as was similarly described in cerebral cortex in humans (Gutekunst *et al.* 1995).

Although we found a slightly increased expression of Htt in TgHD brain, quantitative analysis revealed that the increase was mainly in somatosensory cortex of TgHD. Besides, in some pairs of animals a significant increase was also detected in motor cortex and mainly in caudate nucleus, which is the most affected area in HD brain.

Immunostaing with mouse monoclonal MAB2166 antibody against epitope aa181-810 of Htt delivered relatively weak signal compared to previously described antibodies and therefore the image analysis was not performed.

Interestingly, we successfully detected smaller fragments of Htt and mtHtt in WT and TgHD animal. The fragment of MW=125 kDa represents inserted form of human mtHtt in TgHD minipig. Moreover, we observed fragments with molecular mass less than 50 kDa in TgHD animal, which are supposed to migrate into the nucleus and therefore act cytotoxically. It is interesting to note, that the relationship between the length of the N-terminal Htt fragments and the actual size of these peptides is not as direct as one can presume due to some conformational constraints. That is the reason why we cannot determine the exact length of Htt fragments, which are undoubtedly considered to enter the intranuclear space and form inclusions. Therefore, a systematic analysis of both predicted and observed sizes of different N-terminal Htt peptides should be taken into consideration in efforts to get better knowledge of required size of mtHtt fragment, which would enter the nucleus (Milevski *et al.* 2015). Other factors, which seem to be essencial for this issue and a passive shuttle between cytoplasm and nucleus are the cell-type-specific limits, which has already been reported for some Htt-derived fragments (Trushina *et al.* 2003). Such cell type-specific differences could be a possible explanation of the fact, that in R6/2 transgenic mouse models (89-150Q) is apparent intranuclear accumulation of Htt in striatal neurons (Davies *et al.* 1997).

Second, we performed analysis of mtHtt based on detection of polyQ stretch by 1C2 and 3B5H10 antibodies. The first work which stated that 1C2 antibody is able to detect intracellular inclusions as a hallmark of Huntington´s disease was from Paulson *et al.* (1997). Miller *et al.* (2011) used for recognizing of homomeric polyQ stretch antibody 3B5H10, which in their experiment on BACHD mice showed diffuse shadows in WT nuclear region, but stronger diffuse stain in nucleus of BACHD mouse at 12 months. In our analysis, we also observed more distinctive signal in TgHD minipig, but

the increased immunoreactivity was localized to the areas next to Golgi apparatus and endoplasmic reticulum in striatum and cortex of TgHD minipig brains.

The epitope of 1C2 antibody was found to be a homopolymeric glutamine stretch. The original immunogen TATA Box-binding protein (TBP) is the general transcription factor containing a 38Q stretch (Lescure *et al.* 1994). Other polyQ-containing proteins are recognized by the 1C2, notably those involved in several human neurodegenerative diseases caused by a CAG repeat expansion (Trottier *et al.* 1995). For proteins involved in these neurodegenerative disorders, 1C2 antibody showed remarkable property of detecting much better the pathological proteins that contain a polyQ expansion (37Q) than WT type proteins (Trottier et al 1995). This fact was confirmed in our WB analysis, where use of 1C2 antibody enabled to detect small proteolytic mtHtt fragments in cerebral cortex of TgHD minipig, whereas no fragmentation was observed in WT minipig. Fragmentation of both Htt and mtHtt fragments was detected in WB analysis using mouse monoclonal 3B5H10 antibody, however fragmentation in TgHD animal was much more extensive with presence of smaller proteolytic fragments in contrast to WT animal.

HD manifestation characterized by accumulation and aggreagation of mtHtt have had a leading role for many years. First description of abnormal neuronal membrane ultrastructure in HD was described by Roizin *et al.* (1979) by electron microscope investigation of post mortem human brains. Later the aggregates were discovered in the brain of R6/2 experimental mice model of HD (Davies *et al.* 1997). To date, the puzzling evidence for the presence of aggregates in R6/2, but much lower evidence of the same in the human HD brain finally led DiFiglia *et al.* (1997) to a reassessment of the presence of aggregates in autoptic HD brains. Result of this study was fact, that the most common pattern was to have one aggregate per cell, but also about 5-7% of cells contained two or three aggregates.

Aggregates accumulate primarily in striatum and cortex, whereas their presence in globus pallidus and cerebellum is less often. More recent studies suggested protective role of aggregates playing against the harmful effects of mtHtt (Arrasate *et al.* 2004). In contrary, soluble monomers of mtHtt and Htt oligomers were described to be toxic to cells and to be key factors in process of cellular dysfunction (Lajoie and Snapp 2010).

Htt fragment length and amount, as well as the length of polyQ are main determining factors responsible for aggregares generating. The frequency of aggregates formation is higher in the presence of short N-terminal Htt fragments as biochemical analysis of nuclear and cytoplasmic inclusions showed that nuclear aggregates are composed mostly by the N-terminal fragments of mtHtt. In contrary, extracellular inclusions contain both full-length and truncated mtHtt (Hackam *et al.* 1998).

For assessment of presence of mtHtt aggregates in our transgenic minipig model we used IHC analysis with mouse monoclonal MW8 antibody. In previous experiments on 24m old minipigs have not been detected any aggregates. Notably, our analysis of brain sections of 36m old minipigs probably revealed the first mtHtt aggregates (5-10 μm in diameter). The shape and density of aggregates were similar to those we observed in TgHD (R6/2) mice. We did not see any aggregates in brain sections of WT animals (minipig and mice).

Finally, we carried out investigation of the expression of various proteolytic enzymes from families of caspases, MMPs, KLKs and calpains, namely caspase-3, caspase-8, MMP-9, MMP-10, KLK-10 and calpain-5. As mentioned above, there are many research groups suggesting that the involvement of proteolytic enzymes in HD pathology is remarkable. Some of the enzymes participating in mtHtt cleavage have been already discovered, some are still under investigation, where exactly is their cleavage site on the mtHtt, and there are probably many more, whose role in a toxic fragmentation process within mtHtt remains to be elucidated.

IHC and WB analysis were used for detection of all enzymes. In addition, the Immunofluorescent staining method (IF) was performed for evaluation of caspase-3.

During this study, several minipigs from the F2 generation were sacrificed at the age of 48 moths. Within our longitudinal characterization of minipigs as a model of HD, the next step is to detect and analyse biochemical and molecular genetic changes directly at this age. Therefore, we had an opportunity to get some unique and not very easily obtainable cells, such as RPE cells. The RPE cells might be considered as affected by pathobiochemical changes in HD as Htt is a ubiquitous protein and its mutated form can occur throughout the body. Moreover, RPE is a monolayer of hexagonal shaped neural epithelial cells that have the same embryological origin as the neural retina. They mature right before the neural retina and play a key role in metabolic support of outer re-

tinal cells. Developmentally, the non-neural RPE and the neural retina originate from the same structure – the optic vesicles. Hence, we performed a pilot in vitro experiment striving to outline the presence and potential changes in enzyme levels in these cells. We successfully isolated and cultivated the cells, in spite of the fact that they may be picky as to growing in their environment and seem to be sensitive to pH, and used them for detection of MMP-9 by IF.

Analysis of caspases proved significantly increased levels of caspase-3 in TgHD minipig brain in IHC analysis, where the increased levels of this enzyme were found over the striatum (both caudate nucleus and putamen) and motor cortex of TgHD minipig. This result was confirmed by IF of all tested animals and moreover of R6/2 mouse. By WB we detected higher levels of inactive proenzyme, as well as active form of caspase-3 in TgHD minipigs. Caspase-8 expression was assessed by WB, which showed higher levels of the proenzyme in TgHD individual, whilst the processed form were at the same levels within TgHD and WT animals.

From the family of MMPs, we focus on detection of two enzymes, MMP-9 and MMP-10. Increased levels of MMP-9 processed forms were found in cortex and cerebellum of TgHD minipigs by WB analysis, and also IHC of striatum and somatosensory cortex confirmed this finding and TgHD brain significantly differs from WT one in term of MMP-9 expression. What is more, IF of RPE cells of 48 month old minipigs showed increased levels of MMP-9 in TgHD individual suggesting that those cells may also be affected by pathogenic processes in HD. MMP-10 was detected immunohistochemically in brains of WT and TgHD minipigs with small changes in expression. A small increase of MMP-10 was detected in caudate nucleus of TgHD minipig. We supposed to obtain much higher difference in signal as the activation of MMP-10 was previously described (Miller *et al.* 2010). Therefore, we aim to continue with searching for changes in aging animals, taking into consideration that our result can be influenced by relatively low age of experimental animals as the lifespan of minipigs is about 20 years and the onset of detectable changes at the cellular or whole body levels may be more gradual in contrary to mice models of the disease. Also, the larger scale of experiments would be done for more complex analysis.

Furthermore, the decreased levels of KLK-10 were detected in TgHD minipig brains compared to WT animal, which is in contrast to the other observations, where the

same or increased concentrations occured in TgHD individual. WB analysis suggested little changes in KLK-10 levels. Concretely, a slightly higher level of the enzyme in cortex and a slightly lower level in cerebellum of TgHD were detected.

Calpain-5 was analysed by using both IHC and WB techniques. IHC staining of this enzyme confirmed its strong expression in brains of WT and TgHD animals. However, no difference was observed between them. Also, the results of WB did not show any differences among WT and TgHD minipigs.

Even though the cleavage of full-length Htt releasing smaller N-terminal fragments containing polyQ, which are toxic to neurons, has already been assessed as a crucial step in HD pathogenesis, the cascade of proteolytic events leading to the generation of these toxic properties remains unclear. Commonly used theory is that the mutant fragments are more toxic the shorter they are (Hackam *et al.* 1998, Landles *et al.* 2010), however Graham *et al.* (2006) proposed that some proteolytic fragments are more toxic than the others independently of size.

Very recently, it has also been published that there could be a possible participation of not N-, but C-terminal fragments on HD pathogenesis. El-Daher *et al.* (2015) found that C-terminal fragments induced toxicity via dilation of the endoplasmic reticulum (ER) and increased ER stress. C-terminus bound to dynamin 1 and impaired its activity at ER membranes. They also proposed that when WT full-length Htt is proteolysed, this turns the non-toxic WT Htt into a highly toxic protein.

For future work we are aiming to extend our preliminary results of proteolytic enzymes expression and continue with phenotypical characterization of 36m and 48m old transgenic minipig model of HD, which includes better understanding of proteolytic processes and following drug targeting.

6 CONCLUSION

a. Investigation of the expression of Htt in WT and TgHD minipigs (EPR5526, PW-0595 antibodies) indicated slightly increased levels (non-significant) of Htt in the striatum and cortex (IHC), increased levels in cortex (WB) of TgHD animals.
b. We successfully confirmed cleavage processes of mtHtt and detected small N-terminal fragments of mtHtt using specific antibodies (EPR5526, 1C2).
c. We probably detected first aggregates of mtHtt in the brain of TgHD minipigs.
d. Investigatiton of the expression of caspases, MMPs, KLKs, calpains showed an increase of caspase-3 levels in the striatum and cortex of TgHD (IHC), an increase in cortex of TgHD (WB), an increase in RPE of TgHD (IF), an increase of caspase-8 proenzyme level in the cerebellum of TgHD, a slight increase in the striatum and cortex of TgHD (IHC), an increase in the cortex and cerebellum TgHD (WB), MMP-10 was highly expressed in the striatum and cortex of Tg and WT animals, without significant differences (IHC), a decrease of KLK-10 levels was found in the striatum and cortex of TgHD (IHC), a decrease in cortex of TgHD (WB), calpain-5 was highly expressed in the striatum and cortex of TgHD and WT animals without differences between them (IHC in the striatum and cortex, WB in the cortex).

7 ABBREVIATIONS

3D	three-dimensional
AGERA	agarose gel electrophoresis for resolving aggregates
AS	Academy of Sciences
Asp102	amino acid asparagine 102
Asp586	amino acid asparagine
586BACHD Casp −/−	mouse model with a caspase-6 knockout
BCA	bicinchoninic acid
BDNF	brain derived neurotrophic factor
C1	family of papain-like cysteine proteases
C6R	caspase-6-resistant
Ca^{2+}-ATPase	calcium adenosine triphosphatase
CAG/CAA	trinucleotide repeats (cytosine, adenine, guanine / cytosine, adenine, adenine)
CARD	the caspase recruitment domain
CBBG	Coomassie brilliant blue
cDNA	complementary DNA
cp	cleavage products
CPPT pHIV7	central polypurine tract pHIV7
CR	Czech Republic
CSF	cerebrospinal fluid
Cys	amino acid cysteine
DAB	diaminobenzidine
DAPI	4',6-diamidino-2-phenylindole
DED	the death effector domain
EAE	mouse model of multiple sclerosis
ECL	enhanced chemiluminescence
ED11	a novel peptide inhibitor based on the Htt caspase-6 cleavage site (aa550-560)
EDTA	ethylendiamintetraacetic acid
ER	endoplasmic reticulum
F1, F2, F3, F4	first, second, third, fourth filial generation
FH400-100Q	construct used for transfection
FISH	fluorescent in situ hybridization
GFAP	glial fibrillary acidic protein, used as a marker to distinguish astrocytes from other glial cells
Gln-Ala	glycine, alanine
Gly193	amino acid glycin 193
GRIK2 (GluR6)	glutamate receptor, ionotropic kainate 2 (glutamate receptor 6 gene)
H_2O_2	hydrogen peroxide
H3, H2A.Z, H2B	types of histones
Hdh(111Q/111Q)	construct used for transfection
HEK293T	transgenic mouse model of Huntington´s disease
HEXXH	sequence of matrix metalloproteinases interacting with zinc
His57	amino acid histidine 57
HTT	huntingtin gene

Htt	huntingtin protein
Htt138Q(1-469)	construct used for transfection
Htt15Q(1-469)	construct used for transfection
Htt586	construct used for transfection
Htt-N511-52Q	construct used for transfection
IAPG CR	Institute of Animal Physiology and Genetics
IVLD	cleavage site at position aa586 for caspase-6
KLKs	kallikreins
L1-L4	catalytic center loops of caspases
m-calpains	m-isoform of calpain
mGluRs	metabotropic glutamate receptors
MMPs	matrix metalloproteinases
MRI	magnetic resonance imaging
mRNA	messenger ribonucleic acid
mtHtt	mutated form of huntingtin
MW	molecular weight
NeuN	neuronal nuclear antigen, commonly used as a marker for neurons
NMDA	N-methyl-D-aspartate receptor
NMDARs	N-methyl-D-aspartate receptors
NNGH	N-isobutyl-N- (4-methoxyphenylsulfonyl) glycyl hydroxamic acid
NP-40	tergitol-Type NP-40, nonyl phenoxypolyethoxylethanol
ORF	open reading frame
p10	small subunit of caspases
p20	large subunit of caspases
PBS	phosphate-buffered saline
PBSTx	phosphate-buffered saline with Triton-X-100
PCR	polymerase chain reaction
PET	positron emission tomography
PFA	paraformaldehyde
pFLmixQ145	plasmide comprising cDNA with 145 CAG/CAA repetitions
pH	„power of hydrogen“, numeric scale used to specify the acidity or alkalinity of an aqueous solution
pHIV1-HD-548aaHTT-145Q	construct used for transfection
PIDDosome	PIDD–RAIDD–caspase-2 complex
polyQ	polyglutamine
proKLK	inactive proforms of kallikreins
PTMs	posttranslational modifications
PVP	polyvinylpyrrolidone
RIPA	radioimmunoprecipitation assay buffer
RPE	retinal pigment epithelium
S/T XXGG I/L	cleavage site at position aa402 for matrix metalloproteinase 10
SA	clan of kallikreins
SB	substrate buffer
SDS-PAGE	sodium dodecyl sulfate -polyacrylamide gel electrophoresis
Ser195	amino acid Serine 195
SMAC	second mitochondrial derived activator of caspases

Substance P	neuropeptide acting as a neurotransmitter and as a neuromodulator
TAA repeat	trinucleotide repeats (thymine, adenine, adenine)
TBP	TATA box-binding protein
TgHD	transgenic model of Huntington´s Disease
TIMP1, TIMP2, TIMP3	tissue inhibitor of metalloproteinase 1-3
TTBS	Tris- Tween buffered saline
UCHLI	carboxy-terminal hydrolase L1
UK	United Kingdom
WB	Western blotting
WPRE	woodchuck hepatitis post-transcriptional regulatory element of cis-enhancing element
WT	wild-type
XIAP	X-linked inhibitor of apoptosis
YAC128	transgenic mouse model of Huntington´s disease
α-MEM	minimum essential medium-alpha medium
μ-calpains	μ-isoform of calpain

8 REFERENCES

Andrew SE, Goldberg YP, Kremer B, Telenius H, Theilmann J, Adam S et al. (1993) The relationship between trinucleotide (CAG) repeat length and clinical features of Huntington's disease. *Nat Genet* 4: 398–403

Archibald AL, Bolund L, Churcher C, Fredholm M, Groenen MA, Harlizius B, Lee KT, Milan D, Rogers J, Rothschild MF, Uenishi H, Wang J, Schook LB (2010) Pig genome sequence–analysis and publication strategy. *BMC Genomics* 11: 438

Arrasate M, Mitra S, Schweitzer ES, Segal MR, Finkbeiner S (2004) Inclusion body formation reduces levels of mutant huntingtin and the risk of neuronal death. *Nature* 431: 805–810

Asagiri M, Takayanagi H (2007) The molecular understanding of osteoclast differentiation. *Bone* 40: 251–264

Aylward EH, Codori AM, Rosenblatt A, Sherr M, Brandt J, Stine OC et al. (2000) Rate of caudate atrophy in presymptomatic and symptomatic stages of Huntington's disease. *Mov Disord* 15: 552–560

Barrett AJ, Rawlings ND, Salvesen GS, Woessner JF (2012) Handbook of Proteolytic Enzymes. *Academic Press*

Baumgartner R, Meder G, Briand C, Decock A, D'arcy A, Hassiepen U, Morse R, Renatus M (2009) The crystal structure of caspase-6, a selective effector of axonal degeneration. *Biochem J* 423: 429–439

Baxa M, Hruska-Plochan M, Juhas S, Vodicka P, Pavlok A, Juhasova J, Miyanohara A, Nejime T, Klima J, Macakova M, Marsala S, Weiss A, Kubickova S, Musilova P, Vrtel R, Sontag EM, Thompson LM, Schier J, Hansikova H, Howland DS, Cattaneo E, DiFiglia M, Marsala M, Motlik J (2013) A transgenic minipig model of Huntington's disease. *J Huntingtons Dis* 2: 47–68

Biomarkers Definitions Working Group (2001) Biomarkers and surrogate endpoints: preferred definitions and conceptual framework. *Clin Pharmacol Ther* 69: 89-95

Borrell-Pagès M, Zala D, Humbert S, Saudou F Huntington's disease: from huntingtin function and dysfunction to therapeutic strategies.(2006) *Cell Mol Life Sci* 63: 2642–2660

Brguljan PM, Turk V, Nina C, Brzin J, Krizaj I & Popovic T (2003) Human brain cathepsin H as a neuropeptide and bradykinin metabolizing enzyme. *Peptides* 24: 1977–1984

Brignull HR, Morley JF, Garcia SM, Morimoto RI (2006) Modeling polyglutamine pathogenesis in C. Elegans. *Methods Enzymol* 412: 256–282

Carter RJ, Lione LA, Humby T, Mangiarini L, Mahal A, Bates GP, Dunnett SB, Morton AJ (1999) Characterization of progressive motor deficits in mice transgenic for the human Huntington's disease mutation. *J Neurosci* 19: 3248–3257

Ceru S, Konjar S, Maher K, Repnik U, Krizaj I, Bencina M, Renko M, Nepveu A, Zerovnik E, Turk B, Kopitar-Jerala N (2010) Stefin B interacts with histones and cathepsin L in the nucleus. *J. Biol. Chem.* 285: 10078–10086

Davies SW, Scherzinger E (1997) Nuclear inclusions in Huntington's disease. *Trends Cell Biol* 7: 422

DiFiglia M, Sapp E, Chase K, Schwarz C, Meloni A Young C et al. (1995) Huntingtin is a cytoplasmic protein associated with vesicles in human and rat brain neurons. *Neuron* 14: 1075–1081

DiFiglia M, Sapp E, Chase KO, Davies SW, Bates GP, Vonsattel JP, Aronin N (1997) Aggregation of huntingtin in neuronal intranuclear inclusions and dystrophic neurites in brain. *Science* 277: 1990–1993

Duncan EM, Muratore-Schroeder TL, Cook RG, Garcia BA, Shabanowitz J, Hunt DF, Allis CD (2008) Cathepsin L proteolytically processes histone H3 during mouse embryonic stem cell differentiation. *Cell* 135: 284–294

El-Daher MT, Hangen E, Bruyère J, Poizat G, Al-Ramahi I, Pardo R, Bourg N, Souquere S, Mayet C, Pierron G, Lévêque-Fort S, Botas J, Humbert S, Saudou F (2015) Huntingtin proteolysis releases non-polyQ fragments that cause toxicity through dynamin 1 dysregulation. *EMBO J* [Epub ahead of print]

Emw, December 15, 2009, Structure of the MMP10 protein, Wikimedia Commons, Available from: <https://upload.wikimedia.org/wikipedia/commons/0/0f/Protein_MMP10_PDB_1q3a.png>. [28 August 2015]

Fan MM, Raymond LA (2007) N-methyl-D-aspartate (NMDA) receptor function and excitotoxicity in Huntington's disease. *Prog Neurobiol* 81: 272–93

Gafni J, Ellerby LM (2002) Calpain activation in Huntington's disease. *J Neurosci* 22: 4842–4849

Gafni J, Hermel E, Young JE, Wellington CL, Hayden MR, Ellerby LM (2004) *J Biol Chem* 279: 20211–20220

Gil JM, Rego AC (2008) Mechanisms of neurodegeneration in Huntington's disease. *Eur J Neurosci* 27: 2803–2820

Goldberg Y.P, Nicholson D.W, Rasper D.M, Kalchman M.A, Koide H.B, Graham R.K, Bromm M, Kazemi-Esfarjani P, Thornberry N.A, Vaillancourt J.P, Hayden M.R (1996) Cleavage of huntingtin by apopain, a proapoptotic cysteine protease, is modulated by the polyglutamine tract. *Nature Genet* 13: 442–449

Graham RK, Deng Y, Slow EJ, Haigh B, Bissada N, Lu G, Pearson J, Shehadeh J, Bertram L, Murphy Z, Warby SC, Doty CN, Roy S, Wellington CL, Leavitt BR, Raymond LA, Nicholson DW, Hayden MR (2006) Cleavage at the caspase-6 site is required for neuronal dysfunction and degeneration due to mutant huntingtin. *Cell* 125: 1179–1191

Graham RK, Deng Y, Carroll J, Vaid K, Cowan C, Pouladi MA, Metzler M, Bissada N, Wang L, Faull RL, Gray M, Yang XW, Raymond LA, Hayden MR (2010) Cleavage at the 586 amino acid caspase-6 site in mutant huntingtin influences caspase-6 activation in vivo. *J Neurosci* 30: 15019–15029

Graham RK, Ehrnhoefer DE, Hayden MR (2011) Caspase-6 and neurodegeneration. *Trends Neurosci* 34: 646–656

Hackam AS, Singaraja R, Metzler M, Gunekunst CA, Gan L, Warby S, Wellington CL, Vaillancourt J, Chen N, Gervais FG, Raymond L, Nicholson DW, Hayden MR (2000) Huntingtin interacting protein 1 induces apoptosis via a novel caspase-dependent death effector domain. *J Biol Chem* 275: 41299–41308

Hackam AS, Singaraja R, Wellington CL, Metzler M, McCutcheon K, Zhang T, Kalchman M, Hayden MR (1998) The influence of huntingtin protein size on nuclear localization and cellular toxicity. *J Cell Biol* 141: 1097–1105

Harper PS (2002) Huntington's disease: a historical background. In: Huntington's Disease, 3rd ed. (Bates G, Harper PS, Jones L, eds), pp 3–27. Oxford: *Oxford University Press*

Hermel E, Gafni J, Propp SS, Leavitt BR, Wellington CL, Young JE, Hackam AS, Logvinova AV, Peel AL, Chen SF, Hook V, Singaraja R, Krajewski S, Goldsmith PC, Ellerby HM, Hayden MR, Bredesen DE, Ellerby LM (2004) Specific caspase interactions and amplification are involved in selective neuronal vulnerability in Huntington's disease. *Cell Death Differ* 11: 424–438

Hofmann A, Kessler B, Ewerling S, Weppert M, Vogg B, Ludwig H, Stojkovic M, Boelhauve M, Brem G, Wolf E, Pfeifer A (2003) Efficient transgenesis in farm animals by lentiviral vectors. *EMBO Reports* 4: 1054–60

Huntington's Disease, May 5, 2013, Available from: <http://genetics4medics.com/huntington-disease.html>. [28 August 2015]

Huttenlocher A, Palecek SP, Lu Q, Zhang W, Mellgren RL, Lauffenburger DA, Ginsberg MH, Horwitz AF (1997) Regulation of cell migration by the calcium-dependent protease calpain. *J Biol Chem* 272: 32719–32722

Chan WSA (2014) Paper presented at the HD conference, Cambridge, unpublished

Chen M, Ona VO, Li M, Ferrante RJ, Fink KB, Zhu S, Bian J, Guo L, Farrell LA, Hersch SM, Hobbs W, Vonsattel JP, Cha JH, Friedlander RM (2000) Minocycline inhibits caspase-1 and caspase-3 expression and delays mortality in a transgenic mouse model of Huntington disease. *Nature Med* 6: 797–801

Ikeda H, Yamaguchi M, Sugai S, Aze Y, Narumiya S, Kakizuka A (1996) Expanded polyglutamine in the Machado-Joseph disease protein induces cell death in vitro and in vivo. *Nature Genet* 13: 198–202

Jacobsen JC, Bawden CS, Rudiger SR, McLaughlan CJ, Reid SJ, Waldvogel HJ, MacDonald ME, Gusella JF, Walker SK, Kelly JM, Webb GC, Faull RLM, Rees MI, Snel RG (2010) An ovine transgenic Huntington's disease model. *Hum Mol Genet* 19: 1873–1882

Khorchid A, Ikura M (2002) How calpain is activated by calcium. *Nat Struct Biol* 9: 239–41

Kim M, Lee H-S, LaForet G, McIntyre C, Martin EJ, Chang P, Kim TW, Williams M, Reddy PH, Tagle D, Boyce FM, Won L, Heller A, Aronin N, DiFiglia M (1999) Mutant Huntingtin expression in clonal striatal cells: dissociation of inclusion formation and neuronal survival by caspase inhibition. *J Neurosci* 19: 964–973

Kim J, Cho IS, Hong JS, Choi YK, Kim H, Lee YS (2008) Identification and characterization of new microRNAs from pig. *Mamm Genome* 19: 570–580

Kocurova G, Ardan T (2015) Proteolyticke enzymy v patogenezi HN. *Bioprospect* 1: 23–26

Kovtun IV, Welch G, Guthrie HD, Hafner KL, McMurray CT (2004) CAG repeat lengths in X- and Y-bearing sperm indicate that gender bias during transmission of Huntington's disease gene is determined in the embryo. *J Biol Chem* 279: 9389–9391

Krawitz P, Haffner C, Fluhrer R, Steiner H, Schmid B, Haass C (2005) Differential localization and identification of a critical aspartate suggest non-redundant proteolytic functions of the presenilin homologues SPPL2b and SPPL3. *J Biol Chem* 280: 39515–39523

Kremer B, Goldberg P, Andrew SE, Theilmann J, Telenius H, Zeisler Jutta et al. (1994) worldwide study of the Huntington's disease mutation. *N Engl J Med* 330: 1401–1406

Kulkarni S, Saido TC, Suzuki K, Fox JEB (1999) Calpain Mediates Integrin-induced Signaling at a Point Upstream of Rho Family Members. *J Biol Chem* 274: 21265–21275

Lajoie P, Snapp EL (2010) Formation and toxicity of soluble polyglutamine oligomers in living cells. *PLoS One* 5: e15245

Le S, Bogyo M (2014) Activity-based profiling of proteases. *Annu Rev Biochem* 83: 249–273

Lee X, Ahmed FR, Hirama T, Huber C P, Rose DR, To R, Hasnain S, Tam A & Mort J S (1990) Crystallization of recombinant rat cathepsin B. *J Biol Chem* 265: 5950–5951

Leeflang EP, Zhang L, Tavaré S, Hubert R, Srinidhi J, MacDonald ME et al. (1995) Single sperm analysis of the trinucleotide repeats in the Huntington's disease gene: quantification of the mutation frequency spectrum. *Hum Mol Genet* 4: 1519–1526

Lescure A, Lutz Y, Eberhard D, Jacq X, Krol, Grummt I, Davidson I, Chambon P, Tora L (1994) The N-terminal domain of the human TATA-binding protein plays a role in transcription from TATA-containing RNA polymerase II and III promoters. *EMBO J* 13: 1166–1175

Li J, Yuan J (2008) Caspases in apoptosis and beyond. *Oncogene* 27: 6194–6206
Li SH, Lam S, Cheng AL, Li XJ (2000) Intranuclear huntingtin increases the expression of caspase-1 and induces apoptosis. *Hum Mol Genet* 9: 2859–2867
Li XJ, Li S (2015) Large Animal Models of Huntington's Disease. *Curr Top Behav Neurosci* 22: 149–160
López-Pelegrín M, Ksiazek M, Karim AY, Guevara T, Arolas JL, Potempa J, Gomis-Rüth FX (2015) A novel mechanism of latency in matrix metalloproteinases. *J Biol Chem* 290: 4728–4740
Lunkes A, Mandel JL (1998) A cellular model that recapitulates major pathogenic steps of Huntington's disease. *Hum Mol Genet* 7: 1355–1361
Lüthi AU, Martin SJ (2007) The CASBAH: A searchable database of caspase substrates. *Cell Death Differ* 14: 641–650
Mace PD, Riedl SJ, Salvesen GS (2014) Caspase Enzymology and Activation Mechanisms. In: Methods in enzymology Regulated Cell Death Part A: Apoptotic Mechanisms, Vol 544 (Ashkenazi A, Yuan J, Wells J, eds), pp 161–178. *Elsevier Academic Press*
Mangiarini L, Sathasivam K, Seller M, Cozens B, Harper A, Hetherington C, Lawton M, Trottier Y, Lehrach H, Davies SW, Bates GP (1996) Exon 1 of the HD gene with an expanded CAG repeat is sufficient to cause a progressive neurological phenotype in transgenic mice. *Cell* 87: 493–506
Matsuyama N, Hadano S, Onoe K, Osuga H, Showguchi-Miyata J, Gondo Y, Ikeda JE (2000) Identification and characterization of the miniature pig Huntington's disease gene homolog: Evidence for conservation and polymorphism in the CAG triplet repeat. *Genomics* 69: 72–85
McBride J, Clark R (2014) Paper presented at the HD conference, Cambridge, unpublished
Milewski M, Gawliński P, Bąk D, Matysiak A, Bal J (2015) Complex interplay between the length and composition of the huntingtin-derived peptides modulates the intracellular behavior of the N-terminal fragments of mutant huntingtin. *Eur J Cell Biol* 94: 179–189
Miller JP, Holcomb J, Al-Ramahi I, De Haro M, Gafni J, Zhang N, Kim E, Sanhueza M, Torcassi C, Kwak S, Botas J, Hughes RE, Ellerby LM (2010) Matrix Metalloproteinases Are Modifiers of Huntingtin Proteolysis and Toxicity in Huntington's Disease. *Neuron* 67: 199–212
Miller J, Arrasate M, Brooks E, Libeu CP, Legleiter J, Hatters D, Curtis J, Cheung K, Krishnan P, Mitra S, Widjaja K, Shaby BA, Lotz GP, Newhouse Y, Mitchell EJ, Osmand A, Gray M, Thulasiramin V, Saudou F, Segal M, Yang XW, Masliah E, Thompson LM, Muchowski PJ, Weisgraber KH, Finkbeiner S (2011) Identifying polyglutamine protein species in situ that best predict neurodegeneration. *Nat Chem Biol* 7: 925–934
Moldoveanu T, Hosfield CM, Lim D, Elce JS, Jia Z, Davies PL (2002) A Ca(2+) switch aligns the active site of calpain. *Cell* 8;108: 649–60
Morton AJ, Howland DS (2013) Large genetic animal models of Huntington's Disease. *J Huntingtons Dis* 2: 3–19
Munoz-Sanjuan I, Bates GP (2011) The importance of integrating basic and clinical research toward the development of new therapies for Huntington disease. J *Clin Inv* 121: 476-483
Ona VO, Li M, Vonsattel JPG, Andrews LJ, Khan SQ, Chung WM, Frey AS, Menon AS, Li XJ, Stieg PE, Yuan J, Penney JB, Young AB, Cha JH, Friedlander RM (1999) Inhibition of caspase-1 slows disease progression in a mouse model of Huntington's disease. *Nature* 399: 263–267

Paulson HL, Perez MK, Trottier Y, Trojanowski JQ, Subramony SH, Das SS,Vig P, Mandel JL, Fischbeck KH, Pittman RN (1997) Intranuclear inclusions of expanded polyglutamine protein in spinocerebellar ataxia type 3. *Neuron* 19: 333–344

Petrucelli L, Dawson TM (2004) Mechanism of neurodegenerative disease: role of the ubiquitin proteasome system. *Ann Med* 36: 315–320

Portera-Cailliau C, Hedreen JC, Price DL, Koliatsos VE (1995) Evidence for apoptotic cell death in Huntington disease and excitotoxic animal models. *J Neurosci* 15: 3775–3787

Ramaswamy S, McBride JL, Kordower JH (2007)Animal models of Huntington's disease. *ILAR J* 48: 356–373

Ramos AM, Crooijmans RP, Affara NA, Amaral AJ, Archibald AL, Beever JE, Bendixen C, Churcher C, Clark R, Dehais P, Hansen MS, Hedegaard J, Hu ZL,Kerstens HH, Law AS, Megens HJ, Milan D, Nonneman DJ, Rohrer GA, Rothschild MF, Smith TP, Schnabel RD, Van Tassell CP, Taylor JF, Wiedmann RT,Schook LB, Groenen MA (2009) Design of a high density SNP genotyping assay in the pig using SNPs identified and characterized by next generation sequencing technology. *PloS One* 4: e6524

Ravikumar B, Duden R, Rubinsztein DC (2002) Aggregate-prone proteins with polyglutamine and polyalanine expansions are degraded by autophagy. *Hum Mol Genet* 11: 1107–1117

Roizin L, Stellar S, Liu JC (1979) Neuronal nuclear-cytoplasmic changes in Huntington's chorea: electron microscope investigations. In: Advances in neurology, Vol 23 (Chase TN, Wexler NS, Barbeau A, eds), pp 95–122. New York: *Raven*

Roth J (2009) Neurodegenerace: jeden mechanismus pro mnoho chorob?. *Lek Listy* 7: 17–18

Rubinsztein DC (2002) Lessons from animal models of Huntington's disease. *Trends Genet* 18: 202–209

Sanman LE, Bogyo M (2014) Activity-based profiling of proteases. *Annu Rev Biochem* 83: 249–73

Saudou F, Finkbeiner S, Devys D, Greenberg ME (1998) Huntingtin acts in the nucleus to induce apoptosis but death does not correlate with the formation of intranuclear inclusions. *Cell* 95: 55–66

Sennepin AD, Charpentier Sp Normand T, Sarré C, Legrand A, Mollet LM (2009) Multiple reprobing of Western blots after inactivation of peroxidase activity by its substrate, hydrogen peroxide. *Anal Biochem* 393: 129 –131

Schilling G, Becher MW, Sharp AH, Jinnah HA, Duan K, Kotzuk JA, Slunt HH, Ratovitski T, Cooper JK, Jenkins NA, Copeland NG, Price DL, Ross CA, Borchelt DR (1999) Intranuclear inclusions and neuritic aggregates in transgenic mice expressing a mutant N-terminal fragment of huntingtin. *Hum Mol Genet* 8: 397–407

Schwabish MA, Struhl K (2006) Asf1 mediates histone eviction and deposition during elongation by RNA polymerase II. *Mol Cell* 22: 415–422

Silvestroni A, Faull RLM, Strand AD, Möller T (2009) Distinct neuroinflammatory profile in post-mortem human Huntington's disease: progress toward effective disease-modifying treatments and a cure. *NeuroReport* 20: 1098–1103

Sol-Church K, Frenck J & Mason RW (2000) Mouse cathepsin M, a placenta-specific lysosomal cysteine protease related to cathepsins L and P. *Biochim Biophys Acta* 1491: 289–294

Swindle MM, Makin A, Herron AJ, Clubb FJ, Frazier KS (2012) Swine as models in biomedical research and toxicology testing. *Vet Pathol* 49: 344–56

Trottier Y, Biancalana V, Mandel JL (1994) Instability of CAG repeats in Huntington's disease: relation to parental transmission and age of onset. *J Med Genet* 31: 377–82

Trottier Y, Lutz Y, Stevanin G, Imbert G, Devys D, Cancel G, Saudou F, Weber C, David G, Tora L, Agid Y, Brice A, Mandel JL (1995) Polyglutamine expansion as a pathological

epitope in Huntington's disease and four dominant cerebellar ataxias. *Nature* 378: 403–406

Trushina E, Heldebrant MP, Perez-Terzic CM, Bortolon R, Kovtun IV, Badger JD, Terzic A, Estévez A, Windebank AJ, Dyer RB, Yao J, McMurray CT (2003) Microtubule destabilization and nuclear entry are sequential steps leading to toxicity in Huntington's disease. *Proc Natl Acad Sci U S A* 100: 12171–12176

Turk B, Turk V (2009) Lysosomes as "suicide bags" in cell death: myth or reality? *J. Biol. Chem.* 284: 21783–21787

Vodicka P, Smetana K, Dvorankova B, Emerick T, Xu YZ, Ourednik J, Motlik J (2005) The miniature pig as an animal model in biomedical research. *Ann N Y Acad Sci* 1049: 161–71

Warby SC, Doty CN, Graham RK, Carroll JB, Yang YZ, Singaraja RR, Overall CM, Hayden MR (2008) Activated caspase-6 and caspase-6-cleaved fragments of huntingtin specifically colocalize in the nucleus. *Hum Mol Genet* 17: 2390–2404

Wellington CL, Hayden MR (1997) Of molecular interactions, mice and mechanisms: new insights into Huntington's disease. *Curr Opin Neurol* 10: 291–298

Wellington CL, Singaraja R, Ellerby L, Savill J, Roy S, Leavitt B, Cattaneo E, Hackam A, Sharp A, Thornberry N, Nicholson DW, Bredesen DE, Hayden MR (2000) Inhibiting caspase cleavage of huntingtin reduces toxicity and aggregate formation in neuronal and nonneuronal cells. *J Biol Chem* 275: 19831–19838

Wellington CL, Ellerby LM, Hackam AS, Margolis RL, Trifiro MA, Singaraja R, McCutcheon K, Salvesen GS, Propp SS, Bromm M, Rowland KJ, Zhang T, Rasper D, Roy S, Thornberry N, Pinsky L, Kakizuka A, Ross CA, Nicholson DW, Bredesen DE, Hayden MR (1998) Caspase cleavage of gene products associated with triplet expansion disorders generates truncated fragments containing the polyglutamine tract. *J Biol Chem* 273: 9158–9167

Wexler NS, Lorimer J, Porter J, Gomez F, Moskowitz C, Shackell E et al. (2004) Venezuelan kindreds reveal that genetic and environmental factors modulate Huntington'sdisease age of onset. *Proc Natl Acad Sci U S A* 101: 3498–3503

Wiley HS, VanNostrand W, McKinley DN & Cunningham DD (1985) Intracellular processing of epidermal growth factor and its effect on ligand–receptor interactions. *J Biol Chem* 260: 5290–5295

Yamamoto A, Lucas JJ, Hen R (2000) Reversal of Neuropathology and Motor Dysfunction in a Conditional Model of Huntington's Disease. *Cell* 101: 57–66

Yang D, Wang CE, Zhao B, Li W, Ouyang Z, Liu Z, Yang H, Fan P, O'Neill A, Gu W, Yi H, Li S, Lai L, Li XJ (2010) Expression of Huntington's disease protein results in apoptotic neurons in the brains of cloned transgenic pigs. *Hum Mol Genet* 19: 3983–3994

Yoon H, Laxmikanthan G, Lee J, Blaber SI, Rodriquez A, Kogot JM, Scarisbrick IA, Blaber M (2007) Activation profiles and regulatory cascades of the human kallikrein-related peptidases. *J Biol Chem* 282: 31852–31864

Yoon H, Blaber SI, Debela M, Goettig B, Scarisbrick IA, Blaber M (2009) A completed KLK activome profile: investigation of activation profiles of KLK9, 10, and 15. *Biol Chem* 390: 373–377

Zeitlin S, Liu JP, Chapman DL, Papaioannou VE, Efstratiadis A (1995) Increased apoptosis and early embryonic lethality in mice nullizygous for the Huntington's disease gene homologue. *Nat Genet* 11: 155–163

Zhang Y, Ona VO, Li M, Drozda M, Dubois-Dauphin M, Przedborski S, Ferrante RJ, Friedlander RM (2003) Sequential activation of individual caspases, and of

alterations in Bcl-2 proapoptotic signals in a mouse model of Huntington's disease. *J Neurochem* 87: 1184–1192

Zuccato C, Cattaneo E. (2009) Brain-derived neurotrophic factor in neurodegenerative diseases. *Nat Rev Neurol* 5: 311–322